13 The Crust–Hydrosphere–Atmosphere System

Atmosphere, ocean, and biosphere write their history in the rocks and move on, renewing themselves in a few years or millennia. Their record is preserved in those parts of the lithosphere, growing scarcer as time goes on, that escape the ravages of Zeus and Pluto. Much of this record is chemical; reading it requires the development of chemical hypotheses and models and the formulation of chemical questions to test them.

Gregor, Garrels, Mackenzie, and Maynard (1988)

The Earth has many unique features compared to other planets in the Solar System: abundant (liquid) water on the surface (the oceans cover ~71% of the Earth's surface); an atmosphere with abundant free oxygen and very little CO_2 or CH_4; a chemically evolved crust; and the presence of life (including what we consider to be advanced forms of life). In this chapter we will review the composition of the present atmosphere and oceans, and how they have evolved over the geologic time. Our current knowledge of the evolution of the atmosphere and hydrosphere is quite fragmentary. The conclusions summarized in this chapter are based on models constructed by different authors, each model limited by its own assumptions.

13.1 The present atmosphere

The atmosphere (or air) refers to the envelope of gases that surrounds the Earth and is retained by the Earth's gravity. The Earth's atmosphere has no outer boundary; it gradually becomes thinner with increasing altitude and just fades into space. An altitude of 120 km (75 miles) is where atmospheric effects become noticeable during reentry of spacecrafts. The commonly accepted boundary between the Earth's atmosphere and outer space lies at an altitude of 100 km (62 miles) and is called the *Kármán line*, so named after the Hungarian–American engineer and physicist (1881–1963) who was the first to calculate that around this altitude the Earth's atmosphere becomes too thin for aeronautical purposes (that is, any vehicle above this altitude would have to travel faster than orbital velocity in order to derive sufficient aerodynamic lift from the atmosphere to support itself). The average mass of the total atmosphere is about 5.2×10^{18} kg (Andrews *et al.*, 2004). About 50% of the atmosphere's mass is contained within 5.6 km of the Earth's surface, about 75% within 11 km of the Earth's surface, and about 99.99997% within 100 km of the Earth's surface. The dense part of the atmosphere (pressure > 0.01 bar), accounting for ~97% of mass of the atmosphere, extends to about 30 km from the Earth's surface.

13.1.1 Temperature and pressure distribution in the atmosphere

The temperature of the atmosphere is a direct or indirect consequence of the absorption of solar radiation by resident gas molecules and atoms in the atmosphere. Solar radiation consists predominantly of visible light and the more energetic (shorter wavelengths) ultraviolet (UV) radiation of the electromagnetic spectrum (Fig. 13.1). The absorption by different constituents of the atmosphere occurs at specific wavelengths. The major absorbers are $N_2(g)$, $O_2(g)$, $O_3(g)$, $NO_2(g)$, and particulates (Table 13.1).

On the basis of temperature distribution, the atmosphere can be divided into several layers (Fig. 13.2): *troposphere*, *stratosphere*, *mesosphere*, and *thermosphere*. The troposphere

Introduction to Geochemistry: Principles and Applications, First Edition. Kula C. Misra.

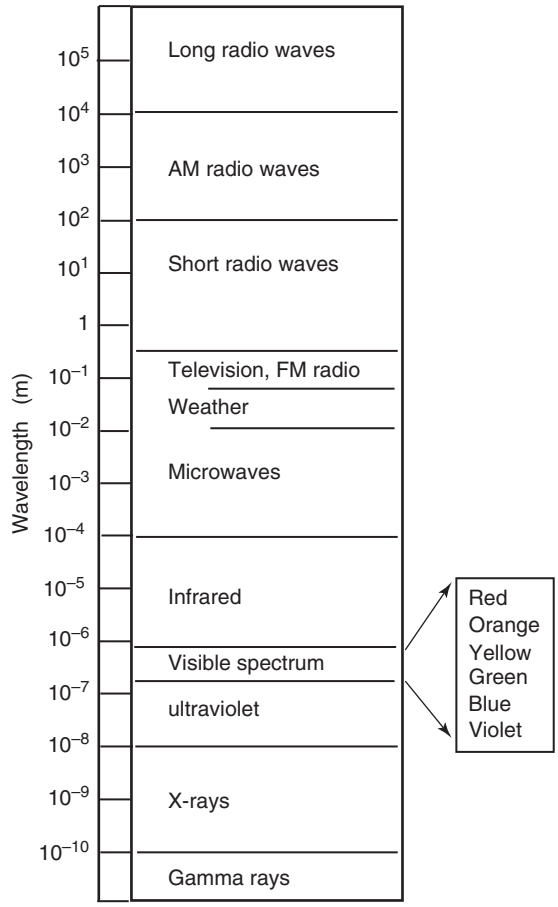

Fig. 13.1 The electromagnetic spectrum. 1 m = 10^6 μm.

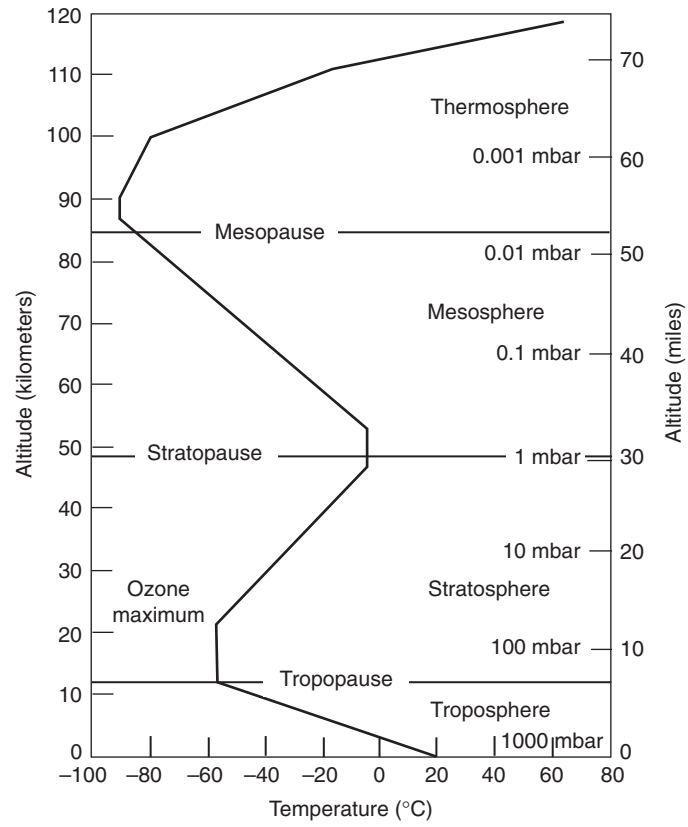

Fig. 13.2 Layers of the Earth's atmosphere based on temperature distribution. Also shown is the exponential decrease in the atmospheric pressure in millibars (mbar) with increasing altitude. Source: http://www.srh.noaa.gov/srh/jetstream/atmos/atmprofile.htm.

Table 13.1 Major absorbers of ultraviolet (UV) radiation in the Earth's atmosphere.

Radiation	Wavelength (μm)	Dominant absorbers	Location of absorption
Far-UV	0.01–0.25	N_2 (g)	Thermosphere, mesosphere
		O_2 (g)	Thermosphere, mesosphere, stratosphere
Near-UV			
UV-C	0.25–0.29	O_3 (g)	Stratosphere
UV-B	0.29–0.32	O_3 (g)	Stratosphere, troposphere
		Particulates	Polluted troposphere
UV-A	0.32–0.38	NO_2 (g)	Polluted atmosphere
		Particulates	Polluted troposphere

1μm (micrometer) = 10^{-6}m (meter). Source of data: Jacobson (2002)

("tropos"=turning), the lowest layer of the atmosphere, extends to between 7 km at the poles and 17 km at the equator, with an average thickness of 11 km. It has a great deal of vertical mixing by convection due to solar heating, and its temperature decreases with increasing elevation because it is heated by radiation reflected back from the Earth's surface. The troposphere contains about 80–90% of the mass of the atmosphere and almost all of the water vapor in the atmosphere (≤4% H_2O); this is the layer where most of the phenomena that we call weather (clouds, rain, snow, storms) occur. The boundary between the troposphere and the stratosphere, the layer above, is called the *tropopause*.

The stratosphere ("stratos" = layered) extends to about 50 km altitude. It contains the "*ozone layer*," which provides a protective shield from the Sun's ultraviolet rays. At its peak concentration in the stratosphere, around an altitude of 20–25 km, the ozone (O_3) density is typically about 5×10^{12} molecules cm^{-3}, which translates to a concentration of only a few parts per million (see Box 13.1). Temperature increases with elevation within the stratosphere because the ozone absorbs solar ultraviolet radiation and then emits it as infrared (heat) radiation. The pressure at the upper boundary of the staratosphere, the *stratopause*, is 1/1000th of that at sea level.

The mesosphere ("meso" = middle) extends to an altitude of about 80–85 km. This is the zone where most meteors burn up

Box 13.1 Mixing ratio

The abundance of a gas in air is commonly expressed as the *mixing ratio by volume*, the fraction of the volume of air occupied by the gas. For example, a mixing ratio of 10 parts per million by volume (ppmv) in air means 10 units of volume of the gas in 106 units of volume of air. This is a convenient way of expressing the abundance of a gas (e.g., a gaseous pollutant in the atmosphere) because we know from the ideal gas equation that volumes occupied by different ideal gases at the same temperature and pressure are proportional to the numbers of molecules of the gases.

(1) *Conversion of parts per million by volume (ppmv) to number of molecules.*
Assuming ideal behavior, the number of molecules per unit volume of any gas, the so-called *Loschmidt's number* (n_0), can be obtained from the ideal gas equation written as (Hobbs, 2000):

$$P = n_0\, k\, T \tag{13.1}$$

where P is the pressure of the gas in pascals, n_0 the number of molecules per air, k the Boltzman's constant = 1.381×10^{-23} J deg^{-1} molecule^{-1}, and T the temperature in Kelvin. At P = 1 atm = 1013×102 Pa, and T = 273.15 K,

$$n_0 = \frac{P}{kT} = \frac{1013 \times 10^2}{(1.381 \times 10^{-23})\,(273.15)} = 2.69 \times 10^{25} \text{ molecules m}^{-3}$$

Suppose that air contains a gaseous species i with a mixing ratio of C_i (ppmv). Since the volumes occupied by gases at the same temperature and pressure are proportional to the number of molecules in the gases,

$$\frac{\text{no. of molecules of } i \text{ in 1 m}^3 \text{ air}}{\text{no. of molecules in 1 m}^3 \text{ air } (= n_0)} = \frac{\text{volume occupied by molecules of } i \text{ in air}}{\text{volume occupied by air}} = C_i$$

So, the number of molecules of i in 1 m^3 air at 273.15 K and 1 atm = C_i (ppmv) n_0

For example, the mixing ratio of methane in dry air is 1.79 ppmv.
Applying the above equation, the number of molecules of methane in 1 m^3 air at 1 atm and 273 K

$= 1.79$ (ppmv) $\times\, n_0 = 1.79 \times 2.69 \times 10^{25} \approx 5 \times 10^{25}$ molecules

Let us also calculate the partial pressure exerted by atmospheric methane, P_{methane}.

C_i (ppmv) = mole fraction of methane in air = 1.79
So, $P_{\text{methane}} = P_{\text{total}} \times C_i = 1 \times 1.79 \times 10^{-6} = 1.79 \times 10^{-6}$ atm.

(2) *Conversion of parts per million by volume (ppmv) to μg m^{-3}.*
At 1 atm pressure and T (K) temperature, the relationship between ppmv and the concentration expressed as μg m^{-3} (micrograms of a gas species per cubic meter of air) is:

$$\mu\text{g m}^{-3} = \frac{\text{(ppmv) (12,187) (molecular mass of the gas species)}}{T\ (\text{K})} \tag{13.2}$$

For example, a mixing ratio of 10×10^{-3} ppmv of the pollutant SO_2 in air at 1 atm and 25°C

$$= \frac{\text{(ppmv) (12,187) (molecular mass of SO}_2\text{)}}{(273.15 + 25)}$$

$$= \frac{(10 \times 10^{-3})\,(12{,}187)\,(64.06)}{298.15} = 26.18\ \mu\text{g m}^{-3}$$

upon entering the atmosphere. In the absence of ozone, there is no source of internal heating, and the temperature decreases with elevation in this layer, and reaches a minimum of around –100°C at the *mesopause*, the upper boundary of mesosphere and the coldest place on the Earth.

Temperature increases with height in the thermosphere from the mesopause to the *thermopause*, the upper boundary of the thermosphere, and may rise to as much as 1500°C. The height of the thermosphere varies with solar activity and may extend up to about 800 km. The International Space Station orbits in the thermosphere, between 320 and 380 km. The heat generated by the absorption of very energetic UV radiation ($\lambda < 0.12\,\mu$m) above approximately 100 km altitude by atoms and molecules of oxygen and nitrogen is the cause of high temperatures in the thermosphere. For example, the UV radiation ionizes oxygen molecules (O_2 + UV photon ⇒ $O_2^+ + e^-$), but many of the released electrons can recombine with the oxygen ions producing a large amount of heat energy ($O_2^+ + e^- \Rightarrow O + O$ + heat energy). The UV radiation with wavelengths in the 0.12–0.30 μm range is absorbed mainly in the mesosphere and stratosphere by molecular oxygen (O_2) and ozone (O_3); nitrogen gas (N_2) is not an effective absorber of these wavelengths. The UV radiation with larger wavelengths ($\lambda > 0.30\,\mu$m) penetrates into the troposphere. The very outermost fringes of the

atmosphere (from 500–1000 km up to 10,000 km), where the gas is so tenuous that collisions between molecules become infrequent, is called the *exosphere*.

The temperature-based atmospheric layers overlap with those based on other characteristics. For example, the *ionosphere*, the part of the atmosphere that is ionized by solar radiation and influences propagation of radio waves to distant places, includes parts of both the mesosphere and the thermosphere.

The atmospheric pressure at any location is a direct consequence of the weight of the overlying air column at that location. The pressure varies with location and time. The average pressure on the Earth's surface is 14.356 lbs per square inch (psi), which is about 2.5% lower than the standard definition of one atmosphere (atm) pressure (14.696 psi or 101.325 kPa) and corresponds to the mean pressure not at sea level but at the mean base of the atmosphere as contoured by the Earth's terrain. The pressure decreases exponentially with increasing altitude (Fig. 13.2), by about a factor of 10 for every 16 km increase in altitude (the *barometric law*). The rapid drop in atmospheric pressure with increasing altitude is the reason why a supplemental supply of oxygen is necessary for climbing very high mountains such as Mount Everest (8.8 km elevation) and why passenger jets (which commonly fly at an altitude of about 10 km) need to have pressurized cabins.

13.1.2 Photochemical reactions in the atmosphere

A *photochemical reaction* is a reaction driven by the interaction of a *photon* of electromagnetic radiation of appropriate wavelength and a molecule, and *photolysis* (or *photodissociation*) refers to the dissociation of a molecule by a photochemical reaction. A photon is the smallest discrete amount of energy that can be transported by an electromagnetic wave of a given frequency. Whether a molecule can be involved in a photochemical reaction depends on the probability of the molecule absorbing a photon of sufficient energy to cause its dissociation.

Photochemical reactions play a key role in many aspects of atmospheric chemistry. An important aspect of such reactions is the production of *free radicals*. A free radical (also referred to simply as *radical*) is an atom or a group of atoms containing an unpaired electron in an outer shell. Free radicals are usually very reactive because of the unpaired electron and therefore short-lived. One of the most important reactive species in the atmosphere is the neutral hydroxyl free radical, $OH^{\bullet}$ (not to be confused with the negatively charged hydroxide ion, OH^{-}), which is formed by the following photochemically induced reaction sequence, starting with the photodissociation of ozone:

$$O_{3(g)} + \text{UV photon} \Rightarrow O_{2(g)} + O_{(g)} \tag{13.3}$$

$$O_{(g)} + H_2O_{(g)} \Rightarrow 2OH^{\bullet}_{(g)} \tag{13.4}$$

Many other photochemical reactions (e.g., the breakdown of $NO_{2(g)}$ and $O_{2(g)}$, and photosynthesis) will be discussed in the following sections.

Example 13–1: Calculation of the minimum wavelength of radiation capable of splitting an oxygen molecule into oxygen atoms

The photodissociation reaction for splitting an oxygen molecule is:

$$O_{2(g)} + \text{UV photon} \Rightarrow O_{(g)} + O_{(g)} \quad (\text{endothermic; } \Delta H^{1}_{r,\,298.15} = +498.4\ \text{kJ mol}^{-1})$$

So, the minimum energy required to split 1 mole of oxygen molecules = 498.4 kJ mol^{-1}

The minimum energy required per molecule of oxygen (E)

$$= \frac{498.4\ \text{kJ mol}}{\text{Avogadro's number}} = \frac{498.4\ \text{kJ mol}^{-1}}{6.022\times10^{23}\ \text{molecules mol}^{-1}}$$
$$= 8.276\times10^{-19}\ \text{J molecule}^{-1}$$

The relationship between E and the wavelength of the emitted radiation (λ) is given by the famous Einstein equation (see equation 2.7),

$$\lambda = \frac{hc}{E} \tag{13.5}$$

where c = speed of electromagnetic waves, and h = Planck's constant = 6.626×10^{-34} J s. Substituting the values of E, c, and h,

$$\lambda = \frac{hc}{E} = \frac{(6.626\times10^{-34}\ \text{J s})\,(2.998\times10^{8}\ \text{m s}^{-1})}{8.276\times10^{-19}\ \text{J molecule}^{-1}}$$
$$= 2.4002\times10^{-7}\text{m} = 0.240\ \mu\text{m}$$

Thus, the minimum radiation wavelength for splitting an oxygen molecule is 0.240 μm.

13.1.3 The Ozone layer in the stratosphere

Chapman mechanism

The bulk of the atmospheric ozone occurs in the stratosphere, where it is produced mostly by interaction of oxygen with UV radiation. In 1930, British geophysicist Sydney Chapman (1888–1970) proposed a series of photochemical reactions, now called the *Chapman mechanism* (or *Chapman reactions*), for production and destruction of ozone, thus for maintaining a steady-state concentration of ozone gas in the stratosphere. At an altitude of approximately 50 km, solar UV radiation of $\lambda < 0.24\ \mu$m has sufficient energy to dissociate O_2 into two atoms of oxygen ($O_{(g)}$), without ionizing it. Each of the two $O_{(g)}$ atoms then combines with $O_{2(g)}$ to form $O_{3(g)}$. The $O_{3(g)}$ molecule cannot accommodate the energy released by the latter reaction without breaking a bond; so for the $O_{3(g)}$ molecule to be a stable product, the reaction needs a catalyst molecule in the neighborhood to absorb the energy. The catalyst molecule commonly is $O_{2(g)}$ or $N_{2(g)}$ because these two molecules

comprise 99% of the atmosphere. The reactions involved in the production of $O_{3(g)}$ may be represented as follows (Hobbs, 2000; Eby, 2004):

$$O_{2(g)} + \text{UV photon} \Rightarrow O_{(g)} + O_{(g)} \quad (\text{endothermic; } \Delta H^1_{r,298.15} = +498.4\,\text{kJ mol}^{-1}) \qquad (13.6)$$

$$O_{(g)} + O_{2(g)} + M \Rightarrow O_{3(g)} + M \quad (\text{exothermic; } \Delta H^1_{r,298.15} = -106.5\,\text{kJ mol}^{-1}) \qquad (13.7)$$

$$O_{(g)} + O_{2(g)} + M \Rightarrow O_{3(g)} + M \quad (\text{exothermic; } \Delta H^1_{r,298.15} = -106.5\,\text{kJ mol}^{-1}) \qquad (13.8)$$

$$3O_{2(g)} + \text{UV photon} \Rightarrow 2O_{3(g)} \quad (\text{net reaction}) \qquad (13.9)$$

where UV photon refers to solar radiation in the 0.2 to 0.22 μm and 0.185 to 0.2 μm wavelength regions, and M represents a catalytic molecule, usually N_2 or O_2, the predominant species in the stratosphere. Reaction (13.7) also occurs in the troposphere, but the oxygen in this case originates from NO_2 photolysis ($NO_2 + h\nu \Rightarrow NO + O$), not from O_2 photolysis.

Ozone is destroyed naturally in the stratosphere (and also in the troposphere) by *photolysis*, which occurs by absorption of solar radiation in the ~0.230 to 0.320 μm wavelength region, leading to regeneration of O_2:

$$O_{3(g)} + \text{UV photon} \Rightarrow O_{2(g)} + O_{(g)} \quad (\text{endothermic; } \Delta H^1_{r,298.15} = +386.5\,\text{kJ mol}^{-1}) \qquad (13.10)$$

$$O_{(g)} + O_{3(g)} \Rightarrow 2O_{2(g)} \quad (\text{exothermic; } \Delta H^1_{r,298.15} = -391.1\,\text{kJ mol}^{-1}) \qquad (13.11)$$

$$2O_{3(g)} + \text{UV photon} \Rightarrow 3O_{2(g)} \quad (\text{net reaction}) \qquad (13.12)$$

Note that when ozone reacts with atomic oxygen, the ozone is destroyed permanently. On the other hand, every molecule of ozone consumed by UV photon produces an oxygen atom, which is free to combine with another $O_{2(g)}$ molecule and form $O_{3(g)}$. Also, $O_{3(g)}$ can be photolyzed all the way down to the Earth's surface, whereas $O_{2(g)}$ can be photolyzed only above about 20 km altitude. This is because all short-wavelength UV radiation required to split $O_{2(g)}$ is absorbed above this altitude.

Two factors that control the production and destruction of ozone are the availability of high-energy (UV) photons, which decreases towards the Earth's surface, and the density of the atmosphere (i.e., the number of gas molecules per unit volume of the atmosphere), which increases towards the Earth's surface. The optimum combination of these two variables acting in opposite directions occurs at an altitude of approximately 15–35 km (at the equator), the region of the so-called "ozone layer," which contains about 90% of our planet's ozone with peak values of only ~10 ppmv, compared to 0–0.07 ppmv in the unpolluted air near the Earth's surface. The maximum ozone concentration is predicted and found at an altitude of approximately 23 km; the maximum altitude varies with time of year and latitude on the Earth (van Loon and Duffy, 2000). The ozone in a given air parcel in the ozone layer is being continuously destroyed by photolysis (equation 13.12) when the parcel is in sunlight, but from the perspective of Chapman reactions the ozone concentration should stay fairly constant over time scales of weeks to months because of regeneration of ozone (equation 13.9) at almost the same rate.

Other reactions for Ozone destruction

Calculations based only on the Chapman oxygen–ozone cycle ($3O_{2(g)} \Rightarrow 2O_{3(g)} \Rightarrow 3O_{2(g)}$) generate the observed vertical profile for $O_{3(g)}$, with the peak $O_{3(g)}$ concentration at the expected altitude, but the predicted concentrations are too high compared with the measured values. This is because there are other pathways that destroy ozone. Most of the catalytic reactions that have been proposed for the removal of stratospheric ozone are of the form

$$X_{(g)} + O_{3(g)} \Rightarrow XO_{(g)} + O_{2(g)} \qquad (13.13)$$

$$XO_{(g)} + O_{(g)} \Rightarrow X + O_{2(g)} \qquad (13.14)$$

$$O_{3(g)} + O_{(g)} \Rightarrow 2O_{2(g)} \text{ (net reaction)} \qquad (13.15)$$

where X represents the catalyst and XO the intermediate product. The important point about such a reaction chain involving a catalyst is that, unless there is an appreciable sink for X, a few molecules of X have the potential to eliminate very large numbers of ozone molecules and atomic oxygen. In anthropologically undisturbed stratosphere, the important catalysts are free radicals of three categories (van Loon and Duffy, 2000): HO_x($H^\bullet$, $OH^\bullet$, $HO_2^\bullet$); NO_x($NO^\bullet$, $NO_2^\bullet$); and ClO_x($Cl^\bullet$, $ClO^\bullet$). Modeling of the ozone chemistry shows that the Chapman mechanism, $NO_{x(g)}$, $HO_{x(g)}$, and $ClO_{x(g)}$ account, respectively, for 20–25%, 31–34%, 16–29%, and 19–20% of O_3 destruction in the stratosphere (Lodders and Fegley, 1998). Let us consider the reactions involving $NO_{(g)}$ (nitric oxide) that dominates in the lower stratosphere and those involving OH that dominates in the upper atmosphere. The destruction of ozone by $ClO_{x(g)}$ is discussed in section 13.3.1.

The major sources of $NO_{(g)}$ in the troposphere are emissions from combustion of fossil fuels and synthesis from atmospheric $O_{2(g)}$ and $N_{2(g)}$ by lightning, and the major sources of $NO_{(g)}$ in the stratosphere are transport from the troposphere and the breakdown of $N_2O_{(g)}$ (nitrus oxide; laughing gas), which is emitted during denitrification by anaerobic bacteria in soils, by bacteria in fertilizers and sewage, and during biomass burning, automobile combustion, and combustion of aircraft fuel. The $N_2O_{(g)}$ molecule is not a free radical; it is a stable species with a tropospheric residence time estimated to be 160 yr. The principal mechanism for its removal from the

troposphere is by migration into the stratosphere where it is converted into $NO^{\bullet}_{(g)}$ by reaction with excited-state oxygen:

$$N_2O_{(g)} + O^{*}_{(g)} \Rightarrow NO^{\bullet}_{(g)} + NO^{\bullet}_{(g)} \quad (13.16)$$

Then, $NO^{\bullet}_{(g)}$ catalyzes the destruction of $O_{3(g)}$:

$$NO^{\bullet}_{(g)} + O_{3(g)} \Rightarrow NO^{\bullet}_{2(g)} + O_{2(g)} \quad (13.17)$$

$$NO^{\bullet}_{2(g)} + O_{(g)} \Rightarrow NO^{\bullet}_{(g)} + O_{2(g)} \quad (13.18)$$

$$O_{3(g)} + O_{(g)} \Rightarrow 2O_{2(g)} \text{ (net reaction)} \quad (13.19)$$

It has been estimated that in the upper atmosphere ~10^5 molecules of O_3 are destroyed before one molecule of $NO_{x(g)}$ is removed from this catalytic ozone destruction cycle; the chain length decreases to ~10 in the lower stratosphere (Jacobson, 2002). Tropospheric $NO^{\bullet}_{2(g)}$ is unlikely to be transferred into the stratosphere because it is readily removed as HNO_3 by $OH^{\bullet}$ ($NO^{\bullet}_{2(g)} + OH^{\bullet}_{(g)} \Rightarrow HNO_{3(g)}$).

Ozone destruction by the highly reactive $OH^{\bullet}$ (which is produced in the stratosphere by the reaction of $O^{*}_{(g)}$ with $H_2O_{(g)}$, $CH_{4(g)}$, and $H_{2(g)}$) involves the free radical $HO^{\bullet}_{2(g)}$ (hydroperoxy radical) as an intermediate product, and can be represented by reactions such as:

$$OH^{\bullet}_{(g)} + O_{3(g)} \Rightarrow O_{2(g)} + HO^{\bullet}_{2(g)} \quad (13.20)$$

$$HO^{\bullet}_{2(g)} + O_{3(g)} \Rightarrow OH^{\bullet}_{(g)} + 2O_{2(g)} \quad (13.21)$$

$$O_{3\,(g)} + O \Rightarrow 2O_{2\,(g)} \text{ (net reaction)} \quad (13.22)$$

As will be discussed later (see section 13.3.1), stratospheric ozone loss has been enhanced in recent years by the anthropogenic infusion of chlorofluorocarbon (CFC) compounds.

13.1.4 Composition of the atmosphere

Approximately 99.9% (by volume) of the Earth's atmosphere is accounted for by nitrogen (78.1%), oxygen (20.9%), and argon (0.9%). There is a nearly uniform mixture of these three gases from the Earth's surface up to ~80 km altitude (including the troposphere, stratosphere, and mesosphere) because turbulent mixing dominates over molecular diffusion at these altitudes. Abundant atmospheric O_2 distinguishes the Earth from all other planets in the solar system. A number of other gaseous species, with concentration levels in parts per million (ppm) to parts per trillion (ppt), make up the rest 0.1% of the atmosphere (Table 13.2).

The composition of the atmosphere reflects a balance among volcanic activity, sedimentation, and life processes, but are the atmospheric gases in thermodynamic equilibrium? We can answer this question by checking if the partial pressures of gases in the atmosphere are consistent with the partial pressures they should have in a system in equilibrium. Let us consider the reaction that links CO_2 and CH_4 in the atmosphere and assume that the gases behave ideally:

$$CH_{4(g)} + 2O_{2(g)} \Leftrightarrow CO_{2(g)} + 2H_2O_{(g)}\ ; \qquad K_{eq} = \frac{P_{CO_2}\ (P_{H_2O})^2}{P_{CH_4}\ (P_{O_2})^2} \quad (13.23)$$

Table 13.2 Average composition of the Earth's unpolluted lower atmosphere (up to an altitude of 25 km).

Gas	Volume%	Source	Estimated residence time
N_2	78.084	Biologic	10^6–10^7 yr
O_2	20.946	Biologic	3000–10,000 yr
Ar	0.934	Radiogenic	Forever
CO_2	0.0383	Biologic, geologic, anthropogenic	2–10 yr
Ne	0.00182	Earth's interior	Forever
He	0.000524	Radiogenic	~10^6 yr
CH_4	0.00017	Biologic, geologic, anthropogenic	2–10 yr
Kr	0.000114	Radiogenic	Forever
H_2	0.000055	Biologic, chemical	4–8 yr
N_2O	0.00003	Biologic, anthropogenic	5–200 yr
Xe	0.000009	Radiogenic	Forever
NO_2	0.0000002	Biologic, anthropogenic	0.5–2 days
O_3	0 to 0.000007	Chemical	100 days

Water vapor (H_2O) is ~0.40% by volume for the whole atmosphere, typically 1 to 4% near the surface. Other species present in the atmosphere at parts per trillion level concentrations include: NO, SO_2, CO, NH_3, H_2S, CS_2, (carbonyl sulfide), CH_3SCH_3 (dimethyl sulfide), methyl chloride (CH_3Cl), methyl bromide (CH_3Br), methyl iodide (CH_3I), hydrogen chloride, CCl_3F (CFC-11 Freon), CCl_2F_2 (CFC-12 Freon), and carbon tetrachloride (CCl_4).

Sources of data: Hobbs (2000); Railsback (2006).

Box 13.2 Residence time of a substance in a reservoir

The *(mean) residence time* (or *mean lifetime*) of a substance (i) in a specified reservoir is defined as the ratio of the mass of the substance in the reservoir (M_i) to either input flux (F_{in}) or the output flux (F_{out}), expressed in terms of mass per unit time, at steady state:

$$\text{Residence time } (\tau) = \frac{M_i}{F_{in} \text{ (or } F_{out})} \tag{13.24}$$

In a steady-state system, the reservoir concentration or mass of a substance does not change with time, so that $F_{in} = F_{out}$, and we can use either of the fluxes to calculate the residence time.

For purpose of illustration, let us calculate the residence time of H_2O in the atmosphere from the following data: amount of H_2O in the atmosphere = 0.13×10^7 kg; amount of H_2O added by evaporation to the atmosphere per year = 4.49 kg (0.63×10^{17} kg from lakes and rivers + 3.86×10^{17} kg from the oceans).

The average residence time of H_2O in the atmosphere

$$= \frac{M_{H_2O}}{F_{in}} = \frac{0.13 \times 10^{17} \text{kg}}{4.49 \times 10^{17} \text{kg yr}^{-1}} = 0.029 \text{ yr} = 10.6 \text{ days}$$

Thus, the average lifetime of a H_2O molecule in the atmosphere, assuming that it is well mixed and in a steady state with respect to H_2O, is about 11 days only!

What is the residence time of H_2O in the oceans? The rivers supply approximately 36×10^3 km^3 of H_2O per year and the volume of the ocean basins is approximately 1350×10^6 km^3. Thus, the average residence time of H_2O in the oceans (or the time that would be taken to "fill" the ocean basins)

$$= \frac{1350 \times 10^6 \text{ km}^3}{36 \times 10^3 \text{ km}^3} = 37{,}500 \text{ yr}$$

The average residence times of dissolved constituents in the oceans vary from millions of years for the highly soluble species (e.g., Na) to approximately 100,000 yr for a soluble but highly bioactive element such as P that is intensely cycled by marine organisms, to a few hundred years or less for relatively insoluble elements such as the REEs. Substances with long residence times can accumulate to relatively high concentrations in a reservoir compared with those with shorter residence times. However, highly reactive substances, even with short residence times, can yield products that cause environmental problems. Residence time is a useful concept because it enables us to evaluate how long a reservoir would take to recover if its chemistry was perturbed, for example, by the addition of a pollutant.

What happens when we perturb a steady-state system, for example, by changing the output flux? Assuming a first-order kinetic model (i.e., the change in the amount of i with time, dM_i/dt, is proportional to its original mass in the reservoir), the integrated rate equation can be written as

$$[M_i]_t = [M_i]_0 \, e^{-kt} \tag{13.25}$$

where k is the rate constant, and $(M_i)_0$ and $(M_i)_t$ denote the amounts of i in the reservoir at time $t = 0$ and some specified time t, respectively. Note that in this model the new steady state for a particular reservoir is approached exponentially.

From the free energy of formation data for the various species (Appendix 5), the equilibrium constant (K_{eq}) for this reaction can be calculated as ~10^{140}, indicating that CH_4 should oxidize readily to CO_2. We can calculate the equilibrium concentration of CH_4 from the concentrations (in vol%) of the other gases in the atmosphere (Table 13.2): O_2 = 20.95%; CO_2 = 0.0383%; and H_2O = 0.4%. Assuming that the volume fractions of these gases are approximately equal to their partial pressures,

$$P_{CH_4} = \frac{P_{CO_2} (P_{H_2O})^2}{K_{eq} (P_{O_2})^2} = \frac{(3.83 \times 10^{-4})(4 \times 10^{-3})^2}{10^{140} (0.2095)^2}$$
$$= \frac{(15.32)(10^{-4})(10^{-6})}{(10^{140})(0.0439)}$$
$$= 349 \times 10^{-10} \times 10^{-140} = 3.5 \times 10^{-148} \text{ atm}$$

Thus, the calculated equilibrium concentration of CH_4 is orders of magnitude less than its actual concentration in the atmosphere (1.7×10^{-6} atm), indicating that the atmospheric gas mixture is not in thermodynamic equilibrium. Most of the gases in the atmosphere are in a *steady state* (i.e., the input of each such gas into the atmosphere is balanced by its output into other reservoirs) with *residence times* (see Box 13.2) ranging from 1–10 Myr for oxygen to a few days or less for some trace constituents (Table 13.2).

Chemical reactions among gaseous species in the atmosphere are dominated by intermolecular collisions, and many are catalyzed by aerosol particles. An *aerosol* is a suspension of fine solid particles and/or liquid droplets in a gas (the term "sol" evolved to differentiate suspensions from solutes in a liquid solution). Examples are smoke, haze over the oceans, volcanic emissions, and smog. Natural aerosol particles

include mineral dust released from the surface, sea salt, biogenic emissions from the land and oceans, and dust particles in volcanic eruptions, but dust in the atmosphere has increased significantly due to human activities such as surface mining and industrial processes. Atmospheric aerosol particles that stay aloft for a while (by Brownian motion) are mostly in the 0.2–2 μm size range, and they serve as nuclei for condensation of water vapor to droplets of water (cloud particles). High concentrations of aerosol particles, most of which are large enough to cause incoherent scattering of visible light, produce a haze in the atmosphere, limiting visibility. Aerosol particles also play a critical role in the formation of smog (see section 13.3.2).

13.2 Evolution of the Earth's atmosphere over geologic time

13.2.1 Origin of the atmosphere

The origin of the terrestrial atmosphere is one of the most puzzling enigmas in the planetary sciences. The Earth probably had a *primary (*or *primordial) atmosphere*, comprised of gases captured gravitationally from the solar nebula. This *solar-type atmosphere*, if it existed, must have been composed, like the Sun itself, of hydrogen and helium. However, marked depletion of the present terrestrial atmosphere in noble gases, by factors of ~10^{-4} to 10^{-11} compared with their abundances in the solar nebula suggests that the solar-type atmosphere dissipated, probably almost completely, when the Solar System was ≤ 1 Myr old (Walker, 1977; Zahnle, 2006).

The Earth's primordial atmosphere was replaced within ~100 Myr by a *secondary atmosphere* (Walker, 1977). Earlier, it was believed that most of the Earth's volatiles were trapped originally in the cold interior of the planet during accretion, and the atmosphere accumulated subsequently when heating of the Earth's interior by radioctive decay gradually released the volatiles through volcanic degassing. More recent models of planetary accretion advocate that the secondary atmosphere formed by shock release and vaporization of chemically bound volatiles contained in the accreting planetesimals. Both qualitatively and quantitatively, the most important of the impact-induced degassed volatiles probably was water vapor. Much of the water accreted by the Earth probably existed in the form of hydrous silicates or was adsorbed onto the dust grains in planetesimals, and entered directly into the atmosphere due to degassing of planetesimals by impact erosion, mainly by dehydration of hydrous silicate minerals (see section 13. 5.1).

Transient steam atmosphere

According to Abe *et al.* (2000), the formation of a transient steam atmosphere started when the mass of the proto-Earth had reached about 0.01 $M_\oplus$ ($M_\oplus$ = Earth mass = 5.97 × 10^{24} kg). Hydrogen likely was a major constituent of such an atmosphere as a consequence of reduction of H_2O by infalling, metallic iron-rich planetesimals (Kasting, 1993). Indirect evidence for the presence of a H_2-rich steam atmosphere is provided by the isotopic composition of noble gases in the atmosphere, some of which appear to have been mass fractionated by the drag created by rapid, hydrodynamic escape of H_2, which carried off the lighter isotopes more easily than the heavy ones. This is believed to be the best explanation for the higher ^{22}Ne:^{20} Ne ratio in the atmosphere than both in the solar wind and the mantle (Zahnle *et al.*, 1988). Xenon ($^{131}_{54}Xe$) is the exception to this trend. Xenon ($^{131}_{54}$ Xe) is depleted in the terrestrial atmosphere by a factor of 4.8×10^4 relative to solar composition, whereas krypton ($^{84}_{36}Kr$) is depleted by a factor of only 3.3×10^4. Also, Xe isotopes are fractionated by 38% amu relative to solar, whereas Kr isotopes are fractionated by only 7.6% amu. This so-called "missing xenon paradox" – the greater depletion and fractionation of the heavier xenon compared to the lighter krypton in the atmosphere, although the abundances of Kr and Xe in the meteorites are about the same – has been attributed by Dauphas (2003) to the terrerstrial atmosphere being formed by contribution from two sources: fractionated nebular gases, and accreted cometary volatiles having low Xe : Kr ratio and unfractionated isotope ratios.

The evolution of an impact-generated steam atmosphere surrounding the accreting Earth, assuming no remnants of the primordial atmosphere, no explosive removal of a portion of the proto-atmosphere by a large impact, and an average of 0.1 wt% H_2O in the accreting planetesimals has been modeled by Matsui and Abe (1986a,b). The surface temperature of an accreting planet depends on the mass and composition of its atmosphere, and the average heat flux from the planet. The latter corresponds to the sum of the net solar flux and, more importantly, gravitational energy flux released from the surface due to accretion. Water vapor plays a key role in controlling the Earth's surface temperature because its strong absorption bands for infrared radiation prevent the impact energy (heat) from escaping into interplanetary space. When the radius of the planet exceeded 40% of its final radius, the blanketing by water vapor (roughly 100 bar), perhaps with some contribution from radioactive decay of short-lived nuclides, would foster surface temperatures high enough to melt the outer portion of the planet and form a magma ocean containing a predictable amount of dissolved H_2O.

Once a surface magma ocean has formed, the mass of the steam atmosphere and the surface temperature and pressure (estimated to have been about 1500 K and 100 bar) would not vary much during further accretion (Matsui and Abe, 1986a). This is because an increase in the surface temperature would increase the degree of melting, thus increasing the size of the magma ocean and causing more H_2O from the atmosphere to be dissolved in it. A decrease in the H_2O content of the atmosphere would decrease the efficiency of the blanketing effect, thereby decreasing the surface temperature, which would then allow the surface to re-solidify and increase the H_2O in the

atmosphere because of outgassing. The exchange of H_2O between the atmosphere and the magma ocean would maintain the abundance of H_2O in the atmosphere just above the critical level required for sustaining a surface magma ocean (Abe *et al*., 2000).

The mass of H_2O left in the proto-atmosphere would be limited by the solubility of H_2O in the silicate melt (which predominantly is a function of temperature), and be practically independent of the H_2O content of the source planetesimals. Considering that the solubility of H_2O in silicate melt is ~1 wt% (under a 100 bar steam atmosphere), comparable to or greater than the concentration of H_2O in the source materials (estimated to be ~0.1 to 1 wt%), almost all of the H_2O would dissolve in the magma ocean. On the basis of thermal evolution models of the growing Earth, Matsui and Abe (1986a,b) predicted that the maximum final mass of H_2O in an impact-generated proto-atmosphere at the end of accretion would be ~10^{21} kg, corresponding to a pressure of ~3×10^7 Pa (or ~3×10^2 bar), which is rather insensitive to variations in the input parameters. They considered the apparent coincidence of the H_2O abundance in the proto-atmosphere with the present mass of the Earth's oceans (~1.4×10^{21} kg) as evidence for an impact origin of the atmosphere and hydrosphere.

Eventually, the sum of accretional and solar heating would drop below the runaway greenhouse threshold, and the steam in the atmosphere would condense and rain out to form a hot proto-ocean of liquid water on the Earth's surface. The average temperature of this ocean, as estimated from oxygen isotope ratios of Archean metasedimentary rocks, would be ~600 K (Matsui and Abe, 1986b). The remaining atmosphere would be dominated by carbon and nitrogen compounds, mainly CO_2, CO, and N_2. The partial pressure of CO_2 in this atmosphere would be 60 to 80 bar if all of the crustal carbon (estimated at ~10^{23} g) were present in the atmosphere as CO_2, or ~10 bar if only about 15% of this carbon resided in the atmosphere before continents began to grow and carbonate rocks began to accumulate (Kasting, 1993). Modeling by Liu (2004) concluded that after accretion and solidification of a "magma ocean," the proto-atmosphere of the Earth would be composed of 560 bar of H_2O and 100 bar of CO_2, and oceans would start to grow when the temperature of the Earth cooled to below approximately 300–450°C.

Venus, which is comparable in size and mass to the Earth, should also have developed an impact-induced proto-atmosphere with approximately the same mass of H_2O. However, whereas H_2O in the Earth's proto-atmosphere could condense to form a hot ocean, it remained in gaseous state in the proto-Venusian atmosphere. The blanketing by atmospheric CO_2 probably resulted in a runaway greenhouse effect on Venus. Oceans did not form or could not stay around because water was converted to water vapor, the increased water vapor in the atmosphere enhanced the greenhouse effect, which in turn caused a further rise of temperature and more evaporation of water, and so on. A possible explanation for the strongly fractionated D : H ratio of the Venusian atmosphere is the photodissociation of H_2O into hydrogen and oxygen by solar UV radiation, and subsequent preferential escape of H_2 to space through a hydrodynamic process (Matsui and Abe, 1986b; Drake, 2005).

In the later stage of accretion, evolution of the atmosphere would depend on the model of accretion envisaged. If the accreting planetesimals remained small, a hot atmosphere and magma ocean would be sustained. On the other hand, any intermittent impact by a large planetesimal (or proto-planet) would likely repeat the steamy atmosphere–magma ocean–water ocean sequence. It is quite conceivable that the ocean was successfully vaporized and rained out with each major impact during the final stages of accretion.

Effect of the Moon-forming giant impact

The effect of the Moon-forming giant impact on the Earth's pre-existing volatiles inventory is not fully resolved. Ahrens (1993) suggested that the preexisting atmosphere was blown off completely by the impact, whereas Peppin and Porcelli (2002) argue that retention of a fraction of the primary, pre-impact atmosphere is an important reqirement for explaining the present abundance and isotopic composition of Xe in the Earth's atmosphere. It is generally agreed that the volatiles were lost from the side of the Earth that was impacted. The loss of volatiles from the other side would depend on whether there was a deep liquid-water ocean on the surface. Model calculations by Genda and Abe (2005) suggest that for a given impact, the fraction of atmosphere lost from a protoplanet covered with a liquid-water ocean would always be larger than that from one without such an ocean, and the loss would increase with decreasing value of R_{mass} (R_{mass} = atmospheric mass/ocean mass). A thin atmosphere above a thick water ocean would be largely expelled, otherwise the atmosphere would be retained. In either case, the entire liquid-water ocean would survive the impact and the water would be retained (Zahnle, 2006, p. 220).

The Moon-forming giant impact melted most of the mantle, forming a deep magma ocean, and vaporized some of the mantle (Canup, 2004), forming an atmosphere of mostly rock vapor topped by ~2500 K silicate clouds (Ahrens, 1993; Peppin and Porcelli, 2002; Zahnle, 2006). The rock vapor condensed into silicates and rained out at a rate of about 1 m per day, and the volatiles became increasingly important constituents of the atmosphere. Much of the Earth's water remained at first in the molten mantle, which later degassed as the mantle froze. By the end of the main accretionary and core-forming events, the residual atmosphere was dominated by a steamy mixture of N_2, CO_2, and H_2O. It also contained minor amounts of reducing gases such as CO and H_2, and trace amounts of noble gases (Des Marais, 1994; Zahnle, 2006). The Earth's surface temperature would depend on how much CO_2 was present and for how long. Model calculations suggest that, as long as most of the Earth's CO_2 remained in the atmosphere, the surface temperature would have been

~500 K. However if carbonates, the main sink of CO_2 in the pre-biotic Hadean eon, could subduct into the mantle, it could have taken as little as 10 Myr to remove 100 bar of CO_2 from the proto-atmosphere (Zahnle, 2006). The surface heat flux dwindled at the end of the Earth's main accretionary phase, and the steam atmosphere rained out to form an ocean. By this account, water has been on the Earth's surface almost from the beginning. Mantle temperatures in the Hadean eon were much higher than today due to greater concentration of radioactive elements and due to thermal energy released during the impact of accretionary bodies. As a result, the Hadean mantle was drier than its modern counterpart, and most of the Earth's water eventually became trapped in the oceans. As we will elaborate later (section 13.5.1), it is unlikely that any known source could have delivered an ocean of water to the Earth after the Moon-forming impact.

The lunar impact-cratering record indicates that the Earth–Moon system continued to be bombarded by large impactors (> 100-km in diameter) until at least 3.8 Ga, and it is likely that the atmosphere gained some H_2O, CO, and NO during this "heavy bombardment period" (4.5–3.8 Ga) if some of the impactors were of cometary or carbonaceous chondritic composition (Chyba, 1987; Kasting, 1993). CO would have been produced by reduction of ambient, atmospheric CO_2 by iron-rich impactors or by oxidation of organic carbon in carbonaceous impactors. NO gas would have been generated by shock heating of atmospheric CO_2 and N_2. The atmosphere during the Hadean eon (4.6–3.8 Ga), however, was essentially devoid of free (molecular) oxygen.

13.2.2 *A warm Archean Earth: the roles of carbon dioxide and methane*

Except for the absence of O_2 and the presence of elevated levels of greenhouse gases such as CO_2 or CH_4, the atmosphere at the beginning of the Archean probably was not very different from what it is now. CH_4 would be a better choice if the Archean was biologically productive, whereas CO_2 would be the better choice if the Earth was lifeless or nearly so (Zahnle, 2006). The Sun's luminosity has been increasing at the rate of ~5% per billion years as a consequence of the gradual conversion of hydrogen into helium inside the Sun's core. The much lower solar luminosity at 4.6 Ga, estimated to be only ~30% of that at present should have caused the Earth's mean surface temperatures to dip below the freezing point of water, resulting in widespread glaciation. The earliest firm evidence for continental glaciation in North America (the *Huronian glaciation* event in eastern Canada) is found in rocks that are 2.2–2.5 Gyr old; the age of the oldest glaciation event, however, may be ~2.9 Ga as recorded in the Archean Mozaan Group of South Africa (Young *et al.*, 1998). The other well-documented Proterozoic glacial period, which actually consists of a series of glacial episodes of global extent and is collectively termed the *Late Precambrian glaciations*, lasted from about 0.8 to 0.6 Ga. The lack of glaciation on the Earth for more than 1.5 Gyr after its birth is credited by most modelers to a much higher partial pressure of the greenhouse gas CO_2, estimated to have been 1–10 bar at 4.5 Ga and decreasing to 0.03–0.3 bar around 2.5 Ga. Mean surface temperature of an atmosphere so rich in CO_2 would be ~85°C, high enough to prevent a very cold Earth in spite of relatively low solar luminosity at that time (Kasting, 1987, 1993; Zahnle, 2006).

Catling *et al.* (2001) cited several reasons why high P_{CO_2} during the Archean is not the most likely solution to the "faint young Sun (FYS) problem," although CO_2 probably played a contributory role. Rye *et al.* (1995) reported that iron lost from the tops of >2.5-Gyr-old paleosol profiles was reprecipitated lower down as silicate minerals, rather than as iron carbonate (siderite), indicating that atmospheric P_{CO_2} must have been $< 10^{-1.4}$ atm, about 100 times today's level of 360 ppm and at least five times lower than that required to compensate for the lower solar luminosity at that time. The mineralogy of the Archean banded iron formations (see Box 13.3) suggests that P_{CO_2} was less than 0.15 bar at 3.5 Ga.

Marine limestones are abundant in the Archean sedimentary record, whereas the opposite should be the case because calcite solubility increases with increasing P_{CO_2} (see Fig. 7.7). Also, there is no evidence for accelerated levels of acid-induced weathering during the Archean that should have resulted from high P_{CO_2}. Catling *et al.* (2001) argued that a relatively high concentration of atmospheric CH_4, not CO_2, was the most likely cause for Archean greenhouse warming. An Archean methanogenic biosphere is suggested also by extremely negative $\delta^{13}C$ values (between –33‰ and –51‰) in a 2.7-Gyr-old paleosol from Western Australia (Rye and Holland, 2000).

It is likely that the Archean Earth contained at least a small amount of CH_4 (1–10 ppmv) formed abiotically from impacts and from serpentinization of ultramafic rocks on the seafloor. At the present time, CH_4 is produced by methanogenic bacteria, most of which metabolize either CO_2 and H_2 from the atmosphere or acetate (represented here as acetic acid) formed from fermentation of photosynthetically produced organic matter:

$$CO_2 + 4H_2 \Rightarrow CH_4 + 2H_2O \quad (13.26)$$

$$CH_3COOH \Rightarrow CH_4 + CO_2 \quad (13.27)$$

Once methanogens appeared, they would have converted most of the available H_2 into CH_4. Photochemical modeling suggests a CH_4 concentration of 1000 ppmv or higher for the Late Archean/Paleoproterozoic atmosphere prior to the drastic rise of O_2 around 2.3 Ga (Kasting, 2005). The surface temperature resulting from such high levels of atmospheric CH_4 would have been enough to prevent a global-scale glaciation. Model-based calculations have shown that an increase in CH_4 from the present-day 1.7 ppmv to 100 ppmv would result in a 12 K increase in surface temperature from 283 to 295 K (Pavlov *et al.*, 2003).

The rise of O_2 around 2.3 Ga (see section 13.2.4) eliminated most of the methane ($CH_4 + O_2 \Rightarrow CO_2 + 2H_2$; $CH_4 + OH\bullet \Rightarrow CH_3 + H_2O$) and probably triggered glaciation during the Paleoproterozoic. Concentrations of CH_4 may have remained much higher (10–100 ppmv, compared to the present-day level of 1.7 ppmv) throughout much of the Proterozoic as a consequence of low concentrations of dissolved O_2 and sulfate in the deep oceans and a corresponding enhancement of organic matter recycling by fermentation and methanogenesis (Kasting, 2005).

13.2.3 Oxygenation of the atmosphere

The oxidation state of the atmosphere – oxic or anoxic – is a measure of the balance between the sources and sinks of oxygen (Box 13.3). The earliest mechanism of oxygen production in the atmosphere probably was photolysis of water vapor and CO_2 by solar UV radiation, which may be expressed as the following sequence of essentially irreversible reactions:

$$H_2O_{(g)} + \text{UV photon} \Rightarrow H^{\bullet}_{(g)} + OH^{\bullet}_{(g)} \quad (13.28)$$

$$CO_{2(g)} + \text{UV photon} \Rightarrow CO_{(g)} + O_{(g)} \quad (13.29)$$

$$O_{(g)} + OH^{\bullet}_{(g)} \Rightarrow O_{2(g)} + H^{\bullet}_{(g)}(\uparrow) \quad (13.30)$$

The escape of the very light H atoms produced in these reactions to space would result in a net addition of O_2 to the atmosphere; without hydrogen escape H_2O would be re-formed. This process, however, did not contribute much to the build-up of O_2 in the atmosphere. Almost all of the O_2 so produced must have been quickly consumed by chemical weathering (after the formation of continental crust), by oxidation of reduced gases (H_2, CO, and H_2S) from volcanoes by reactions such as

$$2H_2 + O_2 \Rightarrow 2H_2O \quad (13.31)$$

$$2CO + O_2 \Rightarrow 2CO_2 \quad (13.32)$$

and by the formation of iron oxides and hydroxides utilizing the Fe^{2+} derived from seawater–oceanic-basalt interaction. Typical atmospheric O_2 levels at this stage were probably on the order of 10^{-14} PAL (*present atmospheric level* = 0.2 atm) or lower (Kasting *et al.*, 1992).

Under the Earth's early, anoxic atmosphere, before the development of an ozone shield, organisms most likely lived underground or in water to avoid exposure to lethal UV radiation, and relied on the conversion of organic or inorganic material to obtain energy. At some point, certain anaerobic bacteria, called *phototrophs*, developed the ability to obtain energy from sunlight by a new process called *anoxygenic photosynthesis*, a process in which reduced chemical species (such as H_2S and H_2) and sunlight provide energy for synthesis of organic substances from CO_2, while more oxidized sulfur compounds or water (but no O_2) are released as byproducts. Examples of such reactions are:

$$CO_{2(g)} + 2H_2S_{(g)} + \text{sunlight} \Rightarrow CH_2O_{(aq)} + H_2O_{(l)} + 2S \quad (13.34)$$

$$CO_{2(g)} + 2H_{2(g)} + \text{sunlight} \Rightarrow CH_2O_{(aq)} + H_2O_{(l)} \quad (13.35)$$

where $CH_2O_{(aq)}$ represents a generic carbohydrate dissolved in water and S represents elemental sulfur. Evidently, anoxygenic photosynthesis did not contribute to the accumultion of free oxygen in the atmosphere.

A marked increase in O_2 production occurred with the advent of *oxygenic photosynthesis*, when cyanobacteria (green algae) appeared on the Earth. Oxygenic photosynthesis is the process in which an organism uses sunlight, water, and CO_2 to synthesize organic matter (e.g., carbohydrates), releasing O_2 as a waste product:

$$CO_{2(g)} + H_2O_{(l)} + \text{sunlight} \Rightarrow CH_2O\ (\text{carbohydrate}) + O_{2(g)} \quad (13.36)$$

The effective addition of molecular O_2 to the atmosphere by photosynthesis depends on how much of the organic carbon is protected from reoxidation by burial in sediments, and how much of the O_2 is consumed by other oxidative reactions such as chemical weathering and oxidation of reduced volcanic gases. At present, respiration and decay reverse this reaction on a time scale of ~10^2 yr, consuming > 99% of the O_2 produced by photosynthesis. A small fraction (0.1–0.2%) of organic carbon does escape oxidation through burial in sediments, resulting in an estimated contribution of $10.0 \pm 3.3 \times 10^{12}$ moles of O_2 per year (Holland, 2002; Catling and Claire, 2005).

Box 13.3 What defines an oxic versus an anoxic atmosphere?

Whether an atmosphere is oxic or anoxic can be described by an oxygenation parameter, K_{oxy}, which is defined as (after Catling and Claire, 2005):

$$K_{oxy} = \frac{F_{source}}{F_{sink}} = \frac{F_{source}}{F_{metamorphic} + F_{volcanic} + F_{weathering}} \quad (13.33)$$

where F_{source} = net flux of O_2 generated (in 10^{12} moles per year), and F_{sink} = O_2 consumed (in 10^{12} moles per year). Net sources of oxygen are: (i) photolysis coupled with loss of H to space (reactions 13.28–13.30); and (ii) oxygenic photosynthesis (reactions 13.35 and 13.38), provided the rate of oxygen production > the rate of organic carbon burial (at present the two rates are equal). O_2 is consumed by the reductants derived from volcanic outgassing and metamorphic reactions (mainly hydrogen-bearing gases such as H_2, H_2S, and CH_4), as well as by oxidative chemical weathering and animal respiration (and, in modern times, by the burning of fossil fuels). The atmosphere is oxic when $K_{oxy} > 1$, and anoxic when $K_{oxy} < 1$. For the present atmosphere, $K_{oxy} \approx 6$, which means that the atmosphere is quite oxic.

The atmospheric O_2 budget is further complicated by the response of other redox-sensitive elements, particularly iron and sulfur. During chemical weathering, sulfur in sulfide minerals, such as pyrite, is oxidized to soluble sulfate (SO_4^{2-}), which is carried by rivers to the ocean, where bacteria reduce sulfate and Fe^{3+} to pyrite (FeS_2), and pyrite burial in sediments is balanced by O_2 production. The reactions involved may be represented as (Canfield, 2005):

$$16H^+ + 16HCO_3^- \Rightarrow 16CH_2O + 16O_2 \quad (13.37)$$

$$8SO_4^{2-} + 16CH_2O \Rightarrow 16HCO_3^- + 8H_2S \quad (13.38)$$

$$2Fe_2O_3 + 8H_2S + O_2 \Rightarrow 8H_2O + 4FeS_2 + 15O_2 \quad (13.39)$$

$$\text{(net reaction) } 2Fe_2O_3 + 8SO_4^{2-} + 16H^+ \Rightarrow 8H_2O + 4FeS_2 + 15O_2 \quad (13.40)$$

At present, pyrite burial contributes $7.8 \pm 4.0 \times 10^{12}$ moles of O_2 per year (Holland, 2002). The burial of organic matter and, to a lesser degree, of pyrite accounts for essentially all the oxygen released to the atmosphere.

13.2.4 The Great Oxidation Event (GOE)

When exactly molecular oxygen first started to accumulate in the atmosphere is a controversial subject. In one scenario, originally proposed by Dimroth and Kimberley (1976) and later promoted by Ohmoto and his collaborators (Towe, 1990; Ohmoto, 1996, 1997; Watanabbe *et al.*, 1997; Beukes *et al.*, 2002), the atmospheric P_{O_2} level has essentially been constant, probably within ±50% of PAL (0.2 atm), since the advent of oxygenic photosynthesis in the Archean. According to the much more popular scenario, first proposed by Cloud (1972) and subsequently championed by a large number of authors (e.g., Walker *et al.*, 1983; Holland, 1984, 1994, 2002, 2006a,b; Kasting, 1993, 2001, 2006; Des Marais, 1994; Karhu and Holland, 1996; Canfield, 1998; Canfield *et al.*, 2000; Kump *et al.*, 2001; Pavlov and Kasting, 2002; Anbar and Knoll, 2002; Shen and Buick, 2004; Catling and Claire, 2005), the atmosphere was essentially devoid of molecular oxygen during the Hadean and Archean eons, but experienced a dramatic rise in the oxygen level during the Paleoproterozoic, around 2.3 Ga (2.4–2.2 Ga). This irreversible transition from fundamentally reducing to oxidizing conditions on the Earth's surface is often referred to as the *Great Oxidation Event* (GOE) (Holland, 1994). It is estimated that the GOE marked a dramatic increase in P_{O_2} from $< 10^{-5}$ PAL (Pavlov and Kasting, 2002) to $>10^{-2}$ PAL and possibly to $>10^{-1}$ PAL (Holland, 1984, 2006a). A chemical equilibrium model by Krupp *et al.* (1994), involving minerals, seawater, and atmospheric gases, yielded a similar scenario: an oxygen-free atmosphere ($P_{O_2} < 10^{-10}$ bar) before ~2.35 Ga, comprised mainly of CO_2 ($P_{CO_2} \leq 1$ bar) and N_2, with minor amounts of H_2 and H_2S. Sverjensky and Lee (2010) have suggested that the rise in atmospheric oxygen resulted in an explosive growth in the diversification of minerals after the GOE because many elements could then occur in more than one oxidation state in minerals formed in near-surface environments. Another major oxidation event occurred at ~0.8–0.7 Ga, more than 1 Gyr after the GOE (see section 11.7.5), just before the appearance of large animals in the fossil record.

Evidence for the Great Oxidation Event

The hypothesis of a marked increase in the atmospheric P_{O_2} at 2.4–2.2 Ga is supported by the following lines of evidence preserved in the rock record.

(1) A large number of paleosols older than about 2.2–2.3 Ga have lost significant amounts of iron, whereas paleosols younger than 1.9 Ga have retained it (Holland, 1984; Rye and Holland, 1998; Yang *et al.*, 2002). The Fe-poor paleosols can be explained by weathering under low oxygen conditions prior to 2.2 Ga (< 0.001 PAL to 0.01 PAL; Rye and Holland, 1998). Iron contained in igneous and metamorphic rocks is dominantly Fe^{2+}. Under an anoxic atmosphere, the iron released during weathering remained as soluble Fe^{2+}, and was carried away by surface water and groundwater. The level of atmospheric O_2 was high enough after 1.9 Ga to retain the iron in the soil by oxidizing Fe^{2+} to insoluble Fe^{3+}.

(2) Continental red beds (sediments with a red coloration due to ferric oxide and hydroxide coatings on quartz grains), which attest to the oxidation of iron, appear for the first time in the rock record only around 2.2 Ga and become abundant after 2.0 Ga. The oldest, reasonably well-dated red beds, closely preceeding the major interval of red bed deposition after 2.0 Ga, occur in the 2224–2090-Myr-old Rooibergg Group in South Africa.

(3) Detrital uraninite ($U^{4+}O_2$) occurs only in rocks older than ~2.3 Ga, as in the uranium deposits hosted by conglomorates in South Africa (Witwatersrand district, ~2.7 Ga) and Canada (Elliot Lake district, ~2.3 Ga), indicating that the atmospheric O_2 was too low during the weathering of the host rock to oxidize uraninite into soluble U^{6+} -bearing species (Smith and Minter, 1980; Schidlowski, 1981; Smits, 1984). Very little or no O_2 in the Archean atmosphere is also indicated by the presence of detrital uraninite, pyrite, and, locally, siderite in 3250–2750 Ma fluvial sandstones and conglomorates in the Pilbara Craton, Australia (Rasmussen and Buick, 1999). Most estimates of O_2 concentration for the survival of detrital uraninite lie between ≤ 0.01 PAL (Holland, 1984) and 0.005 PAL (Kump *et al.*, 2004).

(4) Banded iron formations (BIFs) (Fig. 13.3), are abundant in the sedimentary record prior to 2.4 Ga, but are largely absent between 2.4 and 2.0 Ga (Fig. 13.4). Since Fe(II) species (such as Fe^{2+} and $FeOH^+$) are relatively soluble in

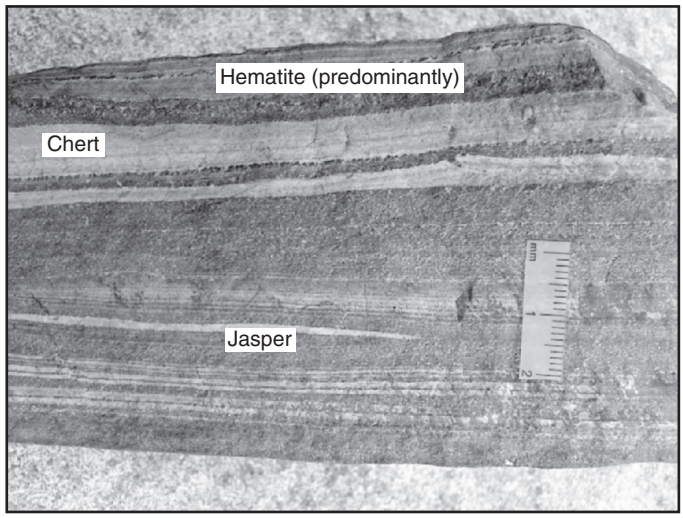

Fig. 13.3 A hand specimen of Archean (~3.0 Ga) banded iron formation from the Buhwa Greenstone Belt, Zimbabwe Craton. (Courtesy Dr Chris Fedo, Department of Earth and Planetary Sciences, The University of Tennessee, Knoxville, USA.)

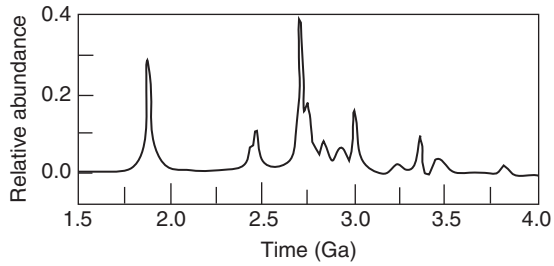

Fig. 13.4 Best estimate of relative abundance of banded iron formations (BIFs) as a function of time. (After Isley and Abbott, Plume-related mafic volcanism and the deposition of banded iron formation, Journal of Geophysical Research, v. 104, p. 15461–15467, 1999. Copyright 1999 American Geophysical Union. Used by permission of American Geophysical Union.)

ocean water, whereas Fe(III) species are not, most models for the formation of BIFs require an anoxic ocean to sustain large quantities of dissolved Fe(II) and some mechanism to precipitate the iron as Fe(III) compounds (see Box 13.4). Because the oxygen in BIFs could have come from several sources, we cannot use BIFs directly to make a quantitative estimate of the O_2 content of the atmosphere, but the time-restricted distribution of BIFs does point to a sudden rise in atmospheric O_2 at ~2.4 Ga.

(5) $\delta^{34}S$ values of sedimentary sulfides (pyrite in fine-grained siliciclastic sediments) show a marked jump to higher values at ~2.4–2.3 Ga. The favored interpretation is that the jump reflects a transition from low concentrations of dissolved SO_4^{2-} (< 1 mM kg^{-1} H_2O) in the oceans under an anoxic atmosphere (O_2 < 0.004 PAL) to higher concentrations of dissolved SO_4^{2-} (>1 mM kg^{-1} H_2O) when the atmosphere turned oxic (see section 11.7.5). This upper limit of O_2 concentration before ~2.4 Ga is in broad agreement with that indicated by the paleosol data.

(6) Mass-independent fractionation of sulfur isotopes (MIF-S) occurs in sediments of Archean and early Proterozoic age (> 2.45 Ga), but not in younger sediments. The loss of the MIF signal is attributed to an increase in the atmospheric oxygen to $>10^{-5}$ PAL between 2.45 and 2.32 Ga (see section 11.7).

(7) Organic carbon is fixed from dissolved inorganic carbon (DIC) by autotrophic processes. Since organic carbon is depleted in ^{13}C, the remaining DIC is enriched in ^{13}C. Carbonate minerals precipitating from ocean water incorporate this DIC, providing a record of $\delta^{13}C$ of marine DIC through time and the intensity of organic carbon burial. Modeling of the intensity of organic carbon burial, the major source of atmospheric O_2, as a function of geologic time by Bjerrum and Canfield (2004) shows a marked transition to high values between 2.4 and 2.2 Ga (Fig. 13.5).

The oxygen jump

What triggered the GOE remains a hotly debated issue. If life existed before 3.8 Ga, it was subjected to intense meteorite bombardment and possibly annihilation. Cyanobacteria, the first oxygenic photosynthesizers, have been identified from organic biomarkers in sediments dated at 2.7 Ga (Brocks *et al.*, 1999), and may have existed since as early as 3.8–3.5 Ga (Buick, 1992; Schopf, 1993; Mojzsis *et al.*, 1996; Shen and Buick, 2004; Tice and Lowe, 2004). Why, then, was there a gap of at least 400 Myr between the emergence of cyanobacteria and the jump in atmospheric oxygen? Some suggested explanations are discussed below.

A rise in the atmospheric O_2 would require an increase in the O_2 source or a decrease in the O_2 sink. An obvious mechanism for an increasing O_2 source would be a long-term increase in organic carbon burial rates, perhaps because of the growth of continental shelves (Godderis and Veizer, 2000), but the carbon isotope data (Fig. 13.5) do not show a systematic increase in the burial rate of organic carbon over geologic time. The atmospheric evolution model of Goldblatt *et al.* (2006) suggests that a mere 3% increase in organic carbon burial would have been enough to trigger the GOE, but such a change is far too small to be detected in the carbon-isotope record.

Another possible cause of the delay in oxygen build-up could be the consumption of oxygen by reduced volcanic gases. At the present time, the O_2 sink provided by the oxidation of volcanic gases accounts for ~25% of the O_2 generated by organic carbon burial; the other ~75% is consumed by oxidative weathering of reduced species in rocks, predominantly of organic carbon, pyritic sulfur, and Fe(II) in shales (Kump *et al.*, 2001). The volcanic sink was certainly much larger during the Archean because of much greater volcanic activity, but the larger O_2 sink would have been offset by a larger release of volcanic CO_2. This, together with the approximately constant $\delta^{13}C$ composition of carbonates (Fig. 13.5), reflecting a

Box 13.4 Banded iron formations (BIFs)

Banded iron formation (BIF), typically, is an iron-rich (~20–40 wt% Fe), siliceous (~40–60 wt% SiO_2), laminated or banded (on scales ranging from < 1 mm to tens of centimeters) sedimentary rock that consists of alternating, millimeter-to-decimeter thick layers of iron-rich minerals (such as magnetite, Fe_3O_4; hematite, Fe_2O_3; and siderite, $FeCO_3$) and silica (SiO_2 as chert or jasper) (Fig. 13.3). Banded iron formations are practically devoid of detrital input, as reflected in their very low Al_2O_3 contents (0–1.8 wt%). They are widely distributed around the world, often as huge deposits, and account for about 90% of the global supply of iron ores. Banded iron formations are important in the context of the evolution of the atmosphere–ocean system because of their time-restricted distribution, and because deposition of BIFs served as a large sink for the atmospheric O_2.

The oldest known BIFs are those of the Isua supracrustal belt (3760 ± 70 Ma; Moorbath *et al.*, 1973). Banded iron formations are quite common in the rock record between ~3.5 and 2.4 Ga, but largely absent from the geologic record between 2.4 and 2.0 Ga. They reappear for a brief interval (2.0–1.8 Ga) in the Paleoproterozoic and then disappear from the rock record quite abruptly after 1.8 Ga (Fig. 13.4). The late Proterozoic (0.85–0.54 Ga) iron formations (Rapitan-type BIFs, which occur in Yukon and NWT of Canada and in the Urucum area of Brazil) are very different from typical BIF in terms of their hematite-dominated mineralogy and stratigraphic settings, especially association with glaciomarine deposits. The Rapitan-type BIFs are thought to be the result of anoxic conditions that arose from stagnation of the oceans beneath a near-global ice cover (referred to as "Snowball Earth").

Most aspects of the genesis of Archean–early Proterozoic BIFs – sources of iron and silica, rhythmic banding of iron-rich and silica-rich layers, precipitation mechanisms for the various facies of BIFs (oxide, silicate, carbonate, and sulfide), spatial and temporal distribution – are controversial and not satisfactorily resolved (James, 1992; Beukes and Klein, 1992; Klein and Beukes, 1992; Morris, 1993; Misra, 2000; Klein, 2005). A comprehensive discussion of the genesis of BIFs is beyond the scope of this book; we will touch only on a few aspects of the story germane to atmospheric oxygen evolution.

The most abundant type of BIF is the Superior-type iron formations, so named because of their abundance in the Lake Superior region of USA and Canada. These predominantly early Proterozoic deposits with well-developed and laterally extensive banding are interpreted to have been deposited on stable continental shelves at depths below the storm wave base (which is at least 200 m in the modern oceans). Prompted by the lack of volcanic association and paucity of detrital components in the Superior-type BIFs, earlier genetic models (e.g., Drever, 1974; Holland, 1984) had invoked a continental source of iron and silica. But the overall REE patterns, positive Eu and negative Ce anomalies, and Nd isotopic data for BIFs ranging in age from 3.8 Ga to 1.9 Ga show that much of the iron and silica were brought from the mantle by mid-oceanic ridge (MOR)-type hydrothermal fluids (Derry and Jacobsen, 1990). As Fe(II) is much more soluble in seawater than Fe(III), the formation of voluminous quantities of BIF requires that large portions of the deep ocean were anoxic to enable the transport of dissolved Fe(II). The dissolved iron was brought to the near-surface regions, probably by wind-induced upwelling of the type that occurs in some modern coastal settings (Klein and Beukes, 1989) or by hydrothermal plumes (Isley, 1995; Isley and Abbott, 1999), and precipitated (at pH > 4) as Fe(III) compounds (here represented by ferric hydroxide, $Fe(OH)_{3(s)}$), believed to be precursors of hematite and magnetite in oxide-facies BIFs. The precipitation occurred by one of the following types of oxidation reactions in the stratified Precambrian ocean.

(1) Indirect biological oxidation, utilizing the dissolved O_2 produced by oxygenic photosynthesis (reaction 13.36) in the *photic zone* of the ocean (the zone, about 100 m for calm and clear water, that is penetrated by sufficient sunlight for photosynthesis to occur), probably in localized "oxygen oases" associated with cyanobacteria blooms,

$$\boxed{3Fe^{2+}_{(aq)} + O_2 + 7H_2O \Rightarrow 3Fe(OH)_{3(s)} + 5H^+} \quad (13.41)$$

(2) Photochemical oxidation of dissolved Fe(II) in the photic zone of the ocean by solar UV radiation (Cairns-Smith, 1978; François, 1986),

$$\boxed{Fe^{2+}_{(aq)} + 3H_2O + \text{UV photon} \Rightarrow Fe(OH)_{3(s)} + 2H^+ + 0.5H_2} \quad (13.42)$$

(3) Direct biological oxidation of Fe(II), the electron donor, catalyzed by anoxygenic phototrophic Fe(II) oxidizing bacteria, which convert CO_2 into biomass using light energy (Widdel *et al.*, 1993; Kappler *et al.*, 2005),

$$\boxed{4Fe^{2+} + CO_2 + 11H_2O + \text{sunlight} \Rightarrow CH_2O + 4Fe(OH)_{3(s)} + 8H^+} \quad (13.43)$$

Although Fe(II) can be oxidized photochemically in simple aqueous systems, such oxidation has not been reported in more complex environments such as seawater at approximately neutral pHs. Also, in the absence of biological silica secretion, the contemporaneous oceans were likely saturated with H_4SiO_4, causing the formation of amorphous Fe-silicate gels and thus limiting the effects of photochemical oxidation. In contrast, both freshwater and marine anoxygenic phototrophs readily oxidize Fe(II) (Widdel *et al.*, 1993; Ehrenreich and Widdel, 1994; Kappler and Newman, 2004) and can account for most, if not all, of the iron in BIFs even if the cell densities of the iron-oxidizing bacteria were much less than found in modern Fe-rich aqueous environments (Konhauser *et al.*, 2002).

An important point in favor of indirect biological oxidation is that primitive O_2-producing photosynthetic bacteria lacked suitably advanced oxygen-mediating enzymes (Cloud, 1973) and, in order to survive, required Fe(II) as an oxygen acceptor. Consequently, these microorganisms would have flourished during periods of abundant supply of Fe(II), leading to $Fe(OH)_3$ precipitation (Crowe *et al.*, 2009). The intervals of limited $Fe(OH)_3$ precipitation, then, may be ascribed to a decrease in Fe(II) supply, causing dwindled population of photosynthetic bacteria.

Whether the oxidation was biotic or abiotic is still unresolved (see section 11.8.1), but it is reasonable to conclude that the intervals of abundant BIFs coincided with an anoxic atmosphere that sustained anoxic conditions over large portions of the deep oceans, thereby permitting the transport of large quantities of iron as dissolved Fe(II) species. Thus, the BIF record provides indirect evidence that the atmosphere turned oxic after ~2.4 Ga. This interpretation implies that a lower level of atmospheric O_2, possibly as low as that before 2.4 Ga, ushered the return of BIF deposition during 2.0–1.8 Ga, which is consistent with a decrease in the calculated fraction of total carbon buried as organic carbon (*f* ratio) as

Box 13.4 (cont'd)

shown in Fig. 13.5. The disappearance of BIFs from the geologic record after 1.8 Ga was perhaps the consequence of very limited supply of dissolved Fe(II) when the deep ocean became oxygenated, a scenario consistent with an oxic atmosphere. Canfield (1998), however, suggested that the deep ocean remained anoxic until the Neoproterozoic, with the Fe(II) being removed by the precipitation of pyrite. In any case, the cessation of BIF deposition eliminated an effective O_2 sink and, thus, contributed to the transition of the atmosphere to an oxygenated state.

A further complication in the BIF story arises from the fact that the major Fe-bearing phases in oxide-facies BIFs, which have not experienced supergene alteration or metamorphism, is magnetite, not hematite or goethite. Conversion of precursor $Fe(OH)_{3(s)}$ to magnetite and siderite at or below the sediment–water interface occurred via several pathways (Johnson *et al.*, 2008a): reactions with seawater Fe^{2+}_{aq} ($2Fe(OH)_{3(s)} + Fe^{2+}_{aq} \Rightarrow Fe_3O_{4(s)} + 2H_2O + 2H^+$; $Fe^{2+} + CO_2 + H_2O \Rightarrow FeCO_3 + 2H^+$); bacteria-catalyzed dissimilatory Fe^{3+}_{aq} reduction (DIR) under Fe^{2+}_{aq}-limited conditions; and DIR in the presence of excess Fe^{2+}_{aq}.

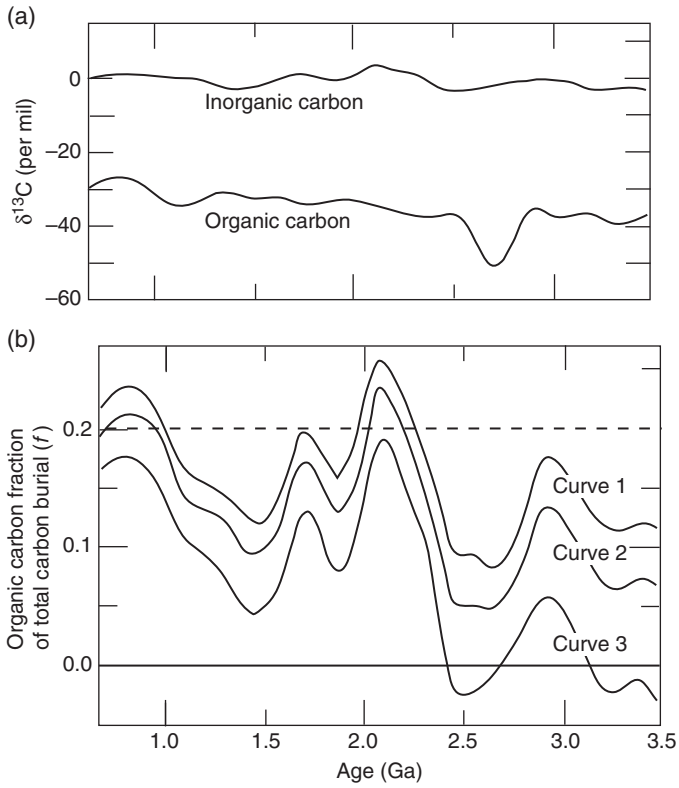

Fig. 13.5 (a) A summary of the isotopic composition of inorganic carbon and organic carbon through geologic time (3.5–0.7 Ga). (b) Reconstructions of the significance of *f* ratio (organic carbon fraction of total carbon burial) through geologic time. Curve 1 does not consider ocean crust carbonatization (OCC). Curves 2 and 3 are based on an isotope gradient of 2% and 5%, respectively, between the surface and deep oceans. (After Bjerrum and Canfield, New insights into the burial history of organic carbon on the early Earth, Geochem. Geophys. Geosyst., v. 5, Q08001, doi:10.1029/2004GC000713 (online), 2004. Copyright 2004 American Geophysical Union. Used by permission of American Geophysical Union.)

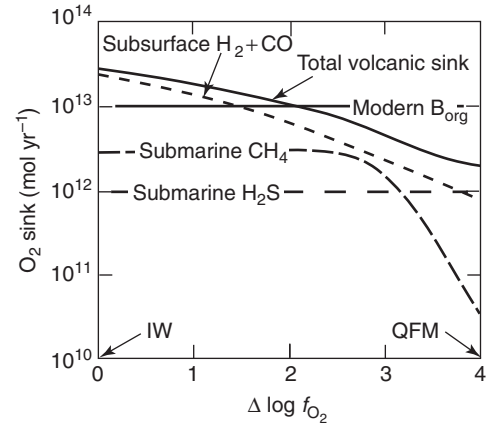

Fig. 13.6 Magnitude of the volcanic O_2 sink as a function of the oxygen fugacity of mantle source regions. B_{org} is the organic carbon burial rate and the presumed rate of O_2 production if most of the organic matter came from oxygenic photoautotrophs. $\Delta \log f_O$ is relative to the iron–wustite (IW) oxygen buffer. Calculations were performed at $T = 1500$ K and $P = 1$ bar for subaerial volcanic gases, and $T = 900$ K and $P = 400$ bar for subaqueous volcanoes. QFM = quartz–fayalite–magnetite oxygen buffer. (After Kump et al., Rise of atmospheric oxygen and the "upside–down" Archean mantle. Geochem. Geophys. Geosyst., v. 2, 1025, doi:1029/2000GC000114 (online), 2001. Copyright 2001 American Geophysical Union. Used by permission of Amerivcan Geophysical Union.)

roughly constant proportion of organic carbon burial, requires that the burial rate of organic carbon was proportionately larger. If oxygenic photosynthesis dominated the production of O_2 during the Archean, then we had an O_2 source that was enhanced in proportion to the volcanic sink. Thus, a higher rate of volcanic outgassing cannot by itself account for the delay in rise of atmospheric O_2 (Kump *et al.*, 2001).

A more plausible explanation for the change in the oxidation state of the atmosphere involves a gradual decrease in the scavenging of atmospheric O_2 due to a corresponding change in the oxidation state of volcanic gases, dominated by H_2 and CO during the early Archean, and escape of H_2 into space (Kasting *et al.*, 1993; Kump *et al.*, 2001; Catling *et al.*, 2001; Holland, 2002; Canfield, 2005).

What caused the change in the oxidation state of volcanic gases? The oxidation state of volcanic gases depends on the oxidation state of upper mantle rocks, where the gases originate: the more oxidized the upper mantle, the more oxidized the volcanic gases. So, for this hypothesis to be viable, the upper mantle must have become progressively more oxidized because of volcanic outgassing of H_2 (and other H-bearing gases, such as CH_4, H_2S, H_2O) by reactions such as (Catling and Claire, 2005)

$$3FeO + H_2O \Rightarrow Fe_3O_4 + H_2 \Rightarrow Fe_3O_4 + 2H\ (\uparrow \text{space}) \quad (13.44)$$

According to Kump *et al.* (2001) the photosynthetic O_2 source exceeded the total volcanic sink when the average f_{O_2} of volcanic gases, no longer dominated by H_2 and CO, rose to a value of 2 log units below the QFM buffer (Fig. 13.6). This marked the transition from an anoxic atmosphere, in which the O_2 sink exceeded the O_2 source, to an oxic atmosphere, in which the O_2 source exceeded the O_2 sink. In a recent article, Kump and Barley (2007) proposed that the anoxic–oxic transition was a consequence of terrestrial volcanism changing from being predominantly submarine during the Archean to being predominantly subaerial at the beginning of the Proterozoic. This is because subaerially erupted volcanic gases have equilibrated with magmas at high temperatures and low pressures, and are dominated by oxidized gases (H_2O, CO_2, and SO_2). Volcanic gases from submarine eruptions, on the other hand, erupt at lower temperatures, and contain higher concentrations of reduced species (H_2, CO, CH_4, and H_2S).

A problem with the above scenario is that the concentrations of redox-sensitive elements, such as Cr and V, in several Archean high-Mg lava flows (komatiites) indicate an oxidation state comparable to, or more oxidizing than, that of the present-day oceanic basalts (Canil, 1997). This apparent discrepancy may be rationalized in several ways: (i) the source regions of komatiites represented pockets of reducing environment in a compositionally inhomogeneous mantle; (ii) the required increase in the f_{O_2} of volcanic gases was actually < 0.5 log units, which is in keeping with the limits set by the Cr and V contents of Archean komatiites (Holland, 2002); and (iii) the oxygen released by oxygenic photosynthesis (reaction 13.36) was largely consumed by the oxidation of continental crust, which, in turn, caused a change in the oxidation state of gases released by metamorphic reactions, independent of the mantle oxidation state (Catling *et al.*, 2001; Catling and Claire, 2005).

Since even a small excess of hydrogen over a steady-state abundance of ~0.1% H_2 (or its equivalent, 0.05% CH_4) could keep the atmosphere in an anoxic state, the anoxic to oxic transformation of the atmosphere must have involved getting rid of most of its H_2 (and CH_4). As suggested by Catling *et al.* (2001), the hydrogen escape rate was probably greatly enhanced by the build up of biogenic methane in the Archean atmosphere and the subsequent photolysis of CH_4. The pertinent methanogenesis reactions are reduction of CO_2 to CH_4 by mantle-derived volcanic H_2,

$$CO_{2(g)} + 4H_{2(g)} \Rightarrow CH_{4(g)} + 2H_2O_{(l)} \quad (13.45)$$

and decomposition of photosynthetically (anoxygenic or oxygenic) produced organic matter to CH_4,

$$2CH_2O_{(aq)} \Rightarrow CH_{4(g)} + CO_{2(g)} \quad (13.46)$$

The photochemistry of CH_4 is complicated, but may be represented by the reactions

$$CH_{4(g)} + \text{UV photon} \Rightarrow C_{(s)} + 4H_{(g)}(\uparrow \text{space}) \quad (13.47)$$

$$C_{(s)} + O_{2(g)} \Rightarrow CO_{2(g)} \quad (13.48)$$

which promoted rapid escape of hydrogen into space. Thus, the combined effect of oxygenic photosynthesis (equation 13.36), methanogenesis (equations 13.45 and 13.46), and hydrogen escape (equations 13.47 and 13.48) resulted in a net gain of O_2.

The availability of phosphorous, a nutrient for cyanobacteria, in the oceans may also have played a role in maintaining an anoxic atmosphere until the disappearance of BIFs. As Fe(III) precipitates strongly adsorb PO_4^{3-} at pH < 9, the very low P content of BIFs translates into very low concentrations of P in BIF-depositing waters of Archean and early Proterozoic oceans, only ~10–25% of present-day concentrations. It is likely that low P availability significantly reduced rates of photosynthesis and organic carbon burial, thus contributing to the prolonged anoxic condition of the atmosphere (Bjerrum and Canfield, 2002, p.159). Marine phosphorite deposits made their first appearance during the GOE, after the cessation of BIF deposition (Holland, 2006a).

According to the conceptual model of Goldblatt *et al.* (2006), the advent of oxygenic photosynthesis gave rise to two simultaneously stable steady states for atmospheric oxygen: a low-oxygen state (< 10^{-5} PAL) and a high-oxygen state (> 5×10^{-3} PAL). In a low-oxygen atmosphere, the lack of an effecive ozone shield allowed oxygen to be rapidly consumed by a UV-catalyzed reaction with biogenic methane ($CH_{4(g)} + 2O_{2(g)} + \text{UV photon} \Leftrightarrow CO_{2(g)} + 2H_2O_{(g)}$). As the oxygen level increased, the shielding of the atmosphere from UV radiation due to the increased level of ozone impeded oxygen consumption, and the atmosphere attained a higher level of oxygen. Thus, the atmospheric budget could change even if other sources and sinks of oxygen remained constant. The model predicts the persistence of a reducing atmosphere for at least 300 Myr after the onset of oxygenic photosynthesis. Goldblatt *et al.* (2006) also predicted that a much larger perturbation would be required to cause a high-oxygen atmosphere to revert back to a low-oxygen state. This might explain why a relatively high level of oxygen persisted following the GOE.

A yo-yo Archean atmosphere?

As discussed earlier, the presence of MIF-S in many sedimentary rocks older than ~2.4 Ga, and its absence in younger rocks, is considered the strongest evidence for a dramatic change from an anoxic atmosphere to an oxic atmosphere around 2.4 Ga. This is because photolysis of volcanic SO_2 gas by ultraviolet radiation in an oxygen-poor atmosphere is the only mechanism known to produce MIF-S. This interpretation, however, is not consistent with the observation recently reported by Ohmoto *et al.* (2006) that the MIF-S signal is absent throughout ~100 m sections of 2.76-Gyr-old lake sediments and 2.92-Gyr-old marine shales in the Pilbara craton, Western Australia. This suggests that these late Archean rocks

preserve a hint of oxic conditions, at least locally, in which rehomogenization of MIF took place. Alternatively, elevated concentrations of other gases in the atmosphere may also have depressed the MIF-S signal during the 2.8–3.0 Ga period (Holland, 2006a).

Examining the MIF-S record for pre-1.6 Ga sedimentary rocks in Australia, Canada, South Africa, and the USA, Ohmoto *et al.* (2006) proposed an Archean "yo-yo atmosphere," which fluctuated from anoxic ($< 10^{-5}$ PAL) before ~3.0 Ga, to oxic ($> 10^{-5}$ PAL or even $> 10^{-2}$ PAL) between ~3.0 and ~2.75 Ga, to anoxic between ~2.75 and 2.4 Ga, and back to oxic after ~2.4 Ga. Anbar *et al.* (2007) reported that the late Archean (2501 ± 8 Ma) Mount McRae Shale in Western Australia is enriched in redox-sensitive transition metals such as Mo and Re. Correlation with organic carbon indicates that these metals were derived from contemporaneous seawater. Mo and Re were probably supplied to Archean oceans by oxidative weathering of crustal sulfide minerals, pointing to the presence of a "whiff of oxygen" in the environment more than 50 Myr before the start of the GOE. The model of Goldblatt *et al.* (2006) mentioned earlier explicitly predicts that the atmosphere was bistable for some time before the GOE. The validity of the "yo-yo atmosphere" hypothesis is still being debated in the scientific community (see discussions by Kasting, 2006; Knauth, 2006; Ohmoto *et al.*, 2006).

13.2.5 A model for the evolution of the atmosphere

Many models have been proposed for the evolution of the atmosphere, but all of them are controversial. The simple conceptual model discussed below is a three-box framework of the atmosphere–ocean system originally proposed by Walker *et al.* (1983) and subsequently refined by Kasting *et al.* (1992) and Kasting (1993). The model does not incorporate the concept of a yo-yo Archean atmosphere. The three "boxes" in this model represent three distinct reservoirs of oxygen: the atmosphere, the surface ocean (the uppermost 75 m or so of water that is stirred rapidly by the action of the wind and, thus, is well mixed), and the deep ocean. The evolution of the atmosphere and the ocean is conceptualized to have progressed in three stages (Fig. 13.7).

Estimated change in the atmospheric O_2 level over geologic time, based on the three-stage model of Kasting *et al.* (1992) and some geologic and biologic data that constrain the model, is presented in Fig. 13.8. During Stage I (prior to the GOE), termed "reducing," both the atmosphere and the ocean were essentially devoid of O_2, although after the arrival of cyanobacteria localized patches of the surface ocean ("oxygen oases") within the photic zone, characterized by high microbial productivity, may have developed substantial concentrations of dissolved O_2. Such "oxygen oases" could have provided an environment conducive to BIF deposition. The deeper oceans were certainly anoxic as evidenced by the occurrence of an abundance of Archean-age BIFs. The occurrence of large marine manganese deposits of

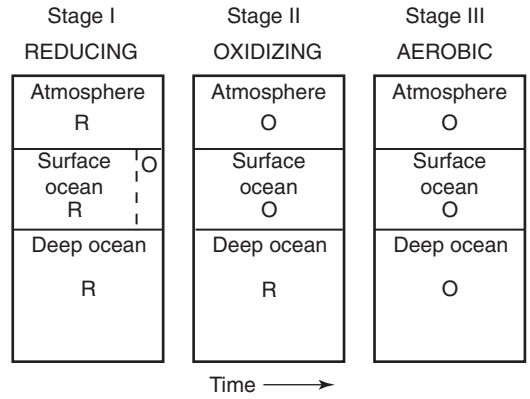

Fig. 13.7 The three–box model of the atmosphere–ocean system pertaining to atmospheric evolution over geologic time proposed by Kasting *et al.* (1992). O = oxidizing, R = reducing. Note that during Stage I, the surface ocean was oxidizing locally.

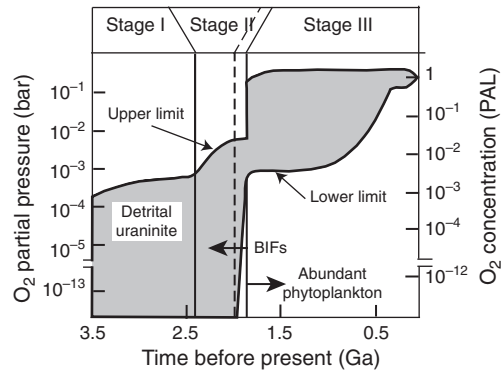

Fig. 13.8 Estimated change in atmospheric O_2 levels through geologic time. The upper and lower limits are constrained by detrital uraninite, paleosols, and the fossil record. (Simplified from J.F. Kasting, H.D. Holland, and L.E. Kump, 1992, *Atmospheric Evolution: the Rise of Oxygen*, Fig. 4.6.1, Cambridge University Press. Used with permission of the publisher.)

Archean age (e.g., the ~3.0-Gyr-old Iron Ore Group, Orissa, India) also points to reducing conditions in the deeper oceans, where Mn^{2+} could accumulate, then upwell into the shallow oceans, and be precipitated there as a constituent of Mn-carbonates or Mn-oxides (Roy, 1997; Holland, 2006a). As mentioned earlier, the atmospheric O_2 level at this stage was generally $< 10^{-5}$ PAL (Pavlov and Kasting, 2002). Independent calculations based on the survival of detrital uraninite imply an atmospheric O_2 level between ≤ 0.01 PAL (Holland, 1984) and 0.005 PAL (Kump *et al.*, 2004).

Stage II (from ~2.4 to ~1.85 Ga), termed "oxidizing," represents a period in which small amounts of O_2 were present in the atmosphere and surface ocean, but the deep ocean remained anoxic, as evidenced by the occurence of large marine manganese deposits of Paleoproterozoic age. Models for BIF deposition suggest an upper limit of ~0.03 PAL for

atmospheric O_2 during Stage II (Kasting, 1993), whereas paleosol data yield O_2 values of less than 0.15 PAL (Klein and Beukes, 1992). Holland (2006a) estimated that the oxygen level during this stage reached about 0.02–0.04 atm. The reason for the lack of BIFs in the rock record between 2.4 and 2.0 Ga is not known, but the reappearance of BIFs between 2.0 and 1.8 Ga implies a return to lower oxygen levels during the later part of the Paleoproterozoic.

The transition from Stage II to Stage III occurred when the deep ocean became oxic, and it is marked by the disappearance of the Superior-type BIFs around 1.85 Ga (Kasting *et al.*, 1993). Possible causes of this transition include a decrease in the supply of Fe^{2+} to the deep sea (probably due to reduced oceanic ridge hydrothermal activity or a transition to an oxygenated ocean), removal of Fe^{2+} as Fe-sulfide precipitates in a sulfidic ocean (Canfield, 1998; Anbar and Knoll, 2002), an increase in the rate of oxygenic photosynthesis, and an increase in the burial rate of organic carbon. A growing body of evidence suggests that precipitation of Fe-sulfides was probably responsible for removing Fe from deep ocean waters (Canfield, 1998; Anbar and Knoll, 2002; Shen *et al.*, 2003; Arnold *et al.*, 2004).

Stage III (1.85–0.85 Ga), termed "aerobic," represents a situation, somewhat similar to the present atmosphere, in which oxygen pervaded the entire system and P_{O_2} was high enough to support aerobic respiration. Calculations suggest that the atmospheric O_2 must have risen to at least 0.02 PAL for the transition to Stage III; otherwise the deep ocean would have remained anoxic as a consequence of the influx of reductants from hydrothermal vents (Kasting, 1993).

The three-box model does not account for the late Proterozoic (0.85–0.54 Ga) Rapitan-type BIFs, which constitute a very different type of BIF and should not be interpreted as necessarily signaling a return to Stage II conditions. The O_2 concentration in the atmosphere and the sulfate concentration in seawater during 0.85–0.54 Ga rose to levels that were probably not much lower than those of the present day (Holland, 2006a).

Calcium sulfate minerals (gypsum or anhydrite), or their pseudomorphs, are scarce before ~1.7–1.6 Ga (Grotzinger and Kasting, 1993), indicating a low concentration of SO_4^{2-} in the pre-1.7 Ga oceans, and therefore a low concentration of oxygen in the contemporaneous atmosphere. On the basis of $\delta^{34}S$ values in marine sedimentary sulfides, Canfield and Teske (1996) argued that atmospheric P_{O_2} values remained at < 5–18% PAL until the late Proterozoic transition. The second line of evidence comes from $\delta^{34}S$ values of carbonate-associated sulfate (CAS), trace amounts of sulfate that substitute for CO_3^{2-} ion in marine carbonate minerals. The amount of CAS increases with increasing sulfate concentration in the solution and, thus, can be used as a proxy for the dissolved sulfate concentration of the contemporaneous ocean. Moreover, CAS trapped in marine carbonates is isotopically buffered against appreciable diagenetic overprint and, therefore, can record the $\delta^{34}S$ of the contemporaneous ocean water (Lyons *et al.*, 2004). Calculations by Kah *et al.* (2004) suggest that marine sulfate concentrations remained low, < 35% of modern values, for nearly the entire Proterozoic. Since lower oceanic sulfate concentrations imply lower rates of pyrite oxidative weathering and, therefore, lower levels of atmospheric P_{O_2}, a significant rise in O_2 may not have occurred until the latest Neoproterozoic (0.54 Ga), just before the Cambrian biological explosion, when sulfate levels may have reached 20.5 mM kg^{-1} H_2O or 75% of present-day levels. The Neoproterozoic jump in atmospheric O_2, probably to not much less than PAL (Holland, 2006a), broadly correlates with a marked increase in organic carbon burial (Fig. 13. 5b).

13.2.6 The Phanerozoic atmosphere

The level of atmospheric O_2 probably reached close to the modern value by the Cambrian biologic explosion. A number of studies (e.g., Berner and Canfield, 1989; Berner, 2001, 2003) have concluded that atmospheric O_2 must have fluctuated significantly during the Phanerozoic, but quantitative modeling has been unsatisfactory in the absence of simple indicators of the O_2 level. Berner and Canfield (1989) have constructed a mathematical model that enables calculation of the level of atmospheric O_2 across the Phanerozoic. In this model, the burial rates of organic carbon and pyrite sulfur, which control the accumulation of atmospheric O_2, are not calculated from $\delta^{13}C$ and $\delta^{34}S$ values of ancient oceans as recorded by sedimentary $CaCO_3$ and $CaSO_4$, respectively. Instead, the burial rates are calculated from an assumed constant worldwide clastic sedimentation rate and the relative abundance and C and S contents of three rock types: marine sandstones and shales, coal basin sediments, and nonmarine clastics (red beds, arkoses).

The "best estimate" of the variation of atmospheric O_2 during the Phanerozoic obtained by Berner and Canfield (1989) is presented in Fig. 13.9. The most striking feature of this plot is

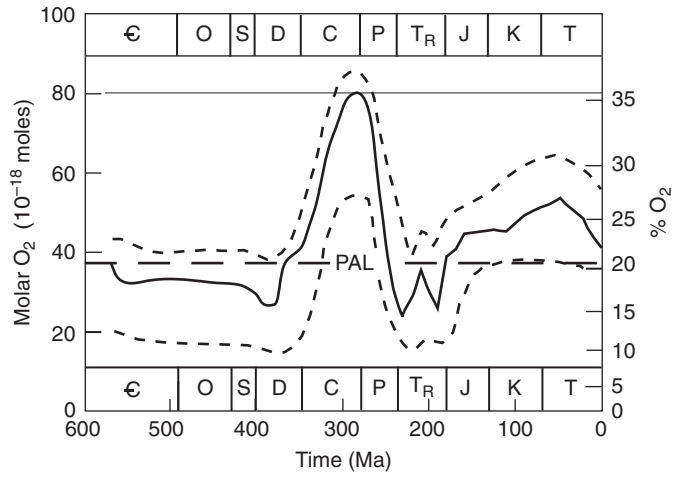

Fig. 13.9 "Best estimate" of atmospheric O_2 during the Phanerozoic as modeled by Berner and Canfield (1989). The values of O_2 shown here should be used in only a qualitative to semiquantitative sense. The dashed lines represent crude error limts, based on their sensitivity analysis. PAL = present atmospheric level of oxygen. (After Berner and Canfield, 1989, Fig. 13, p. 357.)

the pronounced excursion, reaching concentration levels as high as 35% O_2, during the Permo-Carboniferous and its rapid plunge at the end of Permian. The excursion may be ascribed to the evolution of vesicular land plants, which was a new source of organic carbon, and the development of vast lowland swamps where vesicular plants could flourish and then be buried to form coals (Berner, 2004).

Most studies incorporating all known climate forcings implicate CO_2 as the primary driver for the most recent rise in global temperatures (Mann *et al*., 1998; Crowley, 2000; Mitchell *et al*., 2001). The revised GEOCARB model for CO_2 levels during the Phanerozoic (GEOCARB III; Berner and Kothavala, 2001) suggests a similar story – a broad correspondence between the atmospheric CO_2 concentration and glaciation. As shown on Fig. 13.10, CO_2 was low (< 500 ppm) during periods of long-lived and widespread continental glaciations (Permo-Carboniferous, 330–260 Ma, and late Cenozoic, past 30 Myr) and high (>1000 ppm) during intervening warmer periods (Royer *et al*., 2004). The late Ordovician (~440 Ma) represents the only interval during which glacial conditions apparently coexisted with a CO_2-rich atmosphere.

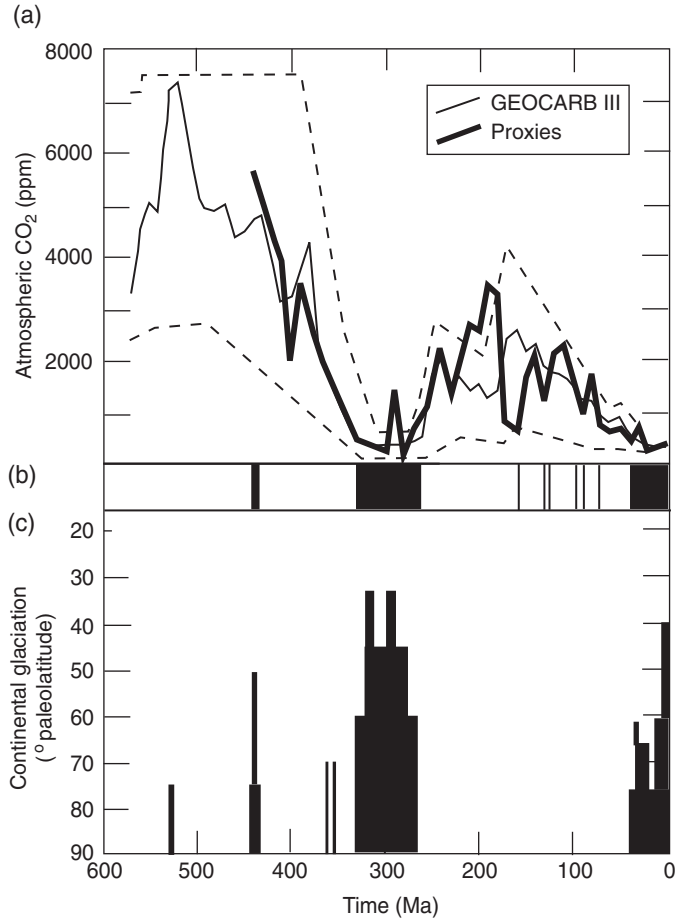

Fig. 13.10 CO_2 and the Phanerozoic climate. (a) Evolution of atmospheric CO_2 over Phanerozoic time according to the GEOCARB III model of Berner and Kothavala (2001). The outer dashed lines represent an estimate of errors in the GEOCARB III model. Also shown for comparison is the graph reconstructed from multiple proxies. (b) Intervals of glacial (solid black) and cool (thin lines) climates. (c) Latitudinal distribution of direct evidence of glaciation, such as tillites and striated bedrock, etc. (Crowley, 1998). (After Royer *et al*., 2004.)

Pavlov *et al*. (2003) have proposed that the long period of warm climate between the Paleoproterozoic (2.5–1.6 Ga) and Neoproterozoic (0.9–0.542 Ga) glaciations was a consequence of the greenhouse effect of the Proterozoic atmosphere bolstered by 100–300 ppm of CH_4. Their calculations for the estimated CH_4 flux in the Proterozoic assume that (i) most of the organic carbon (CH_2O) was initially produced by photosynthesis, and (ii) consumption of CH_4 by methanotrophic bacteria was ineffective in the Proterozoic ocean, which was anoxic at depth and impoverished in sulfate. The Neoproterozoic glaciation could have been initiated by a decrease in CH_4 flux resulting from the second oxygenation event toward the end of the Proterozoic.

Calculations by Berner (2006), using average nitrogen : carbon ratio (N/C) of sedimentary organic matter, coal, and volcanic/metamorphic gases, and existing models of the carbon cycle indicate that the concentration of atmospheric N_2 changed very little (by <1% of the present value) over Phanerozoic time. This means that significant variations of the mass of O_2 during the Phanerozoic resulted in corresponding variations in the total atmospheric pressure.

13.3 Air pollution: processes and consequences

Air pollution refers to the presence in the atmosphere of substances that are potentially harmful to human beings, animals, vegetation, property, or the environment. Air pollutants can be grouped into three broad classes: (i) inorganic gases such as oxides of nitrogen (N_2O, NO, NO_2), sulfur (SO_2, SO_3), and carbon (CO, CO_2), and other inorganic gases (O_3, NH_3, H_2S, HF, HCl, Cl_2, Rn); (ii) volatile organic compounds (e.g., CH_4, higher hydrocarbons, and chlorofluorocarbon compounds such as CFC-11 and CFC-12); and (iii) suspended particulate matter (particularly small particles of solid or liquid substances <10 μm in diameter, commonly denoted as PM-10, which are not very effectively removed by rain droplets). Air pollutants may be primary or secondary. *Primary pollutants* are the direct products of combustion and evaporation (e.g., CO, CO_2, NO_x, SO_x, and volatile organic compounds (VOC)). *Secondary pollutants* are generated in the atmosphere by reaction with primary pollutants (e.g., O_3 formed by photochemical oxidation of O_2, as discussed earlier). The main components of air pollution in the USA are listed in Table 13.3.

13.3.1 Depletion of stratospheric ozone – the "ozone hole"

The ozone in the stratosphere absorbs about 99% of the UV radiation in the 0.23–0.32 μm wavelength region (sometimes referred to as UV-B radiation), thus providing an effective

Table 13.3 The main components of air pollution in the USA, 2008 (fires and dust excluded).

Primary air pollutant	Annual emissions (million tons)	Major anthropogenic sources	Adverse health and environmental effects
Particulates		Fuel combustion, agriculture, unpaved roads, forest fires, oceans (sea salts)	Aggravates respiratory and cardiovascular problems; impairs visibility
PM 10	2		
PM 2.5	1		
Sulfur dioxide (SO_2)	11	Fuel combustion (especially high-sulfur coal; utilities and industrial plants); cement production; volcanoes	Causes sulfurous smog that can aggravate respiratory disease; contributes to acid rain and dry acid deposition; damages materials and vegetation
Carbon dioxide (CO_2)	1592 (carbon)	Fuel combustion (vehicles, power stations), forest fires	Possible global warming
Carbon monoxide (CO)	78	Fuel combustion (especially vehicles)	Reduces the ability of blood to carry oxygen to body tissues; aggravates cardiovascular disease
Nitrogen oxides (NO_x)	16	Fuel combustion (especially vehicles); fertilizers; biomass burning	Causes photochemical smog that can aggravate respiratory problems; contributes to acid rain, dry acid deposition, and ozone and particle formation
Volatile organic compounds (VOC)	17	Fuel combustion, solvents, paints	Increases risk of cancer; contributes to ozone formation

Sources of data: CO_2 data from Carbon Dioxide Information Analysis Center, Oak Ridge National Laboratory website **http://cdiac.ornl.gov**; the rest from US Environmental Protection Agency, Air Quality Trends website http://www.epa.gov/airtrends/aqtrends.html.

shield against the penetration of UV radiation that is harmful to most organisms. Calculations show that an effective ozone shield started to form at an O_2 level of 10^{-3} PAL and became firmly established at an O_2 level of ~10^{-2} PAL (Kasting *et al.*, 1992). In fact, life could not have been sustained on the Earth until there was enough oxygen in the atmosphere to develop an ozone shield for protection from the solar UV radiation. It has been estimated that the incidence of skin cancer in human beings would increase by 2% for every 1% decrease in the concentration of ozone in the stratosphere. Kasting *et al.* (1989) suggested that elemental sulfur vapor (S_8) produced photochemically from volcanogenic SO_2 and H_2S could have played a similar protective role in an anoxic, ozone-free, primitive atmosphere. Some of the earliest organisms were probably thermophillic bacteria that metabolized elemental sulfur.

The stratospheric ozone concentration near the equator, the region of maximum UV photon flux density on the Earth, is fairly constant around 250–300 Dobson units (DU), and it decreases toward the poles but with large seasonal fluctuations at higher latitudes. (The Dobson unit is a unit of measurement of atmospheric ozone columnar density, specifically ozone in the stratospheric ozone layer. It is named after the English physicist and meteorologist G.M.B. Dobson (1899–1976) who in 1928 invented the photoelectric spectrophotometer used in measuring the total ozone over an area from the ground. A Dobson unit for a gas is the amount of gas contained in a layer of the pure gas that is 10^{-5} m in thickness at 1 atm and 0°C; 1 DU = 4.4615×10^{-5} mole m^{-2}). As discussed earlier (Box 13.1), the concentration of O_3 in the stratosphere should be in a steady state because of the balance between production and destruction of O_3, but it is not so because the balance has been destroyed by anthropogenic input of ozone depleting chemicals (ODCs) into the atmosphere.

Significant loss of ozone in the lower atmosphere was first noticed over Antarctica in the 1970s by a research group from the British Antarctic Survey (BAS). In the fall of 1985, BAS scientists reported a much more dramatic depletion in total O_3 column abundance above Antarctica in the austral springs since 1977 – about a 30% decrease relative to pre-1980 measurements – a phenomenon commonly referred to as the "Antarctica ozone hole" (ozone concentration less than 220 DU, which is chosen as the baseline value for an "ozone hole" because total ozone values < 220 DU were not found over Antarctica prior to 1979). The story goes that the measured values were so low and unanticipated that the scientists suspected at first that their instruments were faulty, but measurements with replaced instruments confirmed the earlier results. Many subsequent studies have revealed significant stratospheric ozone depletion in many parts of the world. The most severe depletion has been observed over Antarctica (up to about 70% during September–November, the austral spring), which has now grown to a size greater than that of North America, and to a lesser extent over the Arctic. The "Antarctica ozone hole" is a seasonal event; it typically decreases by 20–25% during January–March.

Box 13.5 Chlorofluorocarbon compounds (CFCs)

Chlorofluorocarbons (CFCs) comprise a group of compounds containing fluorine, chlorine, and carbon atoms. The five main CFCs are CFC-11 (trichlorofluoromethane, $CFCl_3$), CFC-12 (dichlorodifluoromethane, CF_2Cl_2), CFC-113 (trichlorotrifluoroethane, $C_2F_3Cl_3$), CFC-114 (dichlorotetrafluoroethane, $C_2F_4Cl_2$), and CFC-115 (chloropentafluoroethane, C_2F_5Cl). "Freon" is a DuPont trade name for a group of CFCs (including CFC-11 and CFC-12), which are used primarily as refrigerants, but also in fire extinguishers and as propellants in aerosol cans.

Chloroflurocarbon compounds were first synthesized in 1928 by DuPont scientists during a search for a new, nontoxic substance that could serve as a safe refrigerant, replacing ammonia as the standard cooling fluid at that time. Chlorofluorocarbons filled this requirement very well because they are chemically inert (and, therefore, highly stable), nonflammable, nontoxic compounds that are superb solvents. They were considered miracle compounds and soon were in demand for a variety of applications: as coolants in refrigeration and air conditioners; as solvents in cleaners, particularly for electronic circuit boards; and as propellants in aerosols.

Scientists remained unaware of the possible impact of CFCs on the atmosphere until 1970 when the British scientist James Lovelock detected CFC-11 (at concentration levels in parts per trillion) not only in every air sample that passed over Ireland from the direction of London, but also in air samples directly off the North Atlantic uncontaminated by recent urban population. A few years later, in 1974, Mario Molina and Sherwood Rowland demonstrated in their laboratory that CFCs breakdown to form free chlorine radicals ($Cl^{\bullet}_{(g)}$), and predicted that these very reactive radicals could cause environmental problems by catalyzing the destruction of ozone in the stratosphere. Now we know how true that prediction was!

In the 1950s, David Bates and Marcel Nicolet had presented evidence that $OH^{\bullet}$ and $NO^{\bullet}$ could catalyze the recombination reaction $O_{3(g)} + O_{(g)} \Rightarrow 2O_{2(g)}$ (equation 13.19), thereby reducing the amount of stratospheric ozone. Support for this mechanism of ozone depletion came from the suggestion of Prof. Paul Crutzen in 1970 that N_2O gas produced by soil bacteria, fertilizers, and automobile engines with catalytic converters is stable enough to reach the stratosphere, get converted to NO by reaction with atomic oxygen, and catalyze the destruction of ozone (equations 13.10, 13.11, and 13.12).

Ozone can also be removed by reaction with natural chlorine, which is transferred from marine and terrestrial biological sources to the stratosphere mainly as methyl chloride (CH_3Cl), but the natural source accounts for only 25% of the chlorine that is transported across the tropopause. In 1974, Sherwood Rowland, Professor of Chemistry, University of California at Irvine, and his postdoctoral associate Mario J. Molina suggested that long-lived anthropogenic organic halogen compounds, such as chloroflurocarbons (CFCs) and bromofluorocarbons (see Box 13.5), might also catalyze the breakdown of ozone. The prediction turned out to be correct, and Crutzen, Molina, and Rowland were awarded the 1995 Nobel Prize in Chemistry in recognition of their work on stratospheric ozone.

The breakdown of ozone by CFC compounds in the stratosphere (at an altitude of 12–20 km and higher) is a complicated process. The CFC compounds absorb UV radiation in the 190–220 μm range, which results in photodissociation reactions. For example:

$$CF_2Cl_{2(g)}\ (\text{CFC} - 12) + \text{UV photon} \Rightarrow Cl^{\bullet}_{(g)} + CClF^{\bullet}_{2(g)} \quad (13.49)$$

$$CFCl_{3(g)}\ (\text{CFC} - 11) + \text{UV photon} \Rightarrow Cl^{\bullet}_{(g)} + CFCl^{\bullet}_{2(g)} \quad (13.50)$$

A small amount of chlorine is also generated by the breakdown of methyl chloride (CH_3Cl), which is produced biogenically from the oceans, from the burning of vegetation, and from volcanic emissions ($CH_3Cl + h\nu \Rightarrow CH_3 + Cl^{\bullet}$).

Once released from their parent compounds, the highly reactive $Cl^{\bullet}_{(g)}$ can destroy $O_{3(g)}$ molecules through a variety of catalytic cycles, the simplest being a reaction with $O_{3(g)}$ to form an intermediate compound, chlorine monoxide ($ClO^{\bullet}_{(g)}$), and finally $O_{2(g)}$:

$$Cl^{\bullet}_{(g)} + O_{3(g)} \Rightarrow ClO^{\bullet}_{(g)} + O_{2(g)} \quad (13.51)$$

$$ClO^{\bullet}_{(g)} + O_{(g)} \Rightarrow Cl^{\bullet}_{(g)} + O_{2(g)} \quad (13.52)$$

$$O_{3(g)} + O_{(g)} \Rightarrow 2O_{2(g)}\ (\text{net reaction}) \quad (13.53)$$

It is estimated that a single $Cl^{\bullet}_{(g)}$ atom participating in the above catalytic cycle is potentially capable of reacting with 100,000 $O_{3(g)}$ molecules, attesting to the large possible impact of even a small amount of CFC introduced into the stratosphere. A similar catalytic chain reaction would apply to bromine released from synthetic bromofluorocarbon compounds (e.g., CF_2ClBr), and from methyl bromide (CH_3Br) produced by marine plankton, agricultural pesticide (fumigant), and biomass burning. Actually, on an atom-per-atom basis, bromine is even more efficient than chlorine in destroying ozone, but its contribution to ozone destruction is minimal because there is much less bromine in the atmosphere at present. Laboratory studies have shown that F and I atoms participate in analogous catalytic cycles. However, in the Earth's atmosphere, F atoms react rapidly with water and methane to form strongly bound HF, whereas organic molecules that contain I react so rapidly in the lower atmosphere that they do not reach the stratosphere in significant quantities.

Most of the $Cl^{\bullet}_{(g)}$ and $ClO^{\bullet}_{(g)}$ released into the atmosphere (at all latitudes) are quickly tied up in chlorine reservoirs such as chlorine nitrate ($ClONO_{2\,(g)}$) and hydrochloric acid ($HCl_{(g)}$) by reactions such as:

$$ClO^{\bullet}_{(g)} + NO_{2(g)} + M \Rightarrow ClONO_{2(s)} + M \quad (13.54)$$

$$Cl^{\bullet}_{(g)} + CH_{4(g)} \Rightarrow HCl_{(g)} + CH_{3(g)} \quad (13.55)$$

Removal of the chlorine and nitrogen species arrests the destruction of ozone, but not for long. During the austral winter, when the temperature of the Antarctica stratosphere drops below −77°C (−196 K), nitric acid trihydrate (NAT) crystals ($HNO_3.3H_2O$) start to crystallize on small sulfuric acid–water aerosol particles, and $ClONO_{2(g)}$ and HCl are consumed by the following reactions that occur on the surface of the NAT solid particles:

$$ClONO_{2(g)} + H_2O_{(water-ice)} \Rightarrow HOCl_{(g)} + HNO_{3(adsorbed)} \quad (13.56)$$

$$ClONO_{2(g)} + HCl_{(adsorbed)} \Rightarrow Cl_{2(g)} + HNO_{3(adsorbed)} \quad (13.57)$$

However, nitric acid trihydrate cannot survive the increased solar UV radiation during the austral spring, and the catalytic destruction of ozone continues through regeneration of $Cl^{\bullet}_{(g)}$ with the arrival of spring season:

$$HOCl_{(g)} + \text{UV photon} \Rightarrow OH^{\bullet}_{(g)} + Cl^{\bullet}_{(g)} \quad (13.58)$$

$$Cl_{2(g)} + \text{UV photon} \Rightarrow Cl^{\bullet}_{(g)} + Cl^{\bullet}_{(g)} \quad (13.59)$$

It turns out that reactions (13.51) and (13.52) alone cannot account for the very large depletion of O_3 that characterizes the Antarctica ozone hole. A cycle catalyzed by $ClO^{\bullet}_{(g)}$ that appears capable of explaining about 75% of the observed O_3 depletion associated with the ozone hole, without involving atomic oxygen (which is in short supply in the stratosphere), is as follows (Hobbs, 2000; van Loon and Duffy, 2000):

$$ClO^{\bullet}_{(g)} + ClO^{\bullet}_{(g)} + M \Rightarrow ClOOCl_{(g)} + M \quad (13.60)$$

$$ClOOCl_{(g)} + \text{UV photon} \Rightarrow Cl^{\bullet}_{(g)} + ClOO^{\bullet}_{(g)} \quad (13.61)$$

$$ClOO^{\bullet}_{(g)} + M \Rightarrow Cl^{\bullet}_{(g)} + O_{2(g)} + M \quad (13.62)$$

$$2Cl^{*}_{(g)} + 2O_{3(g)} \Rightarrow 2ClO^{*}_{(g)} + 2O_{2(g)} \quad (13.63)$$

$$2O_{3(g)} + \text{UV photon} \Rightarrow 3O_{2(g)} \quad \text{(net reaction)} \quad (13.64)$$

It is now well established that CFC compounds are the chief culprits of stratospheric ozone depletion. The best evidence for this conclusion is the strong inverse correlation between ClO and ozone concentrations in the atmosphere (Fig. 13.11). CFC molecules are much heavier than nitrogen or oxygen but they can reach the stratosphere like other heavy gases, such as argon and krypton, because of wind turbulence that keeps the atmospheric gases well mixed, and because they are insoluble and highly stable. Natural sources of chlorine in the troposphere (mainly HCl from volcanic eruptions, and NaCl sprayed from the oceans) are four to five orders of magnitude larger than anthropogenic sources, but NaCl is highly soluble and quickly removed from the atmosphere by rain water, and measurements have shown that volcanic HCl amounts to only ~3% of the stratospheric chlorine. It is estimated that anthropogenic sources account for about 80% of the stratospheric chlorine.

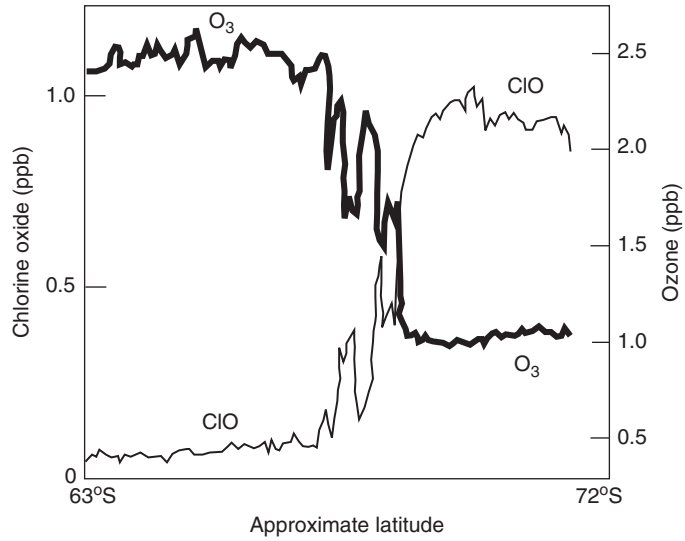

Fig. 13.11 Inverse correlation between chlorine oxide (ClO) and ozone concentrations in the atmosphere over the Antarctic polar region on September 16, 1987. Note that in the high latitudes of Antarctica, the very low ozone concentrations are matched by the relatively high concentrations of ClO produced by the reaction of ozone with Cl. The curves have been smoothed for simplicity. (After Anderson *et al.*, 1991.)

In a report released in 1976, the US National Academy of Sciences concluded that the ozone depletion hypothesis was strongly supported by scientific evidence. Scientists had calculated that if CFC production continued to increase at the going rate of 10% per year until 1990 and then remain steady, the global ozone loss would amount to 5–7% by 1995 and 30–50% by 2050. Responding to this prediction, the USA, Canada, Norway, and Sweden banned the use of CFCs in aerosol spray cans in 1978. Subsequently, as a result of international agreements (Montreal Protocol, 1987; London meeting, 1990; Copenhagen meeting, 1992), various countries have enacted laws for phased reduction and eventual ban on the production and use of CFCs. Promising substitutes, which have practically no ozone destroying potential, include hydrochlorofluorocarbons (HCFCs) and hydrofluorocarbons (HFCs) such as HFC-134a (CH_2FCF_3), HCFC-123 ($CHCl_2CF_3$), HFC-125 (CHF_2CF_3), and HFC-22 (CH_2F_2). The Antarctic "ozone hole," however, is expected to continue to exist for decades because of the longevity of CFCs (between 40 and 150 years) already present in the stratosphere. It is estimated that ozone concentrations in the lower stratosphere over Antarctica will actually increase by 5–10% by 2020 and then return to pre-1980 levels by about 2060–2075.

13.3.2 Smogs

The term "*smog*" was introduced in 1905 by Harold Antoine Des Voeux, a member of the Coal Smoke Abatement Society in London, to describe the combination of smoke and fog

Table 13.4 Comparison of general characteristics of sulfurous smog and photochemical smog.

Characteristics	Sulfurous smog	Photochemical smog
Primary pollutants	$SO_{2(g)}$, CO, carbon particulates	$NO_{(g)}$, $NO_{2(g)}$, CO, organics
Secondary pollutants	H_2SO_4, SO_4^{2-} aerosol	O_3, PAN and other organics, acids, aerosols
Principal sources	Industrial plants, households	Motor vehicles
Temperature	Cool (< 35°F)	Hot (> 75°F)
Relative humidity	High, usually foggy (> 85%)	Low, usually hot and dry (< 70%)
Type of temperature inversion	Radiation inversion	Subsidence inversion
Peak occurrence	Winter months early morning	Summer months around mid-day
Effect on human health	Lung and throat irritation	Eye and respiratory irritation

Sources of data: Raiswell *et al*., 1980; Andrews *et al*., 2004; Eby, 2004.

[sm(oke and f)og], which was then a common feature in several cities throughout Great Britain. *Smoke* is an aerosol composed of solid and liquid particulates and gases, which are emitted when a material undergoes combustion, together with the air that is entrained or otherwise mixed into the mass. The composition of smoke depends on the nature of the combusted material and the condition of combustion, mainly temperature and oxygen supply. Smoke inhalation, the primary cause of death in victims of indoor fires, kills by a combination of thermal damage, poisoning, and pulmonary irritation caused by CO, hydrogen cyanide and other combustion products.

Fog begins to form when water vapor (a colorless gas) condenses into tiny water droplets in the air. Aerosol particles in the air provide the nuclei required for such condensation. Fog normally occurs at a relative humidity near 100% (that is, when the air is saturated with moisture), which is achieved either by adding moisture to the air or by lowering the ambient air temperature. When the air is saturated with moisture, additional moisture tends to condense rather than stay in the air as water vapor.

The floating solid particles and liquid droplets in the smog, dominantly in the 0.2–2 μm size range, cause incoherent scattering of visible light. This results in reduced visibility, which is commonly referred to as *haze*. In addition, smogs are potentially harmful to human health, vegetation, and the environment if they contain pollutants (such as CO, NO_x, O_3, H_2SO_4, VOC, etc.).

There are two main types of smog: (i) *sulfurous smog* (also referred to as London-type or classical-type smog) and (ii) *photochemical smog* (also referred to as Los Angeles-type smog). A comparison of the general characteristics of the two types of smog is presented in Table 13.4.

Sulfurous smog

Most of the world's energy comes from the combustion of hydrocarbons, an oxidation reaction. With plenty of oxygen around, the hydrocarbon (represented here as "CH") is oxidized to CO_2 gas:

$$4CH + 5O_{2(g)} \Rightarrow 4CO_{2(g)} + 2H_2O_{(g)} \quad (13.65)$$

but this poses no direct health threat because CO_2 gas is not toxic. If enough oxygen is not available for combustion, the main product is CO gas:

$$4CH + 3O_{2(g)} \Rightarrow 4CO_{(g)} + 2H_2O_{(g)} \quad (13.66)$$

CO gas is toxic because hemoglobin in our blood takes up CO much faster than it takes up oxygen. With even less oxygen, the product is "smoke" containing particulates of solid carbon that can damage our lungs:

$$4CH + O_{2(g)} \Rightarrow 4C_{(s)} + 2H_2O_{(g)} \quad (13.67)$$

Additional problems arise because of impurities in the hydrocarbon fuels, the most important of which in the context of air pollution is sulfur, which on combustion is converted into SO_2 gas. Sulfurous smog results from the accumulation of smoke from fuels with high sulfur content, such as coal (~0.2 to 7.0 wt% S) and fuel oils (~0.5 to 4.0 wt% S) used in boilers, furnaces, domestic fireplaces, steam turbines, and thermal power stations. Where the atmosphere is humid, the unburnt carbon particles may serve as nuclei for condensation of water droplets. The water droplets become acidic with H_2SO_4 by dissolving atmospheric SO_2 gas, and form an irritating fog. Thus, sulfurous smog is associated with a high concentration of unburned carbon soot as well as elevated levels of atmospheric sulfur dioxide.

Sulfurous smog was a common phenomenon in the mid-20th century in cities such as London (UK.), but it reached a crisis level in the first week of December, 1952, due to the convergence of a series of conditions conducive to the formation of heavy sulfurous smog. On December 4, there was a cloud cover over the city that did not allow much of the incoming solar radiation to penetrate. Consequently, there was no appreciable warming of the lower layers of air, and the temperature at ground level fell precipitously. The air was stagnant, and the relative humidity climbed to 80%, which was sufficiently high to form a dense fog within the polluted city air during the night. Surface temperatures were close to freezing as the next day commenced.

The fog did not dissipate as the Sun rose the next morning. The high albedo of the fog layer limited the penetration of

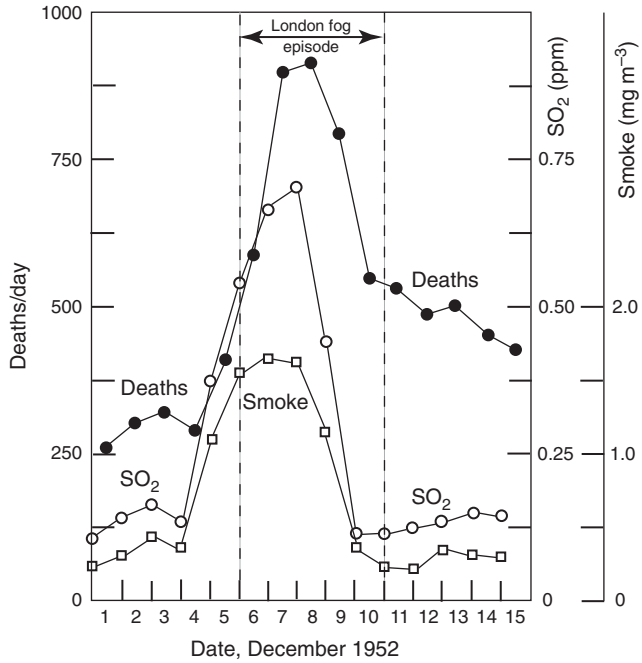

Fig. 13.12 Death toll resulting from the catastrophic London fog episode of December, 1952. Note the high degree of correlation among SO_2, smoke, and number of deaths. (Modified from Wilkins, 1954, Figure 4, p. 10.)

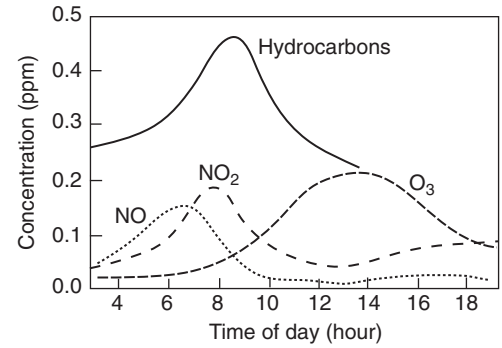

Fig. 13.13 Typical variations in the abundances of some important pollutants, on a 24-h cycle, produced during a photochemical smog event. (After van Loon and Duffy, 2000.)

sunlight to the lower layers of air, and the fog lingered within the Greater London Basin because of exceptionally light winds. By December 6, the noontime temperature had dropped to –2°C (28°F) and the relative humidity had increased to 100%. The cold temperatures and dampness increased the demand for indoor heating in homes and factories; ash, SO_2 gas, and soot from the burning of coal, the primary fuel used in heating, as well as pollutants from automobile exhausts, filled the stagnant air. By December 8, SO_2 reached peak concentrations of ~0.7 ppm (compared to typical annual mean concentration of ~0.1 ppm in polluted cities with large coal usage), and the peak smoke concentrations rose to ~1.7 mg m^{-3}. The resulting smog made breathing very difficult for the Londoners, and in many cases resulted in death. Meteorological conditions improved on December 9 when a breeze developed to remove the stagnant air conditions. The following day a cold front passed through, bringing with it fresh air from the North Atlantic and an end to the smog episode. It is estimated that the so-called "Killer Fog" killed ~4000 people between December 4 and 10 (Fig. 13.12), although it is not certain that the high concentrations of SO_2 and smoke were the sole reasons for the deaths. The low temperatures were probably a significant contributing factor. Sulfurous smog of this magnitude is unlikely to happen again because of much reduced usage of coal as a heating fuel and regulations regarding emissions of SO_2 gas from industrial plants (e.g., UK Clean Air Act of 1956; US Clean Air Act of 1970), but sulfurous smog is still fairly common in early winter mornings in cities with a very large population, a high concentration of coal-burning industrial plants, and humid stagnant air.

Photochemical smog

Photochemical smog was first noticed in Los Angeles during the Second World War; hence, the name Los Angeles-type of smog. It is characterized by high concentrations of a large variety of pollutants such as particulates, nitrogen oxides, ozone, carbon monoxide, hydrocarbons, aldehydes (molecules with a CHO functional group), and sometimes sulfuric acid. (Actually, the term photochemical smog is a misnomer because it involves neither smoke nor fog.) The reactions producing the pollutants are ultimately driven by photochemistry and hence have a diurnal cycle. The effects of the smog are most prominent at mid-day, when solar intensity is highest, and the smog tends to recede at night because of the short half-life of many of the compounds (Fig. 13.13).

Photochemical smog has its origin in the nitrogen oxides and hydrocarbon vapors (e.g., ethylene and butane) emitted by automobiles due to evaporation from fuel tanks and as unburned species in the exhaust, and by industrial plants. These emissions undergo photochemical reactions initiated by sunlight, generating a variety of secondary pollutants, including ozone. Together these products result in smog that pollutes the atmosphere, reduces visibility, and even causes breathing problems. Whereas ozone in the stratosphere plays a very beneficial role, ozone at the ground level is harmful to vegetation and human health, and is the pollutant of primary concern in photochemical smog. The chemical reactions that lead to photochemical smog are extremely complex, and still not completely understood. Outlined below are some of the major chemical reactions considered to be important in the present context.

Although N_2 gas is generally considered as inert, at high temperatures (e.g., in an internal combustion engine) molecular oxygen and nitrogen in the air dissociate into their atomic

states and participate in a series of reactions. The three principal reactions (all reversible) for forming NO are:

$$O_{(g)} + N_{2(g)} \Rightarrow NO_{(g)} + N_{(g)} \quad (13.68)$$

$$N_{(g)} + O_{2(g)} + \Rightarrow NO_{(g)} + O_{(g)} \quad (13.69)$$

$$N_{(g)} + OH_{(g)} + \Rightarrow NO_{(g)} + H_{(g)} \quad (13.70)$$

Note that the oxygen atom produced by reaction (13.69) can enter reaction (13.68) and promote a chain of reactions that produce NO. The net reaction obtained by adding 13.68 and 13.69 is:

$$N_{2(g)} + O_{2(g)} \Rightarrow 2NO_{(g)} \quad (13.71)$$

When the NO gas is exhausted to the open atmosphere, it is oxidized to $NO_{2(g)}$ by the following reactions:

$$2NO_{(g)} + O_{2(g)} \Rightarrow 2NO_{2(g)} \quad (13.72)$$

$$NO_{(g)} + O_{3(g)} \Rightarrow NO_{2(g)} + O_{2(g)} \quad (13.73)$$

$$RO_2^{\bullet} + NO_{(g)} \Rightarrow RO^{\bullet} + NO_{2(g)} \quad (13.74)$$

where $RO^{\bullet}$ and $RO_2^{\bullet}$ are referred to as peroxyl radicals in which R represents the root organic molecule.

The $NO_{2(g)}$ produced by the above reactions undergoes photodissociation at wavelengths below 0.38 μm into $NO_{(g)}$ and $O_{(g)}$, leading to rapid formation of $O_{3(g)}$:

$$NO_{2(g)} + \text{UV photon} \Rightarrow NO_{(g)} + O_{(g)} \quad (13.75)$$

$$O_{2(g)} + O_{(g)} + M \Rightarrow O_{3(g)} + M \quad (13.76)$$

$$\text{(net reaction) } NO_{2(g)} + O_{2(g)} + \text{UV photon} \Rightarrow NO_{(g)} + O_{3(g)} \quad (13.77)$$

where M is a catalytic molecule, most likely N_2 or O_2, that absorbs the excess energy released dring the formation of the ozone molecle. This is the main mechanism by which O_3 is formed *in situ* in the troposphere. However, not much ozone is accumulated directly by reaction (13.77) because it is depleted by the rapid reaction that regenerates NO_2 at the expense of ozone:

$$NO_{(g)} + O_{3(g)} \Rightarrow NO_{2(g)} + O_{2(g)} \quad (13.78)$$

Assuming that the ozone budget is determined by reactions (13.75), (13.76), and (13.78), the steady state concentration of O_3 in urban polluted air should be only ~0.03 ppmv, but typical values are well above this concentration and can reach 0.5 ppmv (Hobbs, 2000). Therefore, there must be other chemical reactions, such as the oxidation of hydrocarbon vapors released through the combustion of petroleum fuels, which also convert NO to NO_2 without consuming O_3. The reactions involving hydrocarbons are quite complex and the ubiquitous $OH^{\bullet}$ radical plays a prominent role in promoting these reactions (e.g., $O^* + H_2O \Rightarrow 2OH^{\bullet}$; $NO_2 + H_2O \Rightarrow NO + 2OH^{\bullet}$). As an example, if the petroleum vapor from vehicles is represented by CH_4, then the the net reaction may be written as

$$CH_{4(g)} + 2O_{2(g)} + 2NO_{(g)} + \text{sunlight} \Rightarrow H_2O_{(g)} + HCHO_{(g)} + 2NO_{2(g)} \quad (13.79)$$

The $OH^{\bullet}$ radical does not appear in the net reaction because it acts as a kind of catalyst. Aldehydes, such as formaldehyde (HCHO) formed by the above reaction, are eye irritants and, at high concentrations, tend to be carcinogens.

Conditions necessary for the development of photochemical smog are a high density of automobiles emitting a large amount of N_2O gas, large concentrations of reactive hydrocarbons (RH) from automobile exhausts and industrial plants, plenty of sunlight (high level of UV radiation), and stagnant air due to thermal inversion (i.e., temperature increasing, instead of decreasing, with altitude). Thermal inversion occurs when a layer of warm air above traps the ground-level cooler air, and prevents the cooler air from rising and dispensing the pollutants. A city which meets these conditions is, for example, Los Angeles, and it is no wonder that photochemical smog is a common phenomenon in this city. Photochemical smog, characterized by the reddish-brown hue of NO_2, is now a common feature of many major cities around the world (e.g., Athens, Bangkok, Mexico City, Beijing, and Tokyo).

13.3.3 Acid deposition

Acid deposition, popularly referred to as "acid rain," is the deposition of acidic gases, aerosol particles, or raindrops on the Earth's surface. The acidity in these deposits result from the formation of sulfuric acid (H_2SO_4), nitric acid (HNO_3), or hydrochloric acid (HCl) in the atmosphere. The main sources of these gases are volcanoes, biological processes on the Earth's surface, and human activities. Summarized below are the reactions pertaining to H_2SO_4, the most important contributor to acid deposition; simlar reactions can be written for HNO_3 and HCl.

Gas-phase transformation of sulfur dioxide gas

The gas-phase transformation mechanism involves the following steps (Jacobsen, 2002): (i) gas-phase oxidation of $SO_{2(g)}$ to $H_2SO_{4(g)}$; (ii) condensation of $H_2SO_{4(g)}$ and water vapor onto aerosol particles or cloud drops to produce a $H_2SO_{4(aq)}$–$H_2O_{(aq)}$ solution; and (iii) dissociation of $H_2SO_{4(aq)}$ to SO_4^{2-} and H^+ in the solution, thereby increasing its acidity. The relevant reactions are presented below:

$$SO_{2(g)} + OH_{(g)}^{\bullet} + M \Rightarrow HSO_{3(g)}^{\bullet} + M \text{ (catalyst)}$$
$$HSO_{3(g)}^{\bullet} + O_{2(g)} \Rightarrow HO_{2(g)}^{\bullet} + SO_{3(g)}$$
$$SO_{3(g)} + H_2O_{(l)} \Rightarrow H_2SO_{4(aq)}$$
$$H_2SO_{4(aq)} \Rightarrow 2H^+ + SO_4^{2-} \quad (13.80)$$

Aqueous-phase transformation of sulfur dioxide

When clouds are present, $SO_{2(g)}$ is consumed at a faster rate than can be explained by gas-phase chemistry alone. This is because of reactions in the liquid water droplets. The aqueous-phase transformation of $SO_{2(g)}$ involves the following steps (Jacobsen, 2002): (i) dissolution of $SO_{2(g)}$ into liquid water drops to produce $SO_{2(aq)}$; (ii) conversion (within the water drops) of $SO_{2(aq)}$ to $H_2SO_{3(aq)}$ and dissociation of $H_2SO_{3(aq)}$ to HSO_3^- and SO_3^{2-}; and (iii) oxidation of HSO_3^- and SO_3^{2-} to SO_4^{2-} (within the water drops). The relevant reactions are listed below:

$$\begin{aligned}
&SO_{2(g)} \Leftrightarrow SO_{2(aq)}\\
&SO_{2(aq)} + H_2O_{(l)} \Leftrightarrow H_2SO_{3(aq)} + H^+ + HSO_3^-\\
&HSO_3^- \Rightarrow H^+ + SO_3^{2-}\\
&HSO_3^- + H_2O_{2(l)} + H^+ \Rightarrow SO_4^{2-} + H_2O_{(aq)} + 2H^+ \text{ (at pH} \le 6)\\
&SO_3^{2-} + O_{3(aq)} \Rightarrow SO_4^{2-} + O_{2(aq)} \text{ (at pH} > 6)
\end{aligned} \tag{13.81}$$

The last reaction is written in terms of SO_3^{2-} and SO_4^{2-} because the HSO_3^-–O_3 reaction is relatively slow and, at pH > 6, most S(VI) exists as SO_4^{2-}.

Gas-phase transformation, which involves condensation onto raindrops, is the dominant process, whereas aqueous phase transformation, which involves dissolution in cloud drops and rain drops, is the more rapid process. The aqueous H^+ produced by these processes is the reason for the acidity of "wet" deposition. The acidity may be partly neutralized by the formation of sulfates, for example, $(NH_4)_2SO_4$ and $(NH_4)HSO_4$ if ammonia is present in the polluted air:

$$2NH_3 + 2H^+ + SO_4^{2-} \Rightarrow (NH_4)_2SO_4 \tag{13.82}$$

$$NH_3 + 2H^+ + SO_4^{2-} \Rightarrow (NH_4)HSO_4 \tag{13.83}$$

Besides deposition in precipitation ("wet" deposition, predominantly rainfall), sulfur is also transferred from the atmosphere to the Earth's surface by "dry" deposition. Dry deposition occurs when SO_2 gas is absorbed or dissolved directly on land by standing water, vegetation, soil, and other surfaces. Also, sulfate particles may settle out of the air or be trapped by vegetation (dry fallout). Dry deposition of SO_2 gas over land depends on the characteristics of the surface, small-scale meteorological effects, and the atmospheric concentration of SO_2. Dry deposition is greater near the emission sources of the gas and decreases rapidly with distance from the source. In some areas, dry acid deposition may be responsible for as much as 25% of total acid deposition (Berner and Berner, 1996).

Whether wet or dry, acid deposition is harmful to aquatic life, vegetation, structures such as buildings and monuments, and human health.

13.3.4 Greenhouse gases and global warming

The energy received by the Earth as a consequence of solar radiation is the source of the Earth's surface temperature, and this is the energy that sustains life on the Earth, and drives many of its processes such as the circulation of air and the hydrologic cycle. The annual mean global energy balance of the Earth–atmosphere system, expressed in terms of 100 arbitrary units of energy associated with the incoming solar radiation at the top of the atmosphere (TOA), is shown in Fig. 13.14. This radiation has wavelengths in the visible light and ultraviolet region of the electromagnetic spectrum. Out of the 100 units, 49 units are absorbed by the Earth, 20 units are absorbed by the atmosphere, and the rest (31 units) are reflected back into space by the Earth's surface (9 units) and atmosphere (22 units). The Earth receives an additional 95 units of energy resulting from absorption by atmosphere and reradiation to the Earth (greenhouse effect), raising the total to 144 units of energy. Thermal equilibrium at the surface of the Earth is achieved by the transfer of 144 units back to the atmosphere: 114 units as longwave (infrared) radiation, 23 units as evapotranspiration, and 7 units by heat fluxes associated with convection, turbulence, etc. Note that at TOA, the incoming 100 units of solar energy is balanced by 31 units of reflected and backscattered radiation and 69 units of outgoing longwave radiation, which ensures thermal equilibrium for the Earth–atmosphere system as a whole.

Greenhouse gases

The Earth's average annual surface temperature is about 15°C, whereas calculations show that, without an atmosphere, the Earth's average surface temperature at present would be a relatively chilly –18°C (0°F) (Kump *et al.*, 2004). This difference of 33°C is attributed to the warming of the atmosphere by absorption of the IR radiation (95 units, Fig. 13.14) returned from the Earth. The warming of the Earth's lower atmosphere due to natural gases that are transparent to most incoming solar radiation, but selectively absorb and reemit a portion of the outgoing thermal-IR radiation, is the natural *greenhouse effect* of the Earth's atmosphere, and the gases responsible for this effect are referred to as *greenhouse gases*. The phenomenon is analogous to the warmth retained inside a greenhouse in our gardens. The glass exterior of a greenhouse, like the greenhouse gases, allows the penetration of incoming solar radiation, but prevents the escape of a portion of the outgoing thermal-IR radiation, resulting in a net increase in the temperature of the interior (much like what happens when a car with closed windows is left in the sun for a while).

The major natural greenhouse gases are CO_2, CH_4, and N_2O. H_2O (water vapor) is also a strong absorber of infrared radiation, but is usually not considered to be a greenhouse gas because human activities have only a small direct influence on the amount of atmospheric water vapor. As mentioned earlier (section 13.2.2), the most plausible explanation for the

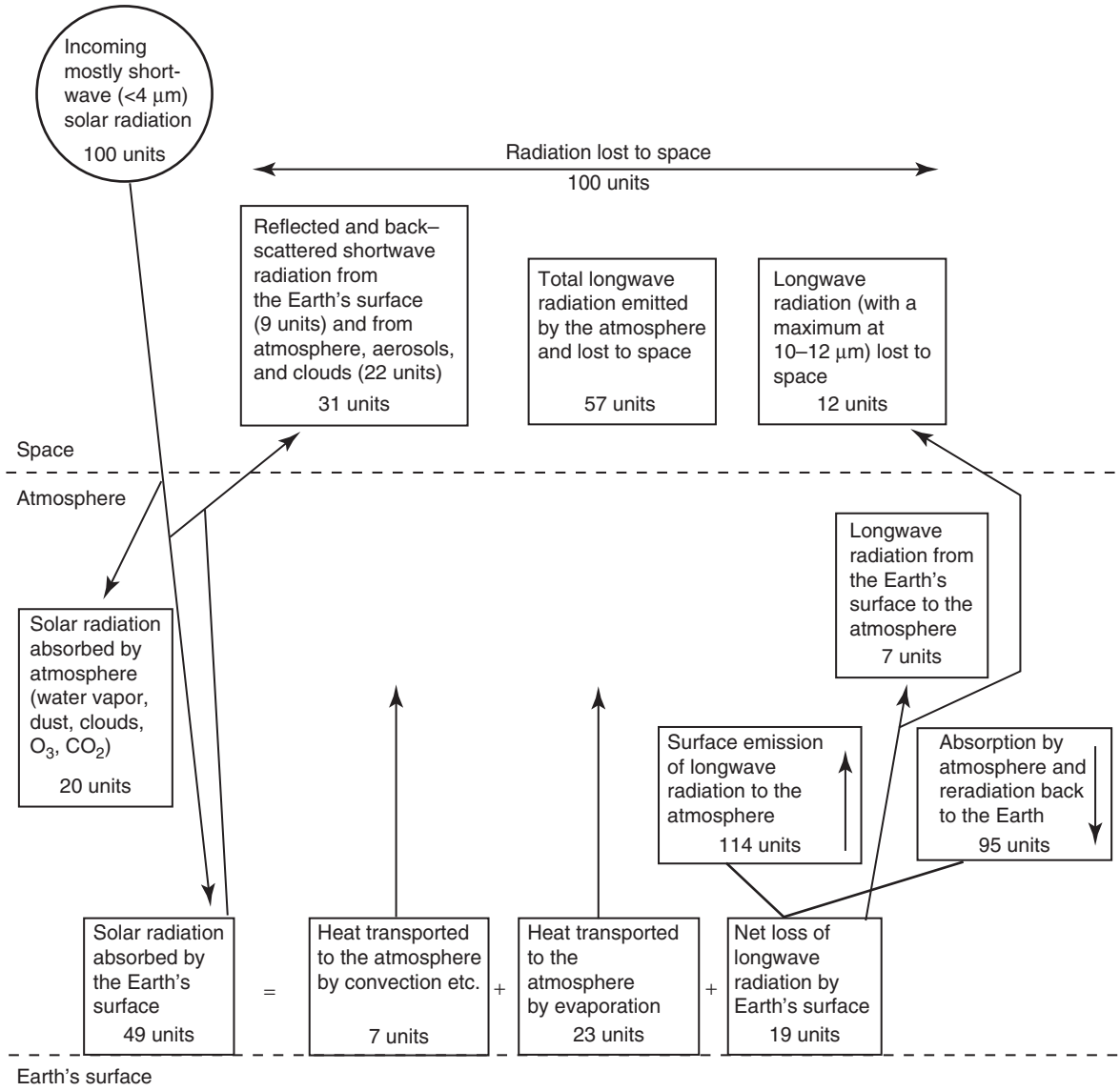

Fig. 13.14 Current estimate of the annual mean global energy balance of the Earth–atmosphere (unpolluted) system expressed in terms of 100 units of incoming solar energy (which represents 342 W m^{-2}) received at the top of the Earth's atmosphere (TOA). (Source of data: Houghton *et al.* (1996).)

absence of glaciation during the Archean, when solar luminosity was 20 to 30% lower than today, is the greenhouse warming due to CH_4 and CO_2 in the atmosphere (Pavlov *et al.*, 2000). Now we are threatened with the likelihood of too high a surface temperature because of sharp increases in the atmospheric concentrations of these gases since the Industrial Revolution, especially since the 1950s (Fig. 13.15). In addition, the atmosphere now contains trace amounts of a number of gases of anthropogenic origin, such as chlorofluorocarbons (CFCs) and hydrofluorocarbons (HFCs), which are exceptionally good absorbers of infrared radiation (in addition to being instrumental in ozone depletion in the stratosphere). The potential increase in the Earth's surface temperature due to increased concentrations of greenhouse gases (and aerosols) in the atmosphere is referred to as *global warming*, which can force global-scale climate changes. Currently recognized warning signs of global warming include an approximately 0.7°C (or 1.3°F) increase in the surface temperature during the 20th century, retreating mountain glaciers, significant melting of the Antarctica ice cap at the edges, and a rise in the sea level by at least 10 cm over the past 100 yr.

The *global warming potential* (GWP) of a greenhouse gas is calculated as the ratio of global warming from one unit mass of the greenhouse gas to one unit mass of carbon dioxide over

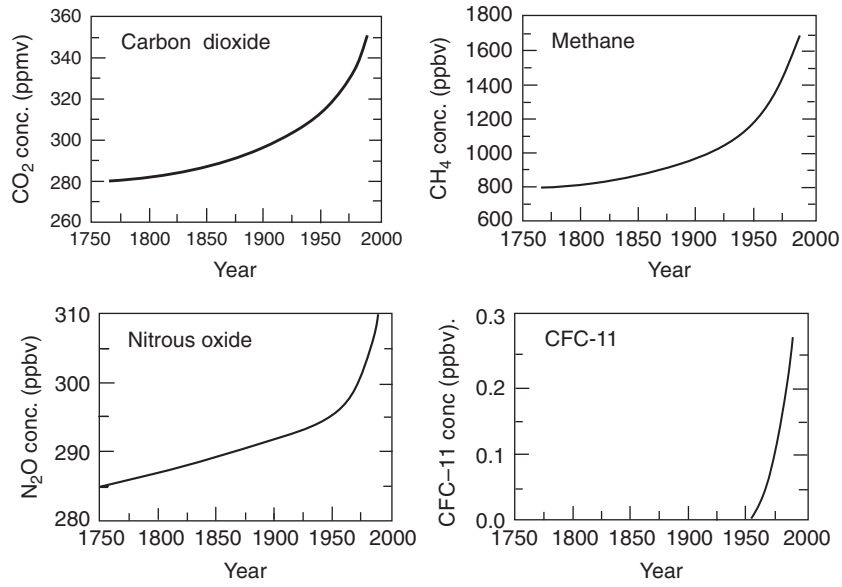

Fig. 13.15 Increases in the concentration of greenhouse gases in the atmosphere since circa 1750. Chlorofluorocarbons (represented by CFC–11), which are entirely anthropogenic in origin, became significant only after 1950. The concentrations of the other gases, which were relatively constant until the 1700s, have increased sharply since then due to human activities, especially combustion of fossil fuels. (After Intergovernmental Panel on Climate Change, 1990.)

Table 13.5 Radiative forcing and global warming potential of greenhouse gases.

Greenhouse gas	Concentration 1990 (ppmv)	Radiative forcing	Total radiative forcing (%)	Lifetime (yr)	Global warming potential (100 yr)
CO_2	354	1.5	61	50–200	1
CH_4	1.72	0.42	17	12	21
H_2O		0.14	6		
N_2O	0.310	0.1	4	120	310
CFC ± 11	0.00028	0.062	2.5	65	3400
CFC ± 12	0.000484	0.14	6	130	7100
Other CFCs		0.085	3.5		

Source of data: Berner and Berner (1966), Intergovernmental Panel on Climate Change (1966), Rodhe (1990), van Loon and Duffy (2000).

a particular time period. The Intergovernmental Panel on Climate Change (IPCC) recommends that GWP be calculated on a 100-year basis. Although CO_2 is considered to be the Earth's main greenhouse gas because of its much higher abundance relative to other greenhouse gases, complex molecules such as CH_4, N_2O, O_3, and the fluorocarbons have much higher global warming potential (Table 13.5).

Radiative forcing

The impact of a factor, such as a greenhouse gas, that can cause climate change is often evaluated in terms of its *radiative forcing*, which is a measure of how the energy balance of the Earth–atmosphere system is influenced when the factor under consideration is altered. Radiative forcing is usually quantified as the rate of energy change per unit area of the globe as measured at the top of the atmosphere, and is expressed in units of Watts per square meter (W m^{-2}). Positive forcings lead to warming of climate, and negative forcings to cooling. The word 'radiative' reminds us that we are looking at the balance between incoming solar radiation and outgoing infrared radiation within the atmosphere, and the word 'forcing' emphasizes that the Earth's radiative balance is being forced out from its normal state.

The principal components of the radiative forcing of climate change over the period from circa 1750 (the beginning of the industrial era) to 2005 are presented in Fig. 13.16. About 60% of the positive radiative forcing is caused by CO_2 (Table 13.4); this is the reason for global concern about the increasing emission of CO_2 to the atmosphere from anthropogenic sources. The greenhouse gases CH_4, N_2O, and halocarbons, despite their combined concentration of ~2 ppmv, have been significant contributors to radiative forcing because of their high global warming potential. Most of the negative forcing is caused by the aerosol particles in the atmosphere, both directly through reflection and absorption of solar and infrared radiation and indirectly through the changes they cause in cloud properties.

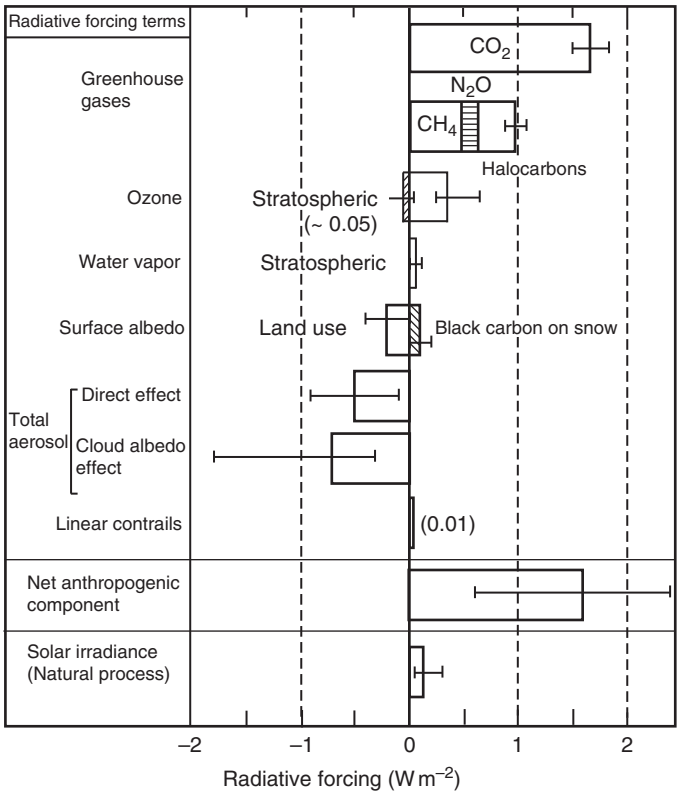

Fig. 13.16 Global average radiative forcing estimates and ranges in 2005, relative to 1750 (the start of the industrial era), for anthropogenic greenhouse gases and other important agents and mechanisms. The thin black line attached to each bar represents the range of uncertainty for the respective value. Positive forcings lead to warming of climate, and negative forcings lead to cooling. Albedo is a measure of the reflectivity of a surface, expressed as the percentage of incoming light that is reflected. Linear contrails refer to linear trails of condensation produced by aircrafts. The only increase in natural forcing of any significance between 1750 and 2005 occurred in solar irradiance. (Adopted from Intergovernmental Panel on Climate Change, 2007.)

The average global temperature has risen by about 0.7°C over the past 100 yr, and the warming trend is likely to continue without substantive changes in global patterns of fossil fuel consumption. It has been estimated that the global average temperature would increase between 1.4 and 5.8°C over the next 100 yr as a result of increases in concentrations of atmospheric CO_2 and other greenhouse gases. Melting of polar ice caps in response to this magnitude of global temperature increase could cause significant rise in average sea level (0.09 to 0.88 m), exposing low-level coastal cities or cities located by tidal rivers such as New Orleans to increasingly frequent and severe floods. In addition, increased concentrations of CO_2 could have a significant impact on the global distribution of vegetation because some plant species respond more favorably to increases in CO_2 than others.

13.4 The hydrosphere

Hydrosphere is the component of the Earth supersystem that includes the various reservoirs of water and ice on or close to the Earth's surface. The global ocean, covering about 71% of Earth's surface to an average depth of 3800 m (12,5000 ft), is the predominant feature of the hydrosphere. The oceans contain ~1370×10^6 km^3 of water and account for 97% of Earth's water; groundwater, rivers, lakes, glaciers and ice caps account for the rest of the hydrosphere.

13.4.1 Composition of modern seawater

The oceans constitute a complex geochemical system of amazingly constant bulk composition. The major dissolved constituents, commonly assumed to be present as ionic species (free ions plus ion pairs formed with ions of opposite charge), are almost the same ones encountered in continental waters: Na^+, Ca^{2+}, Mg^{2+}, K^+, Cl^-, SO_4^{2-}, and HCO_3^- (Table 7.1). These seven constituents account for more than 99% of the dissolved

Table 13.6 Selected minor and trace dissolved constituents of seawater (excluding constituents < 1 mm).

	Concentration			Concentration	
Constituent	**μg kg^{-1} (ppb)**	**μM (micromoles L^{-1})**	**Constituent**	**μg kg^{-1} (ppb)**	**μM (micromoles L^{-1})**
Br^-	66,000–68,000[a]	840–880	H_4SiO_4	<30–5000	<0.5–180
H_3BO_3	24,000–27,000[a]	400–440	NO_3^-	<60–2400	1–40
Sr^{2+}	7700–8100[a]	88–92	NO_2^-	<4–170	<0.1–4
F^-	1000–1600[a]	50–85	NH_4^+	<2–40	<0.1–2
CO_3^{2-}	3,000–18,000	50–300	Orthophosphate	<10–280	<0.1–3
O_2	320–9600	10–300	Organic carbon	300–2000	–
N_2	9500–19,000	300–600	Organic nitrogen	15–200	–
CO_2	440–3520	10–80	Li^+	180–200	26–27
Ar	360–680	9–17	Rb^+	115–123	1.3–1.4

[a]For a salinity of 35%.

Source of data: compilation by Berner and Berner (1996).

constituents in both seawater and river water. The concentrations of ions as shown on Table 7.1 may vary by about ±10% corresponding to changes in salinity (the total dissolved salt content, which varies from 33‰ to 38‰ in the open ocean), but their ratios vary by less than 1% (Wilson, 1975). On the other hand, the concentration ratios of dissolved minor and trace elements relative to chloride do show significant variations from place to place (Table 13.6), especially the constituents such as phosphates and nitrates, which are nutrients for plankton and reflect the metabolic activities of the organisms that are abundant only in the well-lit, upper few tens or hundreds of meters.

Dissolved constituents in seawater are of three kinds: *conservative*, *recycled*, and *scavenged* (Walther, 2009). The concentrations of conservative constituents (such as Br^-, Cl^-, Mg^{2+}, Na^+) relative to other conservative constituents remain constant. This results in a constant concentration versus depth profile for each conservative element, unless its absolute abundance is modified by a change in the volume of seawater. Such constituents usually have long residence times (> 10^6 years) in the ocean. In contrast, recycled and scavenged constituents are nonconservative and their concentrations vary significantly from place to place. Recycled constituents refer to those (such as organic C, H_4SiO_4, Ca^{2+}, NO_3^-, and PO_4^{3-}) that are recycled through the involvement of organisms. Organisms use these constituents as nutrients and, when they die and start sinking toward the ocean floor, their decomposition and dissolution return the constituents to the seawater. Concentrations of such constituents tend to increase with increasing depth. Scavenged constituents (such as Pb, Mn, Sn) are those that are adsorbed onto the surfaces of solid articles; the concentration of a scavenged constituent is strongly influenced by equilibrium and it typically decreases with increasing depth in the ocean. Broecker and Peng (1982) classified the dissolved chemical constituents in seawater as: *biolimiting constituents,* which are almost totally depleted in surface water due to interaction with organisms (examples: NO_3^-, Zn^{2+}, Cd^{2+}, HPO_4^{-2}, H_4SiO_4, and H_4GeO_4); *biointermediate constituents,* which are partially depleted in surface water (examples: Ca^{2+}, Mg^{2+}, C, etc.); and *biounlimited constituents,* which show no measurable depletion in surface water (examples:Na^+, K^+, etc.).

The composition of modern seawater can be accounted for by steady-state mixing of the two major contributors to ocean chemistry, river water (RW) and mid-ocean ridge (MOR) hydrothermal brines, coupled with precipitation of solid $CaCO_3$ and SiO_2 phases (Spencer and Hardie, 1990). The major compositional gradients in the oceans are vertical, driven by biological cycling processes. The main process is removal of constituents from surface seawater by organisms, and destruction of the organism-produced particles after downward movement. Thus, the most dramatic change occurs in the surface water, and deep water is enriched in most constituents relative to suface water. The only major exception is dissolved oxygen. An example from the northern Pacific Ocean

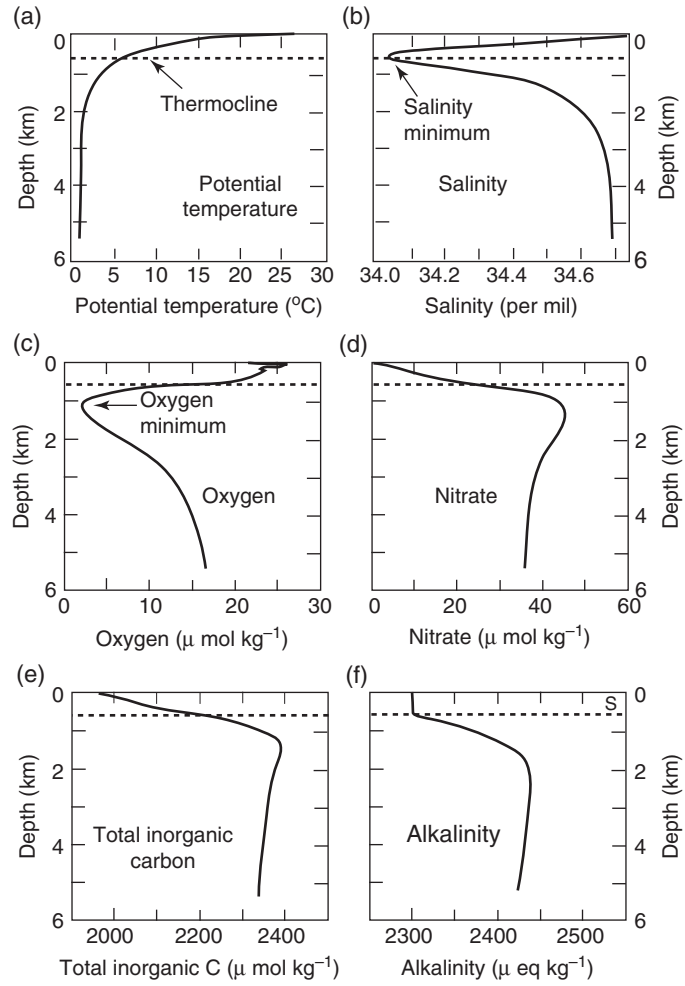

Fig. 13.17 Depth profiles at GEOSECS station 214 in the North Pacific Ocean (32°N, 176°W): (a) potential temperature, (b) salinity, (c) oxygen, (d) nitrate, (e) total dissolved inorganic carbon ($\Sigma CO_2 = CO_2 + HCO_3^- + CO_3^{2-}$), and (f) alkalinity. The dashed line in each figure represents the depth of the salinity minimum. The thermocline is a region (about 1 km thick) of steeply decreasing temperature gradient that separates the surface water (the top 50–300 m that is stirred by the wind and is well mixed) from the deep water. (Modified from Broecker and Peng, 1982, Figure 1-1, p. 4 and Figure 1-2, p. 5.)

(32°N, 176°W) based on data gathered by the Geochemical Ocean Sections program (GEOSECS) during the 1970s is presented in Fig. 13.17. Solar energy is absorbed almost completely within only a few tens of meters of seawater, giving rise to a warm surface zone below which lies a cold ocean, with a nearly constant *potential temperature* of 2°C for most of the deep ocean (Fig. 13.17a). (Water temperatures at depth are generally reported as "potential temperatures," which refer to measured *in situ* temperatures from which the small temperature increase due to compression exerted by the water column has been deducted.) The transitional region between these two zones is called the *thermocline*. As expected, the position of the thermocline varies with distance from the equator and the time

Table 13.7 Influx of dissolved constituents by rivers into the oceans and the time reqauired for these constituents to reach oceanic accounts.

Dissolved constituent	Concentration		Mass in the oceans[c] ($\times 10^{20}$ g)	Annual flux from rivers[d] ($\times 10^{14}$ g)	Time for river fluxes to attain oceanic amounts ($\times 10^{6}$ yr)
	Average river water[a] (ppm)	Average seawater[b] (ppm)			
Cl^-	7.8	19,000	260.3	2.53	102.9
Na^+	6.3	10,500	143.8	2.05	70.2
Mg^{2+}	4.1	1300	17.8	1.33	13.4
SO_4^{2-}	11.2	2650	36.3	3.64	10.0
Ca^{2+}	15.0	400	5.5	4.87	1.1
K^+	2.3	380	5.2	0.75	6.9
HCO_3^-	58.4	140	1.9	18.98	0.1
Br^-	–	65	0.9	–	–
CO_3^{2-}	–	18	0.2	–	–
Sr^{2+}	–	8	0.1	–	–
SiO_2	13.1	6	0.1	4.26	0.02
Organic C	9.6	0.5	0.01	3.12	0.002

[a]Livingstone (1963); [b]Goldberg (1957).

[c]Total mass of ocean water used in the calculation = 1.37×10^{21} kg.

[d]Total river discharge into the oceans per year used in the calculation = 374×10^{14} kg.

of year, and it exercises a major control on the vertical concentration profile of nonconservative dissolved constituents.

The *salinity* of seawater (the total dissolved salts, usually expressed in per mil, ‰) varies from ~30‰, where major rivers discharge into the ocean, to ~40‰ in shallow waters of arid areas, where evaporation is faster than mixing, the average being about 35‰. The vertical salinity profile shows a salinity minimum at a depth of about 600 m, above which the salinity increases toward the surface because of increased evaporation, and a fairly constant salinity in the cold deep ocean (Fig. 13.17b).

Concentrations of dissolved gases in seawater (except for gases such as O_2, CO_2, H_2S, and N_2, which are involved in metabolic processes of organisms) are largely determined by their solubility, which is controlled by the atmospheric partial pressure of the gas. As shown in Fig. 13.17c, the dissolved O_2 content of the surface water in contact with the atmosphere is slightly in excess of its equilibrium value of 0.25 mmol kg^{-1} at 25°C and 1 bar. This is due to the contribution of local photosynthesis to the near-surface O_2 budget. Generally, an oxygen minimum zone develops below the minimum salinity depth because O_2 is consumed during oxidation of organic matter raining down from above. The O_2 level increases in the deep ocean because of the influx of cold oxygenated water that sinks to the bottom of the oceans at the Earth's north and south poles. The present oceans are aerobic because the amount of organic matter is not enough to consume all of the available dissolved O_2. Nitrate is produced as O_2 is consumed, so that the nitrate profile (Fig. 13.17d) has an inverse relationship with that for O_2. The alkalinity of the seawater changes (Fig. 13.17f) mainly because of extraction of Ca by organisms to form $CaCO_3$ skeletal material. Much the $CaCO_3$ skeletal material dissolves after falling to the deep ocean; this accounts for the higher concentration of inorganic carbon ($\Sigma CO_2 = CO_2 + HCO_3^- + CO_3^{2-}$) in the deep ocean (Fig. 13.17e).

The pH of seawater at a given P_{CO_2} is buffered by the complex equilibrium,

$$H_2O + CO_{2(aq)} \Leftrightarrow H_2CO_{3(aq)} \Leftrightarrow H^+ + HCO_3^- \Leftrightarrow 2H^+ + CO_3^{2-} \quad (13.84)$$

The pH varies within the narrow range of ~7.8 to 8.4 because of the relatively small variation in the HCO_3^-:CO_3^{2-} ratio (Skirrow, 1975).

13.4.2 Mass balance of dissolved constituents in seawater

Rivers are the major sources of dissolved and particulate materials in the oceans, and it was once thought that the much higher salinity of the oceans (~35‰ compared to ~< 0.2‰ for average river water) is the result of incremental accumulation of the river load over geologic time. However, the compositions of sedimentary rocks and the nature of the fossil record do not indicate any radical change in seawater composition, at least since the Cambrian Period, and possibly over the past 2 Gyr (Holland, 1972, 1984). The only changes for which there is good evidence are a decrease in the concentration of dissolved silica as siliceous organisms developed in the Precambrian, and fluctuations in the oxidation state of the oceans (see section 13.5.2). At the present rate of salt addition

by rivers, it would require only a few tens of million years at best to account for the mass of ocean salt. Moreover, when the times required to accumulate the individual dissolved constituents in seawater are calculated, the storage times are found to be only a few million years (Table 13.7). It appears that the seawater composition has maintained some sort of steady-state balance over a long time. Then, the questions we are faced with are: how was river water composition modified to seawater composition that is so different (Table 13.7); and how has the steady-state been maintained over geologic time?

Processes capable of modifying the chemistry of seawater, besides addition of constituents by rivers, fall into six categories (Drever *et al.*, 1988; Berner and Berner, 1996).

(1) Biological processes such as the synthesis of soft tissues or organic matter, secretion of skeletal hard parts, and the bacterial decomposition of organic matter upon death (see Berner and Berner, 1996, for a list of major processes of organic matter decomposition in marine sediments). Such processes exert major controls on the concentration of recycled constituents (Ca^{2+}, HCO_3^-, SO_4^{2-}, H_4SiO_4, CO_2, O_2, NO_3^-, and PO_4^{3-}).
(2) Seafloor volcanics–seawater interaction, both high temperature (200–400°C) reactions at mid-oceanic ridge axes and off-axis low temperature reactions.
(3) Reaction of seawater with detrital solids (silicate minerals and clay minerals) transported from the continents. Such reactions may involve an entire detrital mineral, forming generally a more cation-rich mineral (referred to as "reverse weathering," Mackenzie and Garrels, 1966), or affect only the mineral surface by ion exchange, especially of Ca^{2+} for Na^+. Ion exchange is particularly important for trace elements.
(4) Ocean-to-air transfer of cyclic salts (sea-salt particles blown from the ocean surface onto the land).
(5) Precipitation of evaporite and sulfide minerals, an important mechanism for the removal of Na^+, Ca^{2+}, Cl^-, and SO_4^{2-} from seawater.
(6) Special processes that generally affect only one or two constituents. These include porewater burial of Cl^- and Na^+, and a number of processes unique to the nitrogen and phosphorous cycles (nitrification, denitrification, N_2 fixation, adsorption of phosphate on ferric oxides, and authigenic apatite formation).

Input and output processes for several important dissolved constituents have been discussed by Berner and Berner (1996) and are summarized in Table 13.8. It is likely that these processes have been affected by changes in global parameters such as the rate of tectonic uplift, the rate of seafloor spreading, oxic and anoxic events, and biologic evolution. Perhaps, the apparent constancy of the seawater composition through the geologic record was a consequence of the coupled effects of such changes.

Estimates of inputs and outputs reveal that many of the dissolved constituents in seawater are markedly out of balance (Berner and Berner, 1996). For example, the concentrations of Na^+, Cl^-, and SO_4^{2-} have been increasing in the modern era, although they appear to be in balance on a time scale of millions of years. The present imbalance is due to a lack of evaporite basins for the precipitation of halite (NaCl) and gypsum ($CaSO_4.2H_2O$), and because Cl^- and SO_4^{2-} are being added to seawater through anthropogenic pollution. Over the long term (the past 25 Myr), the input and output of Ca^{2+} have been in balance (within the errors of estimation), but the removal of Ca^{2+} from the present oceans (almost entirely by biogenic $CaCO_3$ deposition) considerably exceeds its input, and this is caused by excessively rapid deposition of $CaCO_3$ on the continental shelves as a result of the rapid post-Ice Age rise in sea level.

13.5 Evolution of the oceans over geologic time

13.5.1 Origin of the oceans

Age of the oceans

The occurrence of chemical sediments (such as BIFs) in the 3.8-Gyr-old Isua sequence in west Greenland (Nutman *et al.*, 1997; Whitehouse *et al.*, 1999) is indisputable evidence that liquid water was present on the Earth by that time. A much earlier presence of liquid water on the Earth has been inferred from the ^{18}O-enriched oxygen isotope composition of >3900-Myr-old magmatic zircon crystals recovered from the Jack Hills metasedimentary belt of Western Australia (Mojzsis *et al.*, 2001; Peck *et al.*, 2001; Cavosie *et al.*, 2005). Cavosie *et al.* (2005) reported that preserved magmatic $\delta^{18}O_{V\text{–}SMOW}$ values for individual Jack Hills zircon crystals (4400–3900 Ma) range from 5.3 to 7.3%, increasingly deviating from the mantle range of 5.3 ± 0.3% as the crystals decrease in age from 4400 to 4200 Ma; elevated values up to 6.5% occur as early as 4325 Ma and up to 7.3% by 4200 Ma. A compilation of $\delta^{18}O_{V—SMOW}$ values for zircons ranging in age from 4.4 Ga to 0.2 Ma by Valley *et al.* (2005) shows that $\delta^{18}O_{V—SMOW}$ values >7.5% occur only in zircons younger than 2500 Ma.

Oxygen isotope ratios of magmatic zircon crystals reflect the $\delta^{18}O$ of parental magma and, because of the slow rate of oxygen diffusion in zircon in most crustal environments, unaltered zircon crystals preserve the oxygen isotope ratio attained at the time of crystallization. With rare exceptions, the mantle is a remarkable homogeneous oxygen isotope reservoir, and magmatic zircons in high-temperature equilibrium with mantle magmas have average $\delta^{18}O_{V\text{–}SMOW}$ = 5.3 ± 0.6‰ (Valley, 2003), and this mantle value has remained nearly constant (±0.2‰) over the past 4.4 Gyr (Valley *et al.*, 1998; Mojzis *et al.*, 2001). Closed-system fractional crystallization can result in higher $\delta^{18}O_{V\text{–}SMOW}$(whole rock) values, up to ~6.3‰,

Table 13.8 Major processes affecting the concentration of specific dissolved constituents in seawater numbered in the order of approximate decreasing importance, and the status of their mass balance. (Modified from Berner and Berner, 1996.)

			Mass balance	
Constituent	**Input processes**	**Output processes**	**Long-term budget**	**Present-day budget**
Chloride (Cl^-)	1. Rivers (including pollution)	1. Evaporative NaCl deposition 2. Net ocean–air transfer 3. Porewater burial	B	NB
Sodium (Na^+)	1. Rivers (including pollution)	1. Evaporative NaCl deposition 2. Net ocean–air transfer 3. Cation exchange 4. Volcanics–seawater reaction 5. Porewater burial	B	NB
Sulfate (SO_4^{2-})	1. Rivers (including pollution) 2. Polluted rain and dry deposition	1. Evaporative $CaSO_4$ deposition 2. Biogenic pyrite formation 3. Net ocean–air transfer	B	NB
Magnesium (Mg^{2+})	1. Rivers	1. Volcanics–seawater reaction 2. Biogenic Mg-calcite deposition 3. Net ocean–air transfer	B	?
Potassium (K^+)	1. Rivers 2. High-temperature volcanics–seawater reaction	1. Low-temperature volcanics–seawater reaction 2. Fixation on clay minerals near river mouths 3. Net ocean–air transfer	B	?
Calcium (Ca^{2+})	1. Rivers 2. Volcanics–seawater reaction 3. Cation exchange	1. Biogenic $CaCO_3$ deposition 2. Evaporitic $CaSO_4$ deposition	NB	NB
Bicarbonate (HCO_3^-)	1. Rivers (including pollution) 2. Biogenic pyrite formation	1. $CaCO_3$ deposition	NB	NB
Silica (H_4SiO_4)	1. Rivers 2. Volcanics–seawater reaction	1. Biogenic silica precipitation	?	NB
Phosphorus (PO_4^{3-}, HPO_4^{2-}, $H_2PO_4^-$, organic P)	1. Rivers (including pollution) 2. Rain and dry fallout	1. Burial of organic P 2. $CaCO_3$ deposition 3. Adsorption on volcanogenic ferric oxides 4. Phosphorite formation	B	NB
Nitrogen (NO_3^-, NO_2, organic N)	1. N_2 fixation 2. Rivers 3. Rain and dry deposition	1. Denitrification 2. Burial of organic N	NB	?

B = balanced; NB = not balanced.

in more silicic magmas. $\delta^{18}O_{V\text{–}SMOW}$ values of magmatic zircons significantly higher than ~6.3‰ have been interpreted to require that the host magma incorporate a significant component of recycled continental crust that had been enriched in ^{18}O by interaction with liquid water under surface or near-surface low-temperature conditions during weathering or diagenesis (Mojzsis *et al.*, 2001; Peck *et al.*, 2001).

The above interpretation is consistent with the presence of a hydrosphere of some extent interacting with the crust by ~4.3 Ga, possibly even by ~4.4 Ga, very soon after the formation of the Earth, but it has been questioned by some authors. Hoskin (2005) proposed that the high $\delta^{18}O$ signature could be the result of localized exchange with a high $\delta^{18}O$ (6–10‰ or higher) fluid. Nemchin *et al.* (2006) determined that younger oscillatory zoned Jack Hill zircon crystals (uniquely interpreted as representing crystallization from a melt), including oscillatory zoned cores in complex grains, have $\delta^{18}O$ values lower than 6.5‰, which are within the range for zircons in

high-temperature equilibrium with the normal mantle rocks of $\delta^{18}O = 5.3 \pm 0.6‰$. Nevertheless, as discussed earlier (section 13.2.1), theoretical models indicate that the Earth's atmosphere and oceans had formed within a few tens of millions of years after the end of the main accretion period. The early appearance of oceans, a prerequsite for the origin and evolution of life, has been instrumental in the extensive sequestration of atmospheric CO_2 in the form of sedimentary calcium carbonate minerals (such as aragonite and calcite), thus preventing the development of a runaway greenhouse atmosphere, the likely cause of the lack of a hydrosphere on planet Venus.

Source(s) of water

Where did the Earth's water come from and how did it accumulate to form the oceans? We do not know for sure, but let us discuss some possibilities. Water can be made *in situ* by oxidizing H_2 ($2H_2 + O_2 \Rightarrow 2H_2O$) or organic molecules ($CH_2O + O_2 \Rightarrow CO_2 + H_2O$), but neither works well for the Earth. The former gives a D/H isotopic ratio that is too low, and the latter gives a C/H ratio that is too high (Zahnle, 2006). Besides, there was little free oxygen in the proto-atmosphere for such oxidation reactions on a large scale. Other suggested sources of water in the terrestrial planets include: (i) comets; (ii) hydrous asteroids; (iii) phyllosilicates migrating from the asteroid belt; and (iv) accreting "wet" planetesimals. As discussed below, none of these sources offers a completely satisfactory option.

Comets. For a while, the idea of post-accretion addition of water to an anhydrous proto-Earth from exogenous sources, such as comets and hydrous asteroids, had gained ground because of two reasons. First, it was widely believed that the inner Solar System was too hot for hydrous phases to be thermodynamically stable and be available for accretion. Second, the Earth (and other terrestrial planets) appear to have experienced one or more magma ocean events that would have led to degassing of any existing water acquired in the course of accretion. However, a cometary source of the water (e.g., Deming, 2002; Lunine, 2006) is untenable because of a large discrepancy in hydrogen isotopic ratios. The D : H ratios in the three comets that have been studied so far – Halley, Hyakutake, and Hale-Bopp, all from the Oort Cloud (a spherical shell of cometary nuclei whose average radius is 50,000 AU and which probably has 10^{11} comets) – fall within the range $3.16 \pm 0.34 \times 10^{-4}$, essentially twice the value of 1.56×10^{-4} in Standard Mean Ocean Water (SMOW) (Drake, 2005; Owen and Bar-Nun, 2000). Assuming that these three comets are representative of all comets (a shaky claim as we have not yet sampled any comets from the Kuiper Belt), a late-accreting veneer of volatile-rich material delivered by comets would be limited, variously estimated as < 20% (Abe *et al*., 2000) to ~35% (Owen and Bar-Nun, 2000) to a maximum of 50% (Drake, 2005) of the water in the Earth's oceans; the rest had to be picked up from some other source, such as the solar nebula, with D : H ratio less than that in SMOW. Moreover, Dauphas and Marty (2002) calculated that comets contributed $<0.7–2.7 \times 10^{22}$ g of material to the accreting Earth, which is less than 1% of the mass of water in one Earth ocean (a minimum mass of 1.4×10^{24} g; Matsui and Abe, 1986a). A limitation of the argument against a cometary source of water is the possibility that we are yet to sample representative comets.

Hydrous asteroids. The mass of the Earth continues to grow at present with the addition of 10^6 to 10^7 kg of meteorites each year, and such additions have certainly occurred throughout geologic time. During accretion, the mass flux of material added to the Earth through meteorites is estimated to have been about 2×10^9 times greater than at present. This contribution dropped five to ten orders of magnitude during the first 100 Myr and has continued to decline ever since, except during a resurgence called the *Late Heavy Bombardment* (LHB), an event of intense bombardment by planetary bodies from a dominantly asteroid reservoir between 3.85 and 3.9 Ga (Koeberl, 2006).

The occurrence of up to ~9 wt% water in carbonaceous chondrites raises the possibility that hydrated asteroids could have been the source of Earth's water. From model computations, Morbidelli *et al*. (2000) proposed that the bulk of the water presently on the Earth was carried by a few planetary embryos, originally formed in the outer asteroid belt and accreted by the Earth at the final stage of its formation. Finally, bombardment of comets from the Uranus–Neptune region and from the Kuiper belt delivered no more than 10% of the present water mass. This is the so-called "late veneer," as postulated for the heterogeneous accretion model (see section 12.2.2). However, the ^{187}Os : ^{186}Os ratio of the Earth's primitive upper mantle (~0.1285–0.1305) is significantly higher than that of carbonaceous chondrites (~0.125–0.127), and overlaps that of anhydrous ordinary chondrites (~0.127–0.131), effectively ruling out asteroidal bodies as the source of the "late veneer" (Drake, 2005). It is, however, possible that ordinary chondrites are derived from the metamorphosed outer parts of hydrous asteroids in which case impact of a bulk asteroid could deliver large amounts of water to the accreting Earth.

Phyllosilicates. Ciesla *et al*. (2004) proposed that the source of the Earth's water was phyllosilicate minerals, which formed in the asteroid belt where they were thermodynamically stable, and then migrated into the inner solar system where they were incorporated into the accreting Earth. Since it seems unlikely that phyllosilicates could be decoupled from other minerals and transported into the inner solar system, this hypothesis faces the same objection in terms of Os isotopic composition as stated above for an asteroidal source of water (Drake, 2005).

"Wet" planetesimals. If the accretion disk was too hot for hydrous minerals to form or for phyllosilicate grains migrating from the asteroid belt to survive, the H_2O could have been adsorbed directly onto dust particles prior to their accretion into planetesimals (Drake, 2005). Using a Monte Carlo simulation, Stimpfl *et al*. (2004) have argued that all of the Solar Nebula gases (H_2, He, and H_2O) would interact with the surface of the dust grains, but only H_2O could be adsorbed. Their calculations show that one to three Earth oceans of water could have been adsorbed at temperatures of 500 K to 700 K. Thus, it appears that much or all of the water present on the Earth (as well as on Mars) was indigenous, extracted from the accreting planetesimals. A problem with the "wet" planetisimal hypothesis is that there should be no anhydrous asteroidal bodies in the Solar System, in which case the source of anhydrous chondrites has to be ascribed to metamorphosed, dehydrated parts of hydrous asteroids.

13.5.2 Oxidation state of the oceans

As mentioned earlier (section 13.2.5), except for some "oxygen oases" associated with prolific communities of cyanobacteria, the surface oceans were anoxic under an anoxic atmosphere before the Great Oxidation Event (Stage I, Fig. 13.7). The deeper oceans were almost certainly anoxic as evidenced by the occurrence of large Archean-age marine manganese deposits and BIFs. During Stage II (2.45–1.85 Ga), following the GOE, the atmospheric O_2 level had risen to more than 10^{-1} PAL (i.e., > 0.02 atm), perhaps as high as 0.2–0.4 atm (Holland, 2006a). The concentration of O_2 in much of the shallow oceans was probably close to equilibrium with atmospheric O_2, but the deep oceans continued to remain anoxic during much of the interval between 2.45 and 1.8 Ga (Holland, 2006a), as evidenced by the occurrence of large marine manganese deposits of Paleoproterozoic age.

The interval between 1.8 Ga, the end of prolific BIF deposition, and 0.8 Ga, when the BIF deposition resumed, was a period of environmental stability that has been called the "boring billion" (Holland, 2004). Most of the surface oceans were mildly oxygenated, but the oxidation state of the deep oceans during this time interval is controversial. In the model of Kasting *et al*. (1992), the end of BIF deposition is ascribed to the deep oceans becoming oxic. Also, according to Holland (2006a), the absence of major marine manganese deposits in the geologic record of this interval, whereas they are present both before 1.8 Ga (e.g., the Sausar Group, India, ~2.0 Ga) and after 0.8 Ga (e.g., Penganga Group, India, ~800 Ma), suggests that the deep ocean was mildly oxygenated, perhaps because of a very small delivery rate of organic matter to the deep oceans. The limited availability of organic matter is consistent with the absence of marine phosphorite deposits during this entire interval. An alternative interpretation proposed by Canfield (1998) and supported later by other workers (e.g., Anbar and Knoll, 2002; Shen *et al*., 2003; Poulton *et al*., 2004) attributes the end of BIF deposition to the development of a euxinic (anoxic and sulfidic) deep ocean. Increased atmospheric O_2 levels enhanced sulfide weathering on land and, thus, the flux of sulfate to the oceans. The increased availability of H_2S through sulfate reduction by organic matter (represented here by CH_2O),

$$2CH_2O + SO_4^{2-} \Rightarrow H_2S + 2HCO_3^- \qquad (13.85)$$

removed the Fe(II) dissolved in ocean water as Fe-sulfide precipitates. The abundance of sediment-hosted lead–zinc sulfide deposits in the Mesoproterozoic may be related to an adequate supply of reduced sulfur in anoxic deep oceans (Goodfellow, 1987). Canfield (1998) argued that atmospheric oxygen did not reach the high levels (within a factor of two or three of PAL) required for the deep oceans to be aerobic until the second oxic event in the Neoproterozoic era, as evidenced by the large increase in $\delta^{34}S$ at 0.6–1.0 Ga (Fig. 11.9), which was also contemporaneous with a significant evolutionary radiation of nonphotosynthetic marine sulfide-oxidizing bacteria (Canfield and Teske, 1996). The model of a globally extensive seafloor anoxia persisting for about 1 Gyr after GOE (often referred to as the "Canfield ocean") is claimed to be consistent with significantly lower $\delta^{97/95}Mo$ values for mid-Proterozoic black shales (the Velkerri Formation, McArthur Basin, Australia; the Wollogorang Formation, northern Australia), compared to values of recent euxinic sediments of the Black Sea (Arnold *et al*., 2004). Their data may, however, reflect localized euxinic basins rather than a global-scale euxinic ocean.

Compared to the Mesoproterozoic, the Neoproterozoic era (0.8–0.54 Ga) appears to have been a time of pronounced environmental and biological change on a global scale. Major fluctuations in the $\delta^{13}C$ value of marine carbonates were accompanied by several very large glaciation events, the SO_4^{2-} content of seawater rose to values comparable to that of the modern oceans (Horita *et al*., 2002; Brennan *et al*., 2004), and the level of atmospheric O_2 probably approached modern values by the time of the biological explosion at the Archean to Proterozoic transition (Holland, 2004).

The Neoproterozoic was a time of abundant marine phosphorite deposits in contrast to their absence from the geologic record over the preceding billion years (1.8–0.8 Ga). The increased downward transport of organic matter required for the formation of phosphorite deposits was apparently sufficient to return anoxic conditions in the deep oceans for at least parts of the Neoproterozoic. The striking association of Rapitan-type BIFs with manganese deposits and glacial deposits suggests that anoxia may have been particularly pronounced during the Neoproterozoic glacial periods (Holland, 2006a).

The surface oceans must have been oxygenated throughout the Phanerozoic for the marine life to fluorish, but the oxidation state of the deeper oceans appears to have fluctuated widely. Oceanic anoxia in shelf and abyssal environments, as evidenced by the extensive deposition of black shales, has been

Box 13.6 Evaporites

Salt deposits believed to have formed by evaporation of surficial brines are called *evaporites*. In a barred basin, deprived of replenishment because of isolation from the ocean, evaporation may increase its salinity to cause precipitation of salts (Hsu, 1972). The sequence of precipited salts, as determined by Usiglio in 1849, would be gypsum (when seawater has evaporated to about 19% of its original volume), followed by halite (when the volume has been reduced to about 10% of the original). Further evaporation would produce a whole series of magnesium and potassium salts known as bitterns (Berner and Berner, 1996).

Marine evaporites preserved in the geologic record appear to be of two different compositional types (Kovalevich *et al.*, 1998): (i) $MgSO_4$-type, characterized by an assemblage of potassium and magnesium sulfates (kieserite, kainite, langbeinite, polyhalite), the type of assemblage that would precipitate out of modern evaporated seawater, although locally chloride minerals (such as sylvite, carnallite, and bischofite) may prevail; and (ii) KCl-type (or $MgSO_4$-poor-type), dominated by chloride minerals (sylvite and carnallite, sometimes bischofite) and free of $MgSO_4$ salts. Gypsum, anhydrite, and halite are common to both types. $MgSO_4$-type evaporites are found in the latest Precambrian (Vendian), Mississippian, Pennsylvanian, Permian, Miocene and Quaternary deposits. KCl-type evaporites are found in Cambrian through Mississippian, and Jurassic through Paleogene deposits (Hardie, 1996, p. 279). Intervals of "calcite seas" are approximately coincident with the deposition of KCl-type evaporites and that of "aragonite seas" with the deposition of $MgSO_4$-type evaporites (Fig. 7.8; Hardie, 1996).

The origin of the KCl-type evaporites is controversial because solubility calculations fail to account for the precipitation of sylvite by evaporation of modern seawater and there is no present-day example of a marine evaporite basin precipitating potassium salts. As the K^+ concentration of the oceans is believed to have been fairly constant over the Phanerozoic (Holland, 2004; Demicco *et al.*, 2005), the evaporation of seawater must be combined with a SO_4^{2-}-depleting process in order to explain the syndepositional precipitation of sylvite instead of Mg-sulfates. In addition to post-depositional changes, proposed mechanisms responsible for sulfate depletion are (Holland *et al.*, 1996): (i) secular changes in the composition of seawater resulting from secular variations in seawater chemistry controlled primarily by fluctuations in the mid-ocean ridge hydrothermal brine flux, which, in turn, have been driven by fluctuations in the production of oceanic crust at mid-ocean ridges (Hardie, 1996; Stanley and Hardie, 1998) because seawater recycling through mid-ocean ridges depletes the water in Mg^{2+}, SO_4^{2-}, and Na^+; and (ii) differences in the extent of dolomitization, followed by anhydrite ($CaSO_4$) or gypsum ($CaSO_4.2H_2O$) precipitation, and in the extent of the albitization of clays during the course of seawater evaporation (Horita *et al.*, 1991, 1996).

a recurring feature of the Earth's history (Holland, 1984; Grotzinger and Knoll, 1995). The result was episodic massive release of H_2S (reaction 13.85), which may have been a contributing factor the in the Late Devonian, Late Permian, and Middle Cretaceous mass extinction events (Kump *et al.*, 2005).

13.5.3 Composition of the oceans

Marine evaporite sequences in the rock record and primary fluid (brine) inclusions trapped in primary halite crystals of evaporite beds provide the most important constraints on the composition of ancient seawater (see Box 13.6). Applying our knowledge of the reaction paths for the interpretation of natural evaporite sequences (Harvie *et al.*, 1980), information obtained from brine inclusions in marine evaporite crystals of known age can be used for reconstruction of the contemporary ocean water composition. Evaporation paths for different scenarios can be simulated using, for example, the thermodynamic modeling of the solubility of evaporite minerals by Harvie *et al.* (1984) and the computer program of Sanford and Wood (1991). This approach, however, has some potential limitations: (i) there are no unambiguous criteria for determining marine versus nonmarine origin of evaporites; (ii) the variability among naturally occurring evaporite sequences indicates multiple possible reaction pathways; and (iii) solute concentrations in fluid inclusions may have been significantly modified by diagenesis or brine–rock interactions. Note that there are only a few well-preserved evaporite deposits older than 800 Ma, and so the seawater composition prior to that time is poorly constrained.

In the absence of preserved rocks or fossils, not much can be said about the composition of oceans during the Hadean eon (4.5–3.8 Ga). It is a reasonable guess that Archean oceans contained significant concentrations of Na^+, K^+, Ca^{2+}, Mg^{2+}; Cl^- was certainly the dominant anion in seawater, and the composition and salinity of Archean oceans were not very different from that of present-day seawater (Holland and Kasting, 1992; Holland, 2004). Calcite, aragonite, and dolomite were the dominant carbonate minerals precipitated during the Archean (siderite was a common constituent of BIFs only), implying that the Archean seawater was saturated with respect to $CaCO_3$ and $CaMg(CO_3)_2$. Bedded or massive gypsum/anhydrite formed in evaporitic environments is absent in the Archean (3.8–2.5 Ga) and Paleoproterozoic (2.5–1.8 Ga) record, suggesting a low concentration of SO_4^{2-} in the pre-1.8 Ga oceans. As discussed earlier (section 11.7.5), $\delta^{34}S$ values of marine sedimentary sulfides also indicate low concentration of SO_4^{2-} (< 1 mmol kg^{-1}) in the Archean seawater.

During the Proterozoic, seawater continued to be supersaturated with $CaCO_3$, $CaMg(CO_3)_2$, and SiO_2. Its pH certainly rose in response to decreasing atmospheric P_{CO_2}, and it is likely that its salinity did not differ greatly from that of modern seawater (Holland, 1992). The SO_4^{2-} concentration rose to > 1 mmol kg^{-1} H_2O, but stayed well below the present value of 28 mmol kg^{-1} H_2O for most of the Proterozoic. For example, Shen *et al.* (2002) have proposed that the $\delta^{34}S$ values of pyrite in the Paleoproterozoic (1.72–1.73 Ga) sediments of the McArthur Basin (northern Australia) are best explained if SO_4^{2-} concentration in the contemporary seawater was between 0.5 and 2.4 mmol kg^{-1} H_2O.

Bedded marine evaporite deposits of Neoproterozoic age (900–542 Ma) offer the earliest opportunity to reconstruct the composition of contemporary seawater from brine inclusions in marine halite. For example, fluid inclusions in halite from the 545-Ma Ara Group (southern Oman) are Ca-depleted, Mg-rich, Na–K–Mg–Cl–SO_4 brines (saturated with respect to potash minerals and $MgSO_4$), giving the following reconstructed composition (in mmol kg^{-1} H_2O) for the contemporaneous seawater (Brennan *et al*., 2004): Na^+ = 479; K^+ = 11, Ca^{2+} = 14 (9.5 to 18.5); Mg^{2+} = 52; SO_4^{2-} = 20.5 (16 to 25); Cl^- = 581. These ionic concentrations are similar to those in modern evaporated seawater and fluid-inclusion brines trapped in modern marine halites (Brennan *et al*., 2004):Na^+ = 485; K^+ = 11, Ca^{2+} = 11; Mg^{2+} = 55; SO_4^{2-} = 29; Cl^- = 565.

A major shift in the ocean chemistry occurred in the Early Cambrian, broadly coincident with the "biologic explosion." Fluid inclusions in marine halite crystals from the Early Cambrian (515 Ma) Angarskaya Formation (eastern Siberia) indicate that, compared to Late Proterozoic, the contemporary seawater had a Ca-depleted, Na–K–Ca–Mg–Cl composition, depleted in SO_4^{2-} and Mg^{2+}, but enriched in Ca^{2+}. The reconstructed Angarskaya concentrations (in mmol kg^{-1} H_2O) – Na^+ = 450; K^+ = 9, Ca^{2+} = 37 (33.5 to 40); Mg^{2+} = 44; SO_4^{2-} = 8 (4.5 to 11); Cl^- = 605 (Brennan *et al*., 2004) – are similar to those in other early Paleozoic (Cambrian, Silurian, Devonian) fluid inclusions in marine halites (Lowenstein *et al*., 2001; Horita *et al*., 2002). The coincidence between the large increase in oceanic Ca^{2+} concentration (an approximately threefold increase compared to the Neoproterozoic) and the Cambrian "biologic explosion" probably reflects the effect of the first major biocalcification event.

Numerous fluid inclusion studies (e.g., Hardie, 1996; Kovalevich *et al*., 1998; Horita *et al*., 2002; Lowenstein *et al*., 2001, 2003; Demicco *et al*., 2005) have led to the conclusion that the Phanerozoic seawater composition has alternated between two types of brines related to different evaporite associations: a $MgSO_4$-type, rich in SO_4^{2-} but low in Ca^{2+}; and a KCl-type, rich in Ca^{2+} but low in SO_4^{2-}. In marine evaporites, the secular variation has been recorded in the form of time intervals when potash deposits are characterized by $MgSO_4$ salts, such as polyhalite [$K_2MgCa_2(SO_4)_4.2H_2O$], kieserite ($MgSO_4.H_2O$), and langbeinite [$K_2Mg_2(SO_4)_3$], and time intervals when potash deposits are characterized by KCl salts, such as sylvite (KCl), and the absence or paucity of $MgSO_4$ salts (see Box 13.6). It is significant that periods of $MgSO_4$-type evaporites are synchronous with "aragonite seas" and periods of KCl-type evaporites with "calcite seas" (Fig. 7.8). As discussed earlier (section 7.8.4), secular variations in the major ion chemistry of seawater have occurred probably in response to fluctuations in the ratio of MOR brine flux to river water flux as a consequence of changes in the production of oceanic crust at mid-ocean ridges.

13.6 Geosphere–hydrosphere–atmosphere–biosphere interaction: global biogeochemical cycles

The concept of *biogeochemical cycles* (also referred to as *geochemical cycles*) is a comprehensive expression of interactions within the four components of the Earth supersystem – geosphere (solid Earth), hydrosphere, biosphere, and atmosphere – in terms of global reservoirs of materials and transfer of materials from one reservoir to another. Every element has its own unique biogeochemical cycle, and all of these cycles have ben operating simultaneously. Since the composite is too complex to comprehend, it is convenient to consider the cycles for individual elements (or chemical species) separately. Each biogeochemical cycle is generally portrayed in the form of a *box model* in which the reservoirs are represented by boxes (geometric shapes such as reactangles and circles), whereas the processes linking the boxes and the fluxes between them are denoted by arrows. Each cycle comprises two interconnected components: an *exogenic* component, which operates on the surface of the Earth; and an *endogenic* component, which operates in the interior of the Earth. The two components are linked through tectonics.

It is assumed that, in the absence of anthropogenic perturbations, chemical mass transfer among global reservoirs is *cyclic*, which means that the intake of geologically permanent reservoirs is balanced in the long run by their output so that their size and composition remain, within rough limits, constant over long periods of time. Because biogeochemical processes appear to be cyclic, superimposed on the slow secular evolution of the Earth, the modeling of environmental systems boils down to the modeling of cyclic processes or parts of them. The factors involved in the construction of geochemical cycling models include: (i) identification of sources and sinks of the elements; (ii) definition of the boundaries of the reservoirs; (iii) prediction and evaluation of transport paths; (iv) quantitative knowledge of the masses of the substances in reservoirs, and fluxes into and out of reservoirs (often the most difficult parameters to evaluate); and (v) appropriate mathematical models relating the various variables. For the sake of simplicity, however, we will restrict our attention to qualitative aspects of the biogeochemical cycles of carbon (Fig. 13.18), oxygen (Fig. 13.19), nitrogen (Fig. 13.20), sulfur (Fig. 13.21) and phosphorus (Fig. 13.22), which are of prime importance for the biosphere, the most active geochemical realm at present, and the Earth's surface. Quantitative evaluations of these cycles have been discussed, for example, in Gregor *et al*. (1988), and Berner and Berner (1996).

Comprehensive treatments of these biogeochemical cycles can be found in articles by Houghton (2005), Petsch (2005), Galloway (2005), Brimblecome (2005), and Ruttenberg (2005), all included in the *Treatise on Geochemistry*, vol. 8, 2005, edited by W.H. Schlesinger.

13.6.1 The carbon cycle

The carbon cycle (Fig. 13.18) is important for three reasons (Houghton, 2005): (i) carbon is one of the basic elements of the structure of all life on the Earth, making up ~50% of the dry weight of all living things; (ii) the cycling of carbon approximates

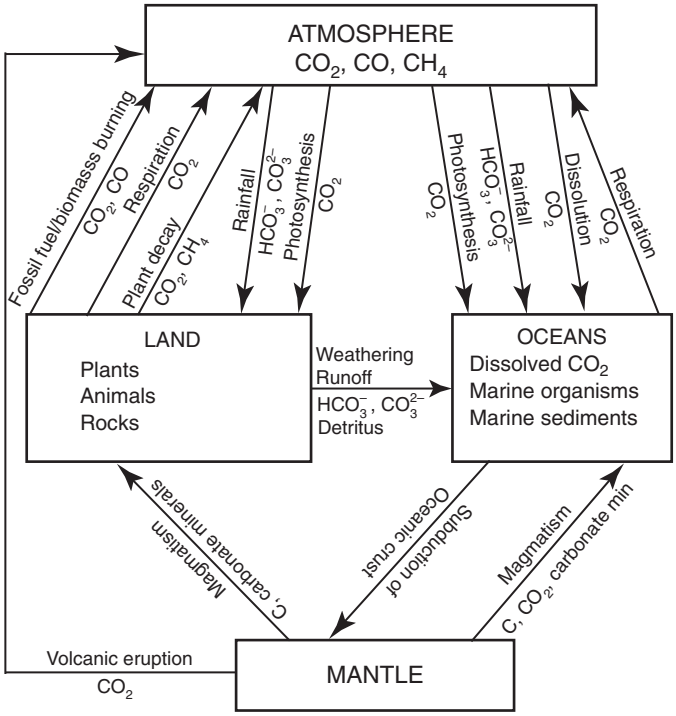

Fig. 13.18 Simplified biogeochemical cycle of carbon. Some $CO_2$and CH_4 are returned to the atmosphere via plant decay. The cycle would be in balance if it were not for human interference such as burning of fossil fuels, cement manufacturing, and deforestation.

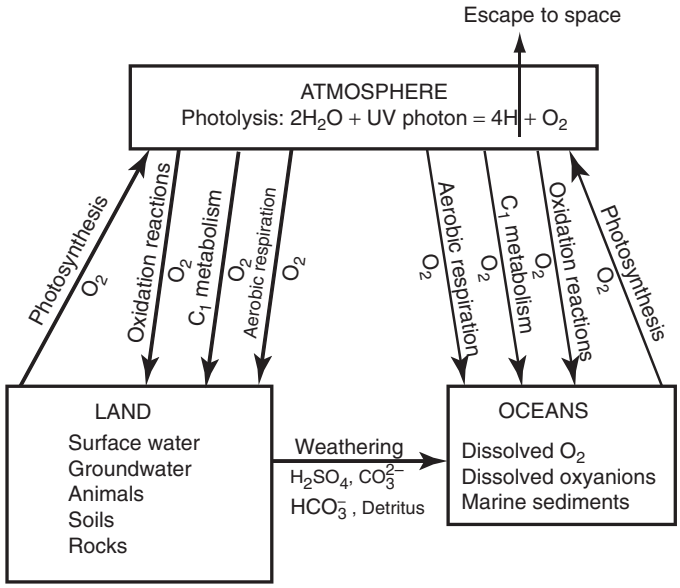

Fig. 13.19 Simplified exogenic biogeochemical cycle of oxygen.

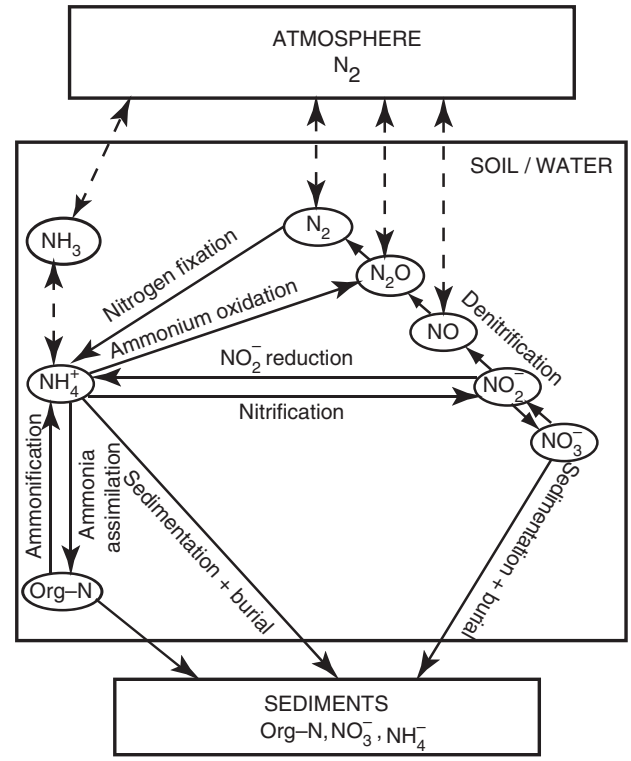

Fig. 13.20 Simplified exogenic biogeochemical cycle of nitrogen. The natural nitrogen cycle has been affected considerably by anthropogenic input of nitrogen gases from various sources.

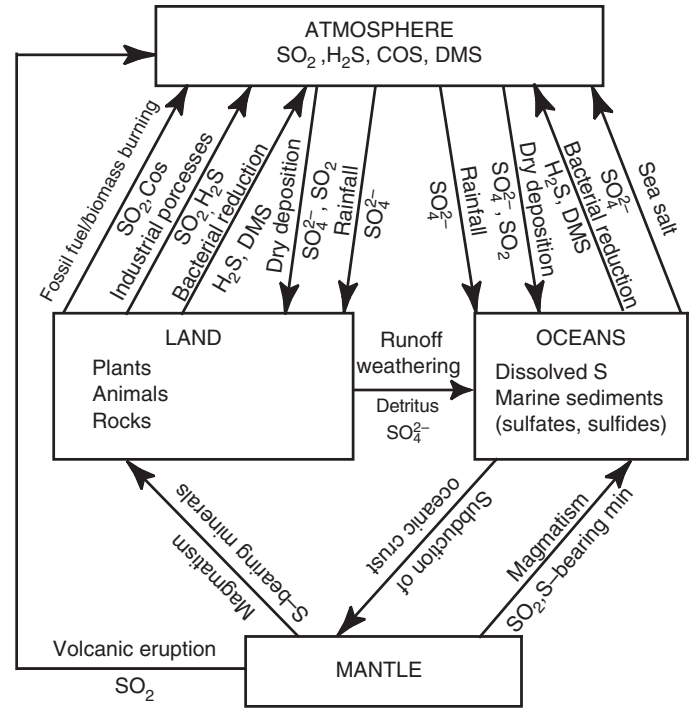

Fig. 13.21 Simplified biogeochemical cycle of sulfur. DMS = Dimethyl sulfide, $(CH_3)_2S$.

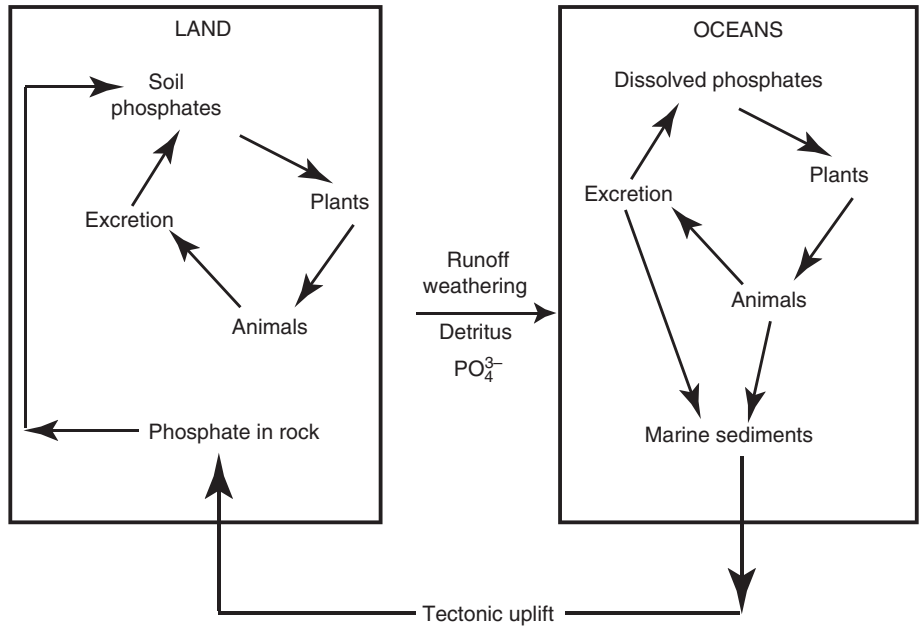

Fig. 13.22 Simplified biogeochemical cycle of phosphorus.

the transfers of energy around the Earth, the metabolism of natural, human, and industrial systems; and (iii) CO_2 and CH_4 are two of the most important greenhouse gases.

The Earth contains ~10^{23} g of carbon, most of it sequestered in carbonate rocks (0.65×10^{23} g) and buried organic matter (0.156×10^{23} g) such as kerogen, oil and natural gas, and coal (Schlesinger, 1997). Only ~0.1% of the carbon (40×10^{18} g) in the Earth's upper crust is cycled throughout active surface reservoirs. The main exogenic reservoirs are the oceans (dissolved organic and inorganic carbon; and marine sediments, mostly in the form of $CaCO_3$), the biosphere (organic matter in plants and animals, with carbon comprising 50% of all living tisues), the land (carbonate rocks and soil carbonate), and the atmosphere (mainly as CO_2 and CH_4, which have played a crucial role in the development of lifeforms and the alteration of Earth's surface environment throughout Earth's history).

Carbon fluxes between the atmosphere and the oceans and between the atmosphere and the continental biosphere are very large. The main processes that control the transfer of carbon among these reservoirs are biological: oxygenic photosynthesis and aerobic respiration by terrestrial plants and phytoplankton (microscopic marine plants that form the base of the marine foodchain) in the oceans (see Chapter 8):

$$\textit{Photosynthesis}: CO_{2\,(g)} + H_2O_{(l)} + \text{sunlight} \Rightarrow CH_2O + O_{2\,(g)} \qquad (8.63)$$

$$\textit{Respiration}: CH_2O + O_{2(g)} \Rightarrow CO_{2(g)} + H_2O_{(l)} + \text{energy} \qquad (8.66)$$

where CH_2O stands for organic compounds such as carbohydrates. Almost all multicellular life on Earth depends on the production of carbohydrates (the most abundant group of organic compounds that includes sugars, starches, and cellulose) by photosynthesis and breakdown of those carbohydrates by respiration to generate the energy needed for movement, growth, and reproduction of organisms. Most, but not all, of the CO_2 extracted from the atmosphere through photosynthesis is returned to the atmosphere through cell respiration and decay of plants. On an annual basis, the amount of carbon involved in photosynthesis and respiration is about 1000 times greater than the amount that moves through the geological component. Nonbiological processes that release CO_2 to the atmosphere include burning of fossil fuels and biomass, cement manufacturing, decay of organic matter, and breakdown of $CaCO_3$. During the past 150 years (~1850–2000) the atmosphere has registered a 30% increase in the amount of carbon, mostly from the combustion of fossil fuels.

The main geochemical processes involved in the cycling of carbon include weathering of rocks exposed by erosion and tectonic upplift, precipitation of minerals, burial and subduction of rocks and sediments at convergent plate boundaries, and volcanism. As discussed earlier, weathering of rocks containing carbonate and silicate minerals is facilitated by carbonic acid (H_2CO_3) formed by reaction of water with atmospheric CO_2 ($CO_{2\,(g)} + H_2O \Leftrightarrow H_2CO_{3\,(aq)}$; reaction 7.36) and by oxidation of organic matter ($CH_2O + O_2 \Rightarrow CO_2 + H_2O \Rightarrow H_2CO_{3\,(aq)}$; reaction 7.85). Dissolved substances produced by weathering reactions such as

$$\underset{\text{calcite}}{CaCO_3} + H_2O + CO_2 \Rightarrow Ca^{2+} + 2HCO_3^- \qquad (13.86)$$

$$\underset{\text{dolomite}}{CaMg(CO_3)_2} + 2H_2O + 2CO_2 \Rightarrow Ca^{2+} + Mg^{2+} + 4HCO_3^- \quad (13.87)$$

$$\underset{\text{wollastonite}}{CaSiO_3} + 3H_2O + 2CO_2 \Rightarrow Ca^{2+} + 2HCO_3^- + H_4SiO_4 \quad (13.88)$$

$$\underset{\text{enstatite}}{MgSiO_3} + 3H_2O + 2CO_2 \Rightarrow Mg^{2+} + 2HCO_3^- + H_4SiO_4 \quad (13.89)$$

are transported to the oceans by rivers, and precipitated as carbonates and silica by reactions such as

$$Ca^{2+} + 2HCO_3^- + Si(OH)_4 \Rightarrow \underset{\text{calcite}}{CaCO_3} + \underset{\text{silica}}{SiO_2} + 3H_2O + CO_2 \quad (13.90)$$

$$Mg^{2+} + 2HCO_3^- + Si(OH)_4 \Rightarrow \underset{\text{magnesite}}{MgCO_3} + \underset{\text{silica}}{SiO_2} + 3H_2O + CO_2 \quad (13.91)$$

The precipitation of calcite (and aragonite) and silica is predominantly biological in the sense that they are precipitated by reef and planktonic organisms to build their skeletons (see sections 7.8.4 and 7.8.5 for abiological and biological precipitation of calcium carbonate). When marine animals and plants die, their remains settle toward the seafloor. Much of this organic debris undergoes decomposition by bacteria and dissolution during their downward journey, replenishing the oceanwater in dissolved CO_2, calcium, silica, and nutrients. The CO_2 is stored in the deeper waters of the oceans for hundreds to a thousand or so years before being returned to the atmosphere by the upwelling of deep ocean waters.

The organic debris that escapes degradation during downward transit accumulates as part of the seafloor sediments. Burial eventually transforms calcite-rich sediments into limestone and the highly altered, finely disseminated organic matter (principally preserved remains of microscopic plant material), called *kerogen*, into oil and gas under appropriate temperature–pressure conditions. Burial of terrestrial plant material, commonly in swampy environments, leads to the formation of different ranks of coal (peat, lignite, bituminous coal, and anthracite) depending on the temperature–pressure conditions experienced by the buried material. The carbon incorporated in sedimentary rocks may be transformed into anthracite or graphite by thermal metamorphism, whereas limestones may recrystalize to form marble.

The carbon cycle continues as seafloor spreading leads to subduction of the seafloor under continental margins. The carbon-bearing material in the subducting slab eventually melts and the carbon is incorporated into magma. Part of the carbon enters crustal igneous rocks formed from this magma and some carbon is released through volcanic eruptions to the atmosphere mostly as CO_2, where the carbon combines wih water and returns to the Earth's surface as H_2CO_3 dissolved in rainwater ($H_2O + CO_2 \Rightarrow H_2CO_3 \Rightarrow H^+ + HCO_3^-$; $HCO_3^- \Rightarrow H^+ + CO_3^{2-}$).

The widespread occurrence of marine carbonate deposits suggests that dissolution of CO_2 in seawater has played an important role in the removal of CO_2 from the Earth's atmosphere. By analogy, the CO_2-rich atmosphere of Mars may be due, at least in part, to the absence of liquid water on the surface. In contrast, the CO_2 atmosphere of Venus may reflect an approximate equilibrium between atmospheric CO_2 and limestone deposits on the surface:

$$CaCO_3 \Leftrightarrow CaO + CO_2 \quad (13.92)$$

13.6.2 *The oxygen cycle*

A unique feature of the Earth among celestial bodies is an abundance of free molecular oxygen (O_2) in its atmosphere. Living organisms depend on oxygen for breathing and for producing energy. Oxygen is also essential for combustion (an oxidation reaction) and it is the ingredient for maintaining the stratospheric ozone shield that provides protection from UV rays. Oxygen is a very reactive element and it readily reacts with most elements of the Periodic Table. Yet, the atmospheric O_2 concenration has been maintained at a fairly constant value (~21% or a partial pressure of oxygen = 0.21 bar) for a long time because of a balance between its production and consumption.

As shown in Fig. 13.19, the main source of atmospheric oxygen is oxygenic photosynthesis by land plants and phytoplankton of the oceans, which produces sugars and oxygen from CO_2 and water in the presence of sunlight:

$$CO_{2(g)} + H_2O_{(l)} + \text{sunlight} \Rightarrow \underset{(8.63)}{CH_2O\ (\text{carbohydrate}) + O_{2(g)}}$$

A small amount of O_2 is also produced by photolysis of water vapor (reactions 13.28 and 13.30), the net reaction for which can be represented as

$$2H_2O_{(g)} + \text{UV photon} \Rightarrow 4H_{(g)} \uparrow + O_{2\,(g)} \quad (13.93)$$

Atomic oxygen formed by photodissociation of molecular oxygen by UV radiation is the major form of oxygen above ~120 km altitude.

The main processes that result in relatively large fluxes of O_2 from the atmosphere to the Earth's surface include: (i) aerobic respiration, the oxidation of organic substrates with oxygen to yield chemical energy ($CH_2O_{(aq)} + O_{2(g)} \Rightarrow CO_{2(g)} + H_2O_{(l)}$; reaction 8.66); (ii) biologically mediated oxidative metabolism of C_1 compounds such as methane, methanol, and formaldehyde, which are common in soils and sediments as the products of anaerobic fermenation reactions (Petsch, 2005); and (iii) various oxidation reactions. Examples of oxidation reactions that consume O_2 include: combustion of fossil fuels and biomass;

oxidation of sulfide to sulfate (e.g., $HS^- + 2O_{2(g)} \Rightarrow SO_4^{2-} + H^+$; reaction 8.68), oxidation of Fe(II) minerals to Fe(III) minerals (e.g., $2Fe^{2+}\ CO_{3(s)} + O_{2(g)} + 2H_2O \Rightarrow 2Fe^{3+}\ OOH + 2HCO_3^-$; reaction 8.67); and oxidation of reduced volcanic gases such as H_2S and CH_4 ($H_2S_{(g)} + O_{2\,(g)} \Rightarrow SO_{2\,(g)} + H_{2\,(g)}$; $CH_{4\,(g)} + O_{2\,(g)} \Rightarrow CO_{2(g)} + 2H_{2\,(g)}$). Aerobic respiration is the most important process of oxygen consumption on the Earth.

A small amount of the Earth's oxygen occurs dissolved in the oceans. Oxygen solubility depends on the temperature, pressure, and salinity. At 1 bar pressure and ~35‰ salinity, the solubility decreases from 11.2 mg L^{-1} (= 349 μmol L^{-1}) at 0°C to 4.6 mg L^{-1} (= 146 μmol L^{-1}) at 50°C. By far the largest reservoir of oxygen is the crust–mantle system, which holds ~99.5% of the Earth's oxygen (compared to only 0.49% in the atmosphere and 0.01% in the biosphere), and is recycled through plate tectonics.

13.6.3 The nitrogen cycle

Nitrogen is an essential constituent of DNA, RNA, and proteins, the building blocks of life. All organisms, therefore, require nitrogen to live and grow. The availability of nitrogen to sustain life should not be a problem, considering that it constitiutes ~79% (by volume) of the Earth's atmosphere, 2.82×10^{20} moles of N_2 gas and much smaller amounts ($\approx 10^{12}$ moles) of six other molecular species (NH_3, NH, N_2O, NO, NO_2, and HNO_3). The N_2 gas is inert and therefore cannot be utilized directly by plants or animals, except by a few primitive bacteria that are capable of converting N_2 gas to NH_3 or NH_4^+, which is the only way organisms can utilize nitrogen directly from the atmosphere. The other significant reservoirs of nitrogen include sediments and sedimentary rocks and, to a lesser extent, the biosphere and dissolved organic compounds in the oceans. The oceans contain a relatively small amount of nitrogen as dissolved N_2 because of its low solubility in water (~0.03 g kg^{-1} at 0°C to ~0.01 g kg^{-1} at 60°C).

Table 13.9 Oxidation states of nitrogen.

Oxidaton state	Examples
–3	NH_3 (ammonia), NH_4^+ (ammonium ion), NH_2^- (amide ion)
–2	N_2H_4 (hydrazine)
–1-	NH_2OH (hydroxylamine), NH_2Cl (chloramine)
0	N_2 (nitrogen gas)
+1	N_2O (dinitrogen oxide or nitrus oxide), $H_2N_2O_2$ (hyponitrus acid)
+2	NO (nitrogen monoxide or nitric oxide)
+3	N_2O_3 (dinitrogen trioxide), HNO_2 (nitrus acid), NO_2^- (nitrite ion)
+4	NO_2 (nitrogen dioxide), N_2O_4 (dinitrogen tetroxide)
+5	N_2O_5 (dinitrogen pentoxie), HNO_3 (nitric acid), NO_3^- (nitrate ion)

The nitrogen cycle (Fig. 13.20) is a little more complicated than the oxygen cycle because nitrogen exists in both organic and inorganic forms as well as in many oxidation states (Table 13.9). Moreover, nitrogen is not involved to any appreciable extent in mineral dissolution and precipitation; it is strictly a biogenic element that is cycled through the action of microorganisms. Thus, microbial processes have a strong, in many cases controlling, influence on the biogeochemistry of nitrogen. Three classes of microorganisms are important in this connection: those that convert N_2 to NH_4^+; those that convert NH_4^+ to NO_3^-; and those that convet NO_3^- back to N_2, thus completing the cycle.

Nitrogen is cycled through the biosphere, atmosphere, and geosphere by six main natural processes, which transform nitrogen from one chemical form to another (Galloway, 2005): (i) nitrogen fixation ($N_2 \Rightarrow NH_3$); (ii) ammonia assimilation ($NH_3 \Rightarrow$ organic N); (iii) nitrification ($NH_4^+ \Rightarrow NO_3^-$); (iv) assimilatory nitrate reduction ($NO_3^- \Rightarrow NO_2^- \Rightarrow NH_4^+$), (v) ammonification (organic N $\Rightarrow NH_4^+$); and (vi) denitrification ($NO_3^- \Rightarrow N_2$).

Nitrogen fixation is the process by which N_2 is converted to any nitrogen compound in which nitrogen has a nonzero oxidation state. The most common is the reduction of N_2 to NH_3 mediated by certain bacteria (e.g., *Rhizobium*, which live in the root nodules of legumes such as peas and beans, and cyanobacteria):

$$2N_{2(g)} + 6H_2O \Rightarrow 4NH_3\ (\text{wihin the organism}) + 3O_{2(g)} \quad (13.94)$$

The NH_3 is released following the death of the organism, and subsequent hydrolysis of NH_3 produces NH_4^+, which can be assimilated by plants:

$$4NH_3 + 4H_2O \Rightarrow 4NH_4^+ + 4OH^- \quad (13.95)$$

Over geologic history, most reactive nitrogen has been formed by biological mediation. In the latter half of the 20th century, however, the Haber–Bosch process for manufacturing NH_3, which is used to make fertilizers and explosives, has been the dominant process on continents for creating reactive nitrogen. This process uses N_2 from the atmosphere and H_2 from fossil fuels (usually natural gas), and operates at high temperature and pressure with a metallic catalyst (see section 9.4.2):

$$N_{2(g)} + 3H_{2(g)} \Rightarrow 2NH_{3(g)} \quad (13.96)$$

Another reactive form of nitrogen, NO gas, is produced by high-energy natural events such as lightning or high-temperature combustion of fossil fuels (as in automobile engines and thermal power plants):

$$N_{2(g)} + O_{2(g)} + \text{electrical /fossil fuel energy} \Rightarrow 2NO_{(g)} \quad (13.97)$$

Ammonia assimilation is the uptake of NH_3 or NH_4^+ by an organism into its biomass in the form of an organic nitrogen compound. All nitrogen obtained by animals can be traced back to the eating of plants at some stage of the foodchain. We may not realize it, but the nitrogen in our food was fixed initially by nitrogen-fixing bacteria.

Nitrification is the aerobic process by which microorganisms oxidize NH_3 to NO_3^- (nitrate ion) and derive energy from the reaction. Actually, nitrification is a combination of two bacterial processes: oxidation of NH_4^+ to NO_2^- (nitrite ion) by one group of bacteria (e.g., *Nitrosomonas*); and oxidation of NO_2^- to NO_3^- by another group of bacteria (e.g., *Nitrobacter*):

$$2NH_4^+ + 3O_2 \Rightarrow 2NO_2^- + 2H_2O + 4H^+ \quad (13.98)$$

$$2NO_2^- + O_2 \Rightarrow 2NO_3^- \quad (13.99)$$

The conversion of nitrites to nitrates is beneficial for plants because accumulated nitrites are toxic to plant life.

Assimilatory nitrate reduction is the uptake of NO_3^- by an organism and incorporation as biomass through nitrate reduction. It is an important process for input of nitrogen for many plants and organisms.

Ammonification is part of the general process of decomposition that converts reduced organic nitrogen ($R–NH_2$) to reduced inorganic nitrogen (NH_4^+) by the action of microorganisms.

Denitrification is the reduction of nitrates back to any gaseous nitrogen species, largely N_2:

$$5CH_2O + 4H^+ + 4NO_3^- \Rightarrow 2N_{2(g)} + 5CO_{2(g)} + 7H_2O \quad (13.100)$$

It is an anaerobic process that is carried out mainly in sediments (and occasionally in the water column) by bacterial species such as *Pseudomonas* and *Clostridium*, and the conversion takes place in the following sequence: $NO_3^- \Rightarrow NO_2^- \Rightarrow NO \Rightarrow N_2O \Rightarrow N_2$. Being a gas, N_2 is likely to be lost readily to the atmosphere. Denitrification is the only nitrogen transformation process that removes nitrogen from ecosystems (essentially irreversibly), thereby approximately balancing the nitrogen fixed by the nitrogen fixers described above.

The natural exogenic nitrogen cycle has been affected considerably by anthropogenic input of nitrogen gases from various sources: ammonium-based chemical fertilizers, automobile exhausts, industrial plants, and sewage facilities such as septic tanks and holding tanks. The various forms of nitrogen in our ecosystems contribute to a number of environmental problems such as photochemical smog and acid rain (as discussed earlier), and creation and growth of eutrophic lakes and oceanic dead zones through algal bloom-induced hypoxia (reduced dissolved oxygen content in a body of water).

13.6.4 The sulfur cycle

Sulfur is a very reactive element and combines directly with many elements, especially with hydrogen and oxygen forming H_2S and many oxides of sulfur, the most important of which are SO_2 and SO_3. Sulfur is also a biologically active element and is cycled readily through the foodchain. Some of the earliest organisms on Earth utilized sulfur compounds, particularly through anoxygenic photosynthesis.

A simplified version of the sulfur biogeochemical cycle is presented in Fig. 13.21. Sulfur from the mantle enters the hydrosphere as a result of alteration/weathering of mafic and ultramafic rocks in the oceans and on land, and by emission of SO_2 during volcanic eruptions. In the present oxic state of the atmosphere, any H_2S in the volcanic emissions is rapidly oxidized to SO_2. Volcanic emissions also release SO_2 directly to the atmosphere. Other sources of sulfur in the atmosphere are: biologically produced H_2S, DMS [dimethyl sulfide, $(CH_3)_2S$] and other organic sulfur compounds (e.g., carbonyl sulfide, COS; carbon disulfide, CS_2), which are readily oxidized to SO_2; SO_2 from burning of fossil fuels and biomass, and industrial processes (e.g., roasting of sulfide ores); and SO_4^{2-} from sea-salt aerosol. Most of the SO_4^{2-} flux is redeposited in the ocean as precipitation and dry-fall. The SO_2 combines with H_2O to form H_2SO_4, which leads to acid deposition (see section 13.3.3) on land and in oceans.

Weathering of sulfur-bearing sediments releases the stored sulfur, which is then oxidized into SO_4^{2-}. The SO_4^{2-} is taken up by plants and microorganisms, and converted into organic forms. Animals consume these organic forms through their food, thereby cycling the sulfur through the foodchain. When organisms die and decay, some of the sulfur is again released as SO_4^{2-} and mostly transported as runoff, although some enters the tissues of microorganisms.

The fate of SO_4^{2-} that enters the oceans and lakes from the atmosphere and as runoff from the land is dominated by anaerobic bacteria (such as *Desulfovibrio desulfuricans*) that reduce SO_4^{2-} to H_2S (reaction 8.71). These bacteria can tolerate a large range of pH and salinity conditions, and they occur widely in marine and lacustrine sediments as well as in the overlying water column if it is sufficiently anoxic ($Eh < +0.100\,V$). The H_2S reacts with metals forming sulfides, predominantly iron sulfide (FeS) that accumulates on the seafloor with marine sediments and eventually recrystallizes to pyrite (FeS_2). In addition, sulfate salts (evaporites), such as anhydrite ($CaSO_4$) and gypsum ($CaSO_4.2H_2O$), are precipated episodically in marine and nonmarine evaporite basins. At the present time, sulfate input into the oceans exceeds the output by a large

amount, the imbalance being due to excessive inputs of anthropogenic sulfur and the absence of large modern-day evaporite basins. The sulfur incorporated in sedimentary rocks is recycled into the hydrosphere in the form of dissolved SO_4^{2-} when the sedimentary rocks are exposed to chemical weathering.

13.6.5 The phosphorus cycle

Phosphorus is an essential element for all organisms and is a key player in fundamental biochemical reacions. It is a critical component of ATP (adenosine triphosphate, $C_{10}H_6N_5O_{13}P_3$), the cellular energy carrier. Adenosine triphosphate contains a large amount of energy stored in its high-energy phosphate bonds; the energy is released when ATP breaks down into ADP (adenosine diphosphate) and utilized for many metabolic processes. Phosphorus, like calcium, is an essential ingradient for vertebrates; in the human body 80% of the phosphorus is found in teeth and bones as organophosphates and in calcium phosphates such as hydrooxyapatite, $Ca_5(PO_4)_3(OH)$, and fluorapatite, $Ca_5(PO_4)_3F$. Organisms cannot directly assimilate phosphorus stored in rocks and soils. Conversion to orthophosphate (PO_4^{3-}), which can be assimilated directly, occurs through geochemical and biochemical reactions at various stages in the global phosphrous cycle (Fig. 13.22).

Very little phosphorus circulates in the atmosphere because at the Earth's normal temperatures and pressures, phosphorus and its compounds are not gases. Thus, the atmosphere is not a reservoir of phosphorus). Sedimentary rocks constitute the largest reservoir of phosphorus. Weathering of continental bedrock results in the dissolution of phosphorus mineals such as apatite ($Ca_{10}(PO_4)_6(OH, F, Cl)_2$) and release of phosphorus as PO_4^{3-} that can be assimilated by organisms. Plants absorb phosphates from soil or water, then bind the phosphate into organic compounds. The phosphorus is passed into animals through successive steps in the foodchain, and eventually returned to the soil or water through the excretion of urine and feces, as well as from the decomposition of plants and animals after death. Much of the phosphates delivered to the oceans (or inland lakes) through runoff, however, are pollutants derived from anthropogenic sources such as mining, leakage of sewage, and use of phosphates for fertilizers, detergents, soft drinks, etc. The phosphorus is transported as soluble PO_4^{3-}, as an adsorbed phase on suspended particles of soil clays and ferric oxides, and as detrital primary apatite and particulate organic compounds. The solubilization/desorption of some of this phosphorus adds to the phosphorus budget of the oceans.

The sole means of phosphorus removal from the ocean or lake water is burial with marine sediments that accumulate on the ocean floor. The phosphatic materials in the sediments include (Berner and Berner, 1996): organic phosphorus compounds (carried to the oceans by rivers, as well as formed in the oceans by photosynthesis) that survive bacterial decay; finely dispersed authigenic calcium phosphate in marine muds of continental margins; phosphate adsorbed on hydrous ferric oxides and incorporated in $CaCO_3$ during growth of calcareous shells. When sediments are stirred up by upwelling, a lot of the phosphorus returns to the surface water and reenters the phosphorus cycle. As is the case with nitrogen, phosphorus undergoes many transfers between deep and surface waters before becoming buried permanently in sediments and locked in the resulting sedimentary rocks. This phosphorus would be released only when the rocks are brought to the surface by tectonic uplift and subjected to weathering.

13.7 Summary

1. On the basis of temperature distribution, the atmosphere can be divided into several layers: troposphere, stratosphere, mesosphere, and thermosphere. The pressure decreases exponentially with altitude, by about a factor of 10 for every 16 km. The stratosphere contains the "ozone layer," which provides a protective shield from the Sun's ultraviolet radiation. The recently discovered depletion of the ozone layer has been caused by the introduction of CFC compounds into the atmosphere from anthropogenic sources.
2. Photochemical reactions play a key role in many aspects of atmospheric chemistry, including the production and destruction of ozone.
3. Three gases – N_2, O_2, and Ar – comprise about 99.9% (by volume) of the atmosphere. Earth is the only planet with abundant atmospheric O_2.
4. The Earth probably had a primary atmosphere composed of H_2 and He captured gravitationally from the solar nebula, but this atmosphere was replaced within ~100 Myr by a secondary atmosphere formed by shock release and vaporization of chemically bound volatiles contained in the accreting planetesimals. Water vapor contained in this steamy atmosphere was the ultimate source of the water in the oceans. A liquid-water ocean similar to modern oceans came into existence at ~4.5 Ga, after the Moon-forming giant impact, by outgassing of a magma ocean when it solidified.
5. The atmosphere during the Hadean (4.5–3.8 Ga) and Archean (3.8–2.5 Ga) was essentially devoid of free (molecular) O_2. Accumulation of free O_2 in the atmosphere had to await the advent of oxygenic photosynthesis, when cyanobacteria appeared on the Earth.
6. Many lines of evidence (BIFs, detrital uraninite, MIF-S, paleosols, etc.) indicate that a dramatic rise in atmospheric P_{O_2}, from $< 10^{-5}$ PAL to $> 10^{-2}$ PAL, occurred during the early Proterozoic, around 2.3 Ga (2.4–2.2 Ga). This is commonly referred to as the Great Oxidation Event (GOE). Another oxidation event occurred at ~0.8–0.7 Ga. Atmospheric O_2 probably reached close to modern values by the Cambrian biologic explosion. The most conspicuous feature of the Phanerozoic scenario was the pronounced excursion, reaching levels as high as 35% O_2, during the Carboniferous–Permian and the rapid decline at the end of Permian.
7. From an environmental perspective, the principal agents of air pollution are: anthropogenic $SO_{2(g)}$ (sulfurous smog, acid deposition); $NO_{x(g)}$ and ground-level ozone

(photochemical smog); $CO_{2(g)}$ and $CH_{4(g)}$ (global warming); and CFC compounds (stratospheric ozone depletion).

8. Theoretical models indicate that the Earth's atmosphere and oceans had formed within a few tens of millions of years after the end of the main accretion period. Much or all of the water present on Earth (as well as on Mars) was indigenous, extracted from the accreting planetesimals.
9. Seven aqueous species – Na^+, Ca^{2+}, Mg^{2+}, K^+, Cl^-, SO_4^{2-}, and HCO_3^- – account for more than 99% of the dissolved constituents in both seawater and river water, and their concentrations are fairly constant (except perhaps that of Ca^{2+}) on a global scale. On the other hand, the concentrations of minor and trace constituents vary significantly. The major compositional gradients in the oceans are vertical, driven by removal of constituents from surface seawater by organisms, and destruction of the organism-produced particles after downward movement.
10. Besides addition of constituents by rivers, several processes are potentially capable of modifying the chemistry of seawater: (i) biological processes; (ii) seafloor volcanics–seawater interaction; (iii) reaction of seawater with detrital silicate and clay minerals transported from the continents; (iv) ocean-to-air transfer of cyclic salts; (v) precipitation of evaporite, sulfide, and phosphate minerals; and (vi) special processes such as porewater burial of Cl^-, nitrification and denitrification, and adsorption of phosphate on ferric oxides.
11. Except for local "oxygen oases," the surface oceans were anoxic under an anoxic atmosphere during the Archean, and the deep oceans continued to remain anoxic until about 1.8 Ga, the end of prolific BIF deposition. The deep ocean was probably sulfidic until 0.8 Ga, when the BIF deposition resumed, and anoxic for at least parts of the Neoproterozoic. The surface oceans must have been oxygenated throughout the Phanerozoic, but the oxidation state of the deeper oceans has fluctuated widely.
12. The seawater composition during the Hadean and Archean was probably not much different from present-day seawater. Seawater continued to be supersaturated with $CaCO_3$, $CaMg(CO_3)_2$, and SiO_2 during the Proterozoic. Its pH certainly rose in response to decreasing atmospheric P_{CO_2}, and it is likely that its salinity did not differ greatly from that of modern seawater. The Phanerozoic seawater composition has alternated between two types of brines related to different evaporite associations: a $MgSO_4$-type, rich in SO_4 but low in Ca; and a KCl-type, rich in Ca but low in SO_4.
13. The biogeochemical cycle of a chemical element (or a chemical species) is a conceptualized representation of its global reservoirs and its transfer from one reservoir to another through chemical and/or biochemical proceses. The biosphere is the most important geochemical realm at present, and the most important biogeochemical cycles are those of carbon, oxygen, nitrogen, sulfur, and phosphorus. The natural cycles of these elements have been significantly affected by input from anthropogenic sources over the past 200 yr.

13.8 Recapitulation

Terms and concepts

Acid deposition
Anoxic
Anoxygenic photosynthesis
Banded iron formation (BIF)
Biogeochemical cycles
Biolimited constituents
Carbon burial
Catalytic reaction chain
Chapman mechanism
Chloroflurocarbon compounds
Euxinic
Evaporites
Exosphere
Free radical
Global warming potential (GWP)
Great Oxidation Event (GOE)
Greenhouse gases
Huronian glaciation
Kármán line
Late Heavy Bombardment
Late Precambrian glaciations
Magma ocean
Mixing ratio
Oxic
Oxygenic photosynthesis
Ozone hole
Ozone layer
Photochemical reaction
Photochemical smog
Photolysis
Photon
Present atmospheric level (PAL)
Primary atmosphere
Primary pollutants
Radiative forcing
Residence time
Salinity
Scavenged constituents
Secondary atmosphere
Secondary pollutants
Snowball Earth stratosphere
Sulfidic ocean
Sulfurous smog
Thermocline
Thermosphere
Troposphere
Ultraviolet radiation

Computation techniques

- Energy required for splitting an atom
- Residence times of constituents in a reservoir
- Calculations pertaining to rates of reactions

13.9 Questions

1. Describe the important events, in chronological order, related to the evolution of the Earth during the first billion years or so after its birth.
2. The concentration of Na^+ in seawater is 460×10^{-3} g kg^{-1} water (Table 7.1) and the mass of seawater = 1.4×10^{24} g
   (a) Calculate the total amount of Na^+ in the oceans.
   (b) Given that the present flux of anthropogenic Na^+ into the oceans is 3.39×10^{12} mol yr^{-1}, how long would it take to increase the concentration of Na^+ in seawater by 10%? Assume no increase in the output flux to counterbalance the increased input.
3. The concentration of ammonia (NH_3) in the atmosphere is 0.456 μg m^{-3} at 0°C and 1 atm. Express the concentration in ppmv and ppbv. The atomic weights of H and N are 1.01 and 14.01, respectively, and the total number of molecules in 1 m^3 of air at 1 atm and 0°C (the *Loschmidt's number*) is 2.69×10^{25}.
4. Using the data given below, calculate the residence times of the solutes in seawater. The amount of water flowing from rivers to oceans = 3.74×10^{19} g yr^{-1}, and the amount of water in oceans = 1.35×10^{24} g.

Solute	Conentration in rivers (ppm)	Concentration in seawater (ppm)	Solute	Conentration in rivers (ppm)	Concentration in seawater (ppm)
Cl	6	19,350	Ca	13	412
Na	5	10,7860	K	1	399
SO_4	8	2712	HCO_3	52	145
Mg	3	1294	Si	10	10

5. What would be the equilibrium pH value of rainwater if atmospheric SO_2 gas were its only dissolved constituent?

   $SO_{2(g)} + H_2O_{(l)} \Leftrightarrow H_2SO_{3(aq)} \qquad K_1 = 2.0$
   $H_2SO_{3(aq)} \Leftrightarrow H_2SO^-_{3(aq)} + H^+ \qquad K_2 = 2.0 \times 10^{-2}$

   Assume that the activity of SO_2 gas in the atmosphere is 5×10^{-9} bar.
6. Assuming that P_{CO_2} in the Earth's early Archean atmosphere was 10^{10} bar, what would be the likely pH of rainwater in equilibrium with the atmospheric P_{CO_2}? Calculate the solubility of calcite in equilibrium with this water. Assume $a_i = m_i$. [Hint: see section 7.5.1.]
7. Climate modeling suggests that the Earth's atmospheric CO_2 concentration by the end of the 21st century will be close to 700 ppmv and global mean surface temperature could be 1.4–5.8°C warmer than in AD 2000. Explain qualitatively the likely impact of this scenario on (i) the pH of the rainwater, (ii) the pH of surface water in equilibrium with calcite, and (iii) the saturation state of surface seawater with respect to calcite.
8. The photolysis of water may be represented by the following reaction series:
   H_2O + UV photon ⇒ H + OH
   OH + OH ⇒ O + H_2O
   O + OH ⇒ O_2 + H
   O + O + M ⇒ O_2 + M
   (a) How many water molecules are needed to produce one molecule of O_2 by this reaction series?
   (b) What is a necessary condition for net addition of O_2 by this reaction series?
9. The combination of CO_2 with photolysis reaction series for H_2O (Q. 13.8) yields the following reaction series:
   H_2O + UV photon ⇒ H + OH
   CO_2 + UV photon ⇒ CO + O
   CO + OH ⇒ CO_2 + H
   OH + OH ⇒ O + H_2O
   O + O + M ⇒ O_2 + M
   Write down the net balanced reaction.
10. Methane gas (CH_4) comprises 7×10^{-5} % by mass of the Earth's atmosphere. What is the residence time of the gas in the atmosphere if it is being lost to the methane sinks at the rate of 4×10^{11} kg yr^{-1}. Estimated mass of the Earth's atmosphere = 5×10^{18} kg.
11. Calculate the residence time of Na^+ in the oceans using the following data: total riverine discharge into the oceans = 37.4×10^{15} L yr^{-1}; average concentration of Na^+ in riverine water = 0.313×10^{-3} mol L^{-1} (Gregor *et al.*, 1988, p. 26); total amount of water in the oceans = 10^{21} kg (Andrews *et al.*, 2004, p. 192); and average concentration of Na^+ in the oceans = 460×10^{-3} mol L^{-1}.
12. For the reaction

    $CO_{2(g)} + 4H_{2(g)} \Leftrightarrow CH_{4(g)} + 2H_2O_{(g)}$

    the equilibrium constants and partial pressures in the primitive atmosphere are as follows:

$K_{eq}(300\ K) = 5.2 \times 10^{19}$; $K_{eq}(500\ K) = 2.7 \times 10^{12}$
$P_{H_2O} = 3.0 \times 10^{-2}$ bar ; $P_{CO_2} = 3.0 \times 10^{-4}$ bar;
$P_{H_2} = 5.0 \times 10^{-5}$ bar

Calculate P_{CH_4} at 300 K and 500 K.

13. A catalytic cycle of reactions that might have contributed to the formation of H_2 from H in the early atmosphere of the Earth is

$$H + CO + M \xrightarrow{k_1} HCO + M$$

$$H + HCO \xrightarrow{k_2} H_2 + CO$$

$$2H \Rightarrow H_2 \text{ (net reaction)}$$

Assuming steady state, calculate the concentration of the radical HCO, given the following: concentration of CO = 1.0×10^{12} molecules cm^{-3}; concentration of M = 2.5×10^{19} molecules cm^{-3}; $k_1 = 1.0 \times 10^{-34}\ cm^6\ s^{-1}$ $molecule^{-2}$; and $k_2 = 3.0 \times 10^{-10}\ cm^3\ s^{-1}$ $molecule^{-1}$

14. Suppose, the conversion of ozone into molecular oxygen can be achieved by the following elementary reactions:

$O_3 \Leftrightarrow O_2 + O$
$O_3 + O \Leftrightarrow 2O_2$

What is (i) the overall chemical reaction, (ii) the intermediate, (iii) the rate law for each elementary reaction, and (iv) the rate-controlling elementary reaction, if the rate law for the overall reaction is
rate = $k\ [O_3]^2\ [O_2]^{-1}$
where k is the rate constant.

15. Calculate the rate for the reaction $Cl^{\bullet} + O_3 \Rightarrow ClO^{\bullet} + O_2$ at 30 km and 235 K. Assume that $[Cl^{\bullet}] = 5.0 \times 10^{11}$ molecules cm^{-3}, and $[O_3] = 2.0 \times 10^{12}$ molecules cm^{-3}. The rate equation is rate = $k\ [Cl]\ [O_3]$. For the Arrhenius equation, $A = 2.8 \times 10^{12}$, and $E_a = 21$ kJ mol^{-1}.

16. The amount of carbon in the crust is ~10^{20} kg. If all this carbon were present in the atmosphere as CO_2, what would be the atmospheric P_{CO_2}? Amount of carbon (inorganic) in the atmosphere = 58×10^{15} moles (Faure, 1991, p. 437).

17. In the upper atmosphere, O_3 is dissociated by ultraviolet radiation by the reaction $O_{3(g)} + UV \Rightarrow O_{2(g)} + O$. What is the energy of a 3400×10^{-8} cm photon that is absorbed in the process? What is the energy absorbed for a mole of these photons?

18. Photosynthesis involves the absorption of light of wavelength 440 nm and emission of radiation of wavelength 670 nm. What is the energy available for photosynthesis by this process?